

dental materials

Journal for Oral and Craniofacial Biomaterials Sciences

www.demajournal.com

**Abstracts of the Academy of Dental Materials Annual Meeting,
03-05 October 2019 - Jackson Hole, USA**

Available online at www.sciencedirect.com

This journal is part of **Science Direct**'s free alerting service which sends tables of contents and favourite topics for Elsevier books and journals. You can register by clicking "Alerts" at www.sciencedirect.com

ScienceDirect



Indexing Services

Dental Materials is indexed by *Index Medicus*, *BIOSIS*, *Current Contents*, *SciSearch*, *Research Alert*, *UnCover*, *Reference Update*, *UMI*, *Silver Platter*, *Excerpta Medica*, *CAB International* and *CINAHL*. The journal is available in microfilm from *UMI*.



0109-5641 (2019) 35:S1;1-0

Printed by Henry Ling Ltd., The Dorset Press, Dorchester, UK

Available online at www.sciencedirect.com

ScienceDirect



Official Publication of the Academy of Dental Materials

dental materials

Editor-in-Chief

David C Watts PhD FADM, *University of Manchester School of Dentistry, Manchester, UK.*

Editorial Advisor

Nick Silikas PhD FADM, *University of Manchester School of Dentistry, Manchester, UK.*

Editorial Assistant

Diana Knight, *University of Manchester School of Dentistry, Manchester, UK.*

E-mail: dentistry.dentmatj@manchester.ac.uk

Official Publication of the Academy of Dental Materials

Editorial Board

Kenneth Anusavice <i>University of Florida, USA</i>	Garry J.P. Fleming <i>Trinity College Dublin, IRELAND</i>	Ulrich Lohbauer <i>University of Erlangen-Nuremberg, Erlangen, GERMANY</i>	Patricia N.R. Pereira <i>University of Brasilia, BRAZIL</i>
Stephen Bayne <i>The University of Michigan, USA</i>	Alex S.L. Fok <i>The University of Minnesota, USA</i>	Grayson W. Marshall <i>University of California, San Francisco, USA</i>	John Powers <i>University of Texas at Houston, USA</i>
Roberto R Braga <i>University of São Paulo, BRAZIL</i>	Jason A. Griggs <i>The University of Mississippi, USA</i>	Sally Marshall <i>University of California, San Francisco, USA</i>	N. Dorin Ruse <i>University of British Columbia Vancouver, CANADA</i>
Lorenzo Breschi <i>Università di Bologna, ITALY</i>	Reinhard Hickel <i>Ludwig-Maximilians University of Munich, GERMANY</i>	Jukka P. Matinlinna <i>University of Hong Kong, CHINA</i>	Paulette Spencer <i>University of Kansas, USA</i>
Paulo Francisco Cesar <i>University of Sao Paulo – São Paulo, BRAZIL</i>	Nicoleta Ilie <i>Ludwig-Maximilians University of Munich, GERMANY</i>	Bart van Meerbeek <i>Katholieke Universiteit, Leuven, BELGIUM</i>	Jeffrey W. Stansbury <i>University of Colorado, USA</i>
Martin Y.M. Chiang <i>NIST, Gaithersburg, USA</i>	Satoshi Imazato <i>Osaka University, JAPAN</i>	Yasuko Momoi <i>Tsurumi University, Yokohama, JAPAN</i>	Michael Swain <i>University of Sydney, AUSTRALIA</i>
Pierre Colon <i>Université Denis Diderot, FRANCE</i>	Klaus Jandt <i>Friedrich-Schiller Universität Jena, GERMANY</i>	Mutlu Ozcan <i>University of Zurich, SWITZERLAND</i>	Arzu Tezvergil-Mutluay <i>University of Turku, FINLAND</i>
Brian Darvell <i>University of Birmingham, UK</i>	J. Robert Kelly <i>University of Connecticut, USA</i>	Will Palin <i>University of Birmingham, UK</i>	John E. Tibballs <i>Nordic Institute of Dental Materials, NORWAY</i>
Alvaro Della Bona <i>University of Passo Fundo, BRAZIL</i>	Matthias Kern <i>University of Keil, GERMANY</i>	David Pashley <i>Georgia Regents University, USA</i>	Pekka K. Vallittu <i>University of Turku, FINLAND</i>
George Eliades <i>University of Athens, GREECE</i>	Karl-Heinz Kunzelmann <i>Ludwig-Maximilians University of Munich, GERMANY</i>	Huakun (Hockin) Xu <i>The University of Maryland Dental School, MD, USA</i>	John C. Wataha <i>University of Washington, USA</i>
Jack Ferracane <i>Oregon Health Sciences University, USA</i>	Paul Lambrechts <i>Katholieke Universiteit, Leuven, BELGIUM</i>	Mangala P. Patel <i>Queen Mary University of London, UK</i>	Spiros Zinelis <i>University of Athens, GREECE</i>
Marco Ferrari <i>University of Siena, ITALY</i>			

Academy of Dental Materials

President: Jeff Stansbury

Local event organizer: RES Seminars

Executive Manager: Deanna Hilton/ Lynn Reeves

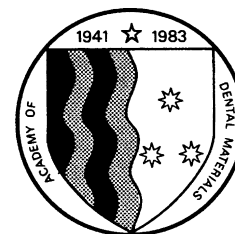
**ACADEMY OF DENTAL MATERIALS
CORPORATE MEMBERS**

3M ESPE



GC Dental Company





Contents

- e1 **Chemical characterization of clay material and effects on gingival healing**
B. Akon-Laba, B. Doukouré, G. Maroua, A. Aké
- e1 **Influence of dentin biomodification on bond strength and MMP activity**
M.A. Ferretti, K. Rischka, G.F. Abuna, M.C.A.J. Mainardi, F.H.B. Aguiar
- e2 **Two-body wear of glass-ceramics after sliding fatigue using three-dimensional inspection**
L.M.M. Alves, A.M.O. Dal Piva, J.P.M. Tribst, T.J.A. Paes-Junior, A.L.S. Borges, M.A. Bottino, Y. Zhang, R.M. Melo
- e2 **Curing protocols' effect on micro-flexural strength using different light-curing units**
A.O. Al-Zain, J.A. Platt
- e3 **Bone Regeneration with Extracellular Matrix Hydrogels from Porcine-Bladder and Bovine-Bone**
A.R. Ayala-Ham, J.A. López-Gutierrez, G. Jiménez Gastélum, G.Y. Castro-Salazar, J.G. Romero-Quintana, E.L. Silva-Benitez, J.E. Soto-Sainz, E.M. Aguilar-Medina, J. Sarmiento-Sanchez, R. Ramos-Payan
- e3 **Dynamic heat profile generated on pulpal-wall by various curing lights**
F. Baabdullah, E. Kilinc, C. Garcia-Godoy, S.A. Antonson
- e4 **Anti-Biofilm and Mechanically Stable Bioactive Composite for Root Caries Restorations**
A.A. Balhaddad, M. Ibrahim, M.D. Weir, H.H.K. Xu, M.A.S. Melo
- e5 **Dentin Matrix Stability and Gelatinolytic Activity with a Polyphenol-Enriched Extract**
E.C. Bridi, R.T. Basting, F.M.G. França, C.P. Turssi, F.L.B. Amaral, M.A. Foglio, R.T. Basting
- e5 **Wear Behavior of Translucent Zirconia after Chewing Simulation**
M. Borba, Y. Zhang, T. Okamoto, M. Zou, M.R. Kaizer
- e6 **Adhesives containing calcium phosphate: bond strength, micro-permeability and collagen degradation**
M.D.S. Chiari, Y. Alanía, A.K. Bedran-Russo, R.R. Braga
- e6 **Comparative research of bacteria gram-negative and positive on ti-30ta alloy**
P. Capellato, D. Sachs, A.P.R.A. Claro, G. Silva, C.A.C. Zavaglia
- e7 **Proanthocyanidin Gel on Acquired Pellicle Enamel at Initial Erosion**
F. Cardoso, A.P. Boteon, G.G. Dallavilla, D. Rios, H.M. Honório
- e7 **Azobenzene Hydrogels as Stimuli-Responsive, Antibacterial Oral Drug Delivery Networks**
C. Carpenter, G.M. Kehe, D. Nair, M. Schurr
- e8 **Analgesic-loaded pva films for tooth extraction: effect on blood coagulation**
B.I. Cerda-Cristerna, V.H. Flores-Valencia, J.L. Suárez-Franco, E.L. Galindo-Reyes, J.C. Flores-Arriaga
- e8 **Effect of surface finishing on flexural strength of translucent y-tzps**
K.N. Monteiro, R.P. Nigro, P.F. Cesar
- e9 **Shear bond strength comparison of self-adhesive resin cements**
L. Chen, R. Wang, B.I. Suh
- e9 **Universal adhesive improved bond strengths of self-adhesive resin cements**
L. Chen, B.I. Suh
- e9 **Condition for a valid exposure reciprocity law in dental composites**
S.V. Palagummi, T. Hong, Z. Wang, C.K. Moon, M.Y.M. Chiang
- e10 **Additive manufacturing of photopolymerizable thiol-ene thermoplastics**
K.K. Childress, M.D. Alim, J.J. Hernandez, J.W. Stansbury, C.N. Bowman
- e10 **Study on testing methods for efficacy of tooth manicure products**
J.W. Choi, S.Y. Yang, J.S. Kwon, S.B. Lee
- e11 **Effect of an experimental etchant on dentin bond-strength over time**
A. Comba, T. Maravic, E. Mancuso, S.R. Cunha, E. Mayer-Santos, M. Cadenaro, A. Mazzoni, L. Breschi

Indexing Services

Dental Materials is indexed by *Index Medicus*, *BIOSIS*, *Current Contents*, *SciSearch*, *Research Alert*, *UnCover*, *Reference Update*, *UMI*, *Silver Platter*, *Excerpta Medica*, *CAB International* and *CINAHL*. The journal is available in microfilm from *UMI*.

Available online at www.sciencedirect.com

ScienceDirect

This journal is part of **Science Direct's** free alerting service which sends tables of contents and favourite topics for Elsevier books and journals. You can register by clicking "Alerts" at www.sciencedirect.com



ELSEVIER

Amsterdam • Boston • London • New York • Oxford • Paris • Philadelphia • San Diego • St. Louis

- e11 **Effect of Er,Cr:YSGG laser conditions on debonding ysz ceramic**
L.R. Corby, D.S. Remley, D.M. Hutto, K.S. Jodha, J.A. Griggs, L. Contreras, S.M.S. Marocho
- e12 **3D Printed PBAT/BAGNb scaffolds: in vitro and in vivo analysis**
G. Balbinot, L.M. Ulbrich, V.C.B. Leitune, D. Ponzoni, R.M.D. Soares, F.M. Collares
- e13 **Chemical bonding and micromechanical interlocking to dental zirconia substrate**
N. Alsalem, B. Hajhamid, C. Lorenzetti, S. Barreto, G.M. De Souza
- e13 **Color and whiteness stability of composites after bleaching and aging**
A.D. Bona, M.L. Vidal, J. Xavier, O.E. Pecho
- e14 **WITHDRAWN**
- e14 **Biomechanical analysis of zirconia implant-supported crowns**
N. Kaur, H. Sherrill, Y. Duan
- e14 **Dental sealant modified biofilm inhibitor: effect on streptococcus mutans growth**
J.F.B. Fonseca, C.T.P. Araújo, A.B. Meireles, C.A. Santos, P.M. Alcântara, P.C.P. Paiva, M.H. Canuto
- e15 **Effect of mechanical properties of adhesives on bond strength**
K. Fujimori, A. Arita, T. Kumagai
- e15 **Effect of hybrid zinc-based particle with ionic liquid in adhesive**
I.M. Garcia, V.S. Souza, J.D. Souza, F. Visioli, J.D. Scholten, F.M. Collares
- e16 **Methacrylic resin compatibilization via reactive and inert nanogels**
D. Gautam, J.W. Stansbury, D.P. Nair
- e16 **Mechanical properties of 3d-printed dental implant guide by sterilization methods**
H.B. Go, S.Y. Im, B.S. Lim, K.M. Kim, J.S. Kwon
- e17 **Efficacy of PILP-method for remineralization of artificial and natural lesions**
M. Bacino, E. Babaie, G.W. Marshal, L.L. Gower, S. Habelitz
- e17 **Fluoride ion release/recharge behavior of ion-releasing restorative materials**
Y.Hokii, C. Carey, M. Heiss, G. Joshi
- e18 **SEPB fracture toughness of six dental zirconias**
T. Hill, R. Fachko, G. Tysowsky
- e18 **In vitro biocompatibility of extracellular matrix scaffolds with stem cells**
G.J. Gastélum, A. Ayala-Ham, J. López-Gutierrez, R. Ramos-Payan, G. Castro-Salazar, J. Romero-Quintana, J. Soto-Sainz, E. Aguilar-Medina, L. Espinoza-Cristobal, E. Silva-Benitez
- e19 **Monolithic zirconia structural degradation induced by aging and surface treatments**
M.R. Kaizer, R.C. Hintz, C.E.P. Borges, A.B.F. Fernandes, G. Serpa, C. Rodrigues, L. Wambier, G.M. Correr, Y. Zhang, C.C. Gonzaga
- e19 **Osteogenic and mechanical effect of ZrO₂-bioactive glasses bone graft substitute**
T.Y. Kang, J.H. Ryu, J.Y. Seo, K.M. Kim, J.S. Kwon
- e20 **Photocontrollable viscosity and hydrophilicity of nanogel based antibacterial dental adhesives**
G. Kehe, R. Trivedi, K. Patel, D. Nair
- e20 **Contrast ratio of bulk fill composite resins with different thicknesses**
P.V. Manozzo Kunz, M.R. Kaizer, G.M. Correr, L.F. Cunha, C.C. Gonzaga
- e21 **Evaluation of bond strength to dentin of universal adhesive systems**
M.C.A. Lago, C.L. Mendes, H. Annibal, C.P.P. Assis, L.J.R. Oliveira, M.S. Albuquerque, V.L. Nascimento, A. Nascimento, P.M. Alcantara, R. Braz
- e22 **Influence of biosilicate and propolis on adhesive bond strength**
R. Geng-Vivanco, R. Tonani-Torrieri, A.B. Silva, F.M. Oliveira, F.C.P. Pires-De-Souza
- e22 **Characterization of a new dental resin composite containing nano-MgO**
J. Fu, B.S.H. Tonin
- e22 **Effect of shockwave on desensitizer penetration into dentinal tubules**
I.B. Lee, C.H. Lee
- e23 **Influence of Water Storage Periods on Properties of Resin Materials**
A.F. Lima, M.V. Salvador, C.H. Saraceni
- e23 **Biocompatibility of endodontic repair cements with pulp cells**
J.A. López-Gutierrez, M. Bermúdez, A.R. Ayala-Ham, G.J. Gastélum, G.Y. Castro-Salazar, R. Ramos-Payan, J.G. Romero-Quintana, J.E. Soto-Sainz, E.L. Silva-Benitez, E.M. Aguilar-Medina
- e24 **Water sorption property of experimental nanocomposite**
H.Y. Marghalani
- e24 **Increased cariogenic biofilm formation on under-cured bulk fill composites**
M.A.S. Melo, H. Maktabi, M. Ibrahim, A. Balhaddad, Q. Alkhubaizi, A.P.P. Fugolin, C.S. Pfeifer, H. Strassler
- e25 **Microstructure of new lithium-disilicate CAD/CAM block**
T. Miyake, K. Kato, S. Akiyama, T. Azuma, K. Yamamoto, K. Kojima, K. Nagaoka, K. Shiraki, A. Fujimoto, T. Sato, T. Kumagai
- e25 **Inhibition of streptococcus mutans biofilms on azopolymer composite restorations**
D.I. Mori, G.M. Kehe, M.J. Schurr, D.P. Nair
- e26 **Effect of experimental S-PRG giomer®-based toothpastes on dentin hydraulic conductance**
V. Mosquim, G.S. Zabeu, G.A. Foratori-Junior, L.S. Condi, R.A. Caracho, D. Rios, L. Wang
- e26 **Antimicrobial Effects of Zinc-Fluoride Releasable Glass-Ionomer Cement on Fusobacterium Nucleatum**
Y. Nagano, D. Mori, T. Kumagai
- e27 **WITHDRAWN**

- e27 **Effect of ceramic on degree of conversion of cements**
Q.N. Souza, G. Pizzolatto, A.D. Bona, M. Borba
- e27 **Design optimization of all-ceramic crowns**
R. Ottoni, J.A. Griggs, P.H. Corazza, M. Borba
- e28 **Effect of Light Tip Optical Design on Dental Radiometer Accuracy**
W.M. Palin, M. Hadis, A.C. Shortall
- e29 **Evaluation of bone regeneration at socket-filled extraction sites with PRF**
G. Park, G. Kurgansky, A. Torroni, L.F. Gil, R. Neiva, L. Witek, P. Coelho
- e29 **Stress relaxation behavior in glassy methacrylate networks containing thiourethane-based oligomers**
S.H. Lewis, A.P.P. Fugolin, J.L. Ferracane, C.S. Pfeifer
- e30 **Dentin adhesives modified with DMSO: cell viability and produced cytokines**
C.T.A. Pimenta, A.B. Meireles, I.M. Ottoni, I. D'angellis, P. Barroso, B. Avelar-Freitas, G.E. Brito-Melo
- e30 **Effectiveness of a universal adhesive used as silane-coupling agent**
T.S. Porto, A.J. Faddoul, S.Y. Park, F.F. Faddoul, M.F. De Goes
- e31 **Effect of preheating on rheological properties of resin composites**
D.L.N. Poubel, S.J.L. Sousa, I.D.O. Pereira, F.C. Cunha, A.P.D. Ribeiro, P. Pereira, F.C.P. Garcia
- e31 **Resin cements light-cured through different hybrid cad/cam materials**
J.P.D. Moraes, L.O. Brasil, M.Z.D. Picolo, M. Giannini, V. Cavalli
- e32 **Microstructure and mechanical properties of stabilized zirconia ceramics**
S. Rada, E. Culea, M. Rada
- e32 **Improvement of resin-based composites physico-mechanical characteristics after thermal post-cure**
C.M. Hardy, D. Dive, J.G. Leprince, L.D. Randolph
- e33 **Physico-mechanical properties of 3d-printed resin used as temporary crown/bridge restoration**
F.A.P. Rizzante, T.L. Bueno, G.M.F. Guimarães, G.F. Moura, R. Roperto, T.S. Porto, F. Faddoul, A.Y. Furuse, G. Mendonça
- e33 **Effect of Chemical Catalysis on Hydrogen Peroxide Bleaching Efficacy**
C.R.G. Torres, L.F. Cornelio, A.B. Borges
- e34 **Physico-Chemical Properties and Cytocompatibility of 36 Commercially Available “Graphene” Materials**
V. Rosa, R. Melhotra
- e34 **Bulk-Fill Composites Based on an Elastomeric Methacrylate Monomer**
M.G. Rocha, J.F. Roulet, D.C.R.S. Oliveira, M.A.C. Sinhoreti, A.B. Correr
- e35 **Monomer Combination's for Bulkfill Applications'**
L.D. Pereira, M.P.C. Neto, L.M. Cavalcante, L.F. Schneider
- e35 **RCT Papers in Prosthesis - Compliance with Consort Guidelines – A SR**
N. Meckelburg, A. Reis, A. Loguerio, M. Schroeder
- e35 **Interfacial Gap and Fracture Resistance of Indirect CAD-CAM Restorations**
N. Scotti, E.A. Vergano, A. Baldi, G. Zoppetto, R.M. Tempesta, M. Alovisei, D. Pasqualini, A. Comba, E. Berutti
- e36 **Bond strengths Of universal adhesives achieved by different dentin-etching approaches**
M. Sebold, C.B. André, M. Giannini
- e36 **Effect of surface treatments on bond of cad/cam composite block**
L. Chen, T. Sedlacek, B.I. Suh
- e37 **Control of dynamic material property development in photopolymers using photochromism**
P.K. Shah, J.W. Stansbury
- e37 **Effect of tooth-brushing with microcurrent on dentinal tubule occlusion**
G. Kim, Y. Shin
- e38 **Ultrasonic activation of different solutions on root canal dentin**
J.E. Soto-Sainz, J.A. Espinoza-Rodriguez, C. Samano-Valencia, A.R. Ayala-Ham, G.Y. Castro-Salazar, N.V. Zavala-Alonso, R. Ramos-Payan, E.M. Aguilar-Medina, E.L. Silva-Benitez, J.G. Romero-Quintana
- e38 **Resin property control throughout conversion based on nanogel functionalization**
M. Barros, J. Vigil, J. Stansbury
- e39 **Physicochemical study of Biodentine™-dentine tissue interphase**
J.L. Suárez-Franco, B.I. Cerda-Cristerna, A. Suárez-Porras, R.E. Flores-Ventura, M. Trujillo-Hernández, R. Trueba-García
- e39 **Reinforcement of dental adhesives with bio-inspired monomers**
C. Szczepanski, C. Ligo
- e40 **Inhibitory effects of various ions released from surface active fillers**
I. Salim, R. Seseogullari-Dirihan, S. Imazato, A. Tezvergil-Mutluay
- e40 **Fracture resistance of short-fiber resin composite bilayers**
J. Tiu, R. Belli, U. Lohbauer
- e41 **Dentin changes associated with patient age and cavity site**
A.T. Weerakoon, I.A. Meyers, S. Roy, C. Cooper, T.R. Cox, N.D. Condon, C. Sexton, D.H. Thomson, P.J. Ford, A.L. Symons
- e41 **Structural and mechanical effects of ionizing radiation on human enamel**
M. Wendler, G. Jerez, I. Luque-Martinez, M. Lopez, A. Bedran-Russo, M. Muñoz
- e42 **Endocrown luting procedures: analysis of dual luting cements conversion rate**
S. Chirico, A. Ionescu, L. Breschi, E. Brambilla, M.M. Gagliani
- e42 **Stress relaxation via covalent dynamic bonds in nanogel containing resins**
G. Gao, X. Han, N. Swan, X. Zhang, C. Bowman, J. Stansbury

Paffenbarger Award Finalists

- e43 **P1. 3D printable resins combining extreme strength with toughness**
R. Bailey, M. Barros, P.K. Shah, J.W. Stansbury
- e43 **P2. Development of porous calcium-hydroxide-linked scaffolds for dentin cell-homing therapy**
E.A.F. Bordini, F.B. Cassiano, E.S. Bronze-Uhle, L.E. Pacheco, G. Zabeo, J. Hebling, M.C. Bottino, C.A.D.S. Costa, D.G. Soares
- e44 **P3. Photoreactive nanogels for local treatment of the oral cavity**
H. Escobedo, J.W. Stansbury, D.P. Nair
- e44 **P4. Mini-interfacial fracture toughness when bonding indirect restorations with light-curable composite**
C.M.F. Hardy, V. Landreau, M. Valassis, B. Mercelis, B. Van Meerbeek, J.G. Leprince
- e45 **P5. Rechargeable dual function dental sealant against cariogenicity of streptococcus mutans**
M.S. Ibrahim, A.S. Ibrahim, A.A. Balhaddad, M.D. Weir, T.W. Oates, H.H.K. Xu, M.A.S. Melo
- e45 **P6. Dark-curing photoinitiators that extend the cure depth in composite materials**
K. Kim, J. Sinha, A.M. Salazar, C.B. Musgrave, J.W. Stansbury
- e46 **P7. Development of higher substituted thiols for improved thiol-ene dental materials**
K. Long, A. Ortego, M. Olin, C. Bowman
- e47 **P8. Residual stresses in bilayer crowns: a vfem study**
C.S. Rodrigues, S. Dhital, L.G. May, J. Kim, Y. Zhang

Marshalls Award Finalists

- e47 **M1. Methacrylamide-methacrylate hybrid monomers for dental applications**
A. Fugolin, M.G. Logan, S. Lewis, J.L. Ferracane, C.S. Pfeifer
- e48 **M2. Antimicrobial properties of PMMA resin containing graphene**
A.C. Ionescu, S. Sauro, P.M. Pires, A. López-Castellano, A.M. Alambiaga-Caravaca, E. Brambilla
- e49 **M3. Mechanical and antimicrobial properties of novel bioactive dental restorative composites**
C.B. Tanaka, F. Gonçalves, D.P. Lopes, L.H. Catalani, R.R. Braga, J.J. Kruzic

Paffenbarger Award Finalists

- P1.** 3D Printable Resins Combining Extreme Strength with Toughness. **R. Bailey**^{*1}, M. Barros ¹, P. K. Shah ², J. W. Stansbury ^{1,2} (¹ Department of Craniofacial Biology, University of Colorado Anschutz Medical Campus, USA; ² Department of Chemical & Biological Engineering, University of Colorado Boulder, USA)
- P2.** Development of Porous Calcium-Hydroxide-Linked Scaffolds for Dentin Cell-Homing Therapy. **E.A.F. Bordini**^{*1,3}, F.B. Cassiano ¹, E.S. Bronze-Uhle ², L.E. Pacheco ², G. Zabeo ², J. Hebling ¹, M.C. Bottino ³, C.A. De Souza Costa ¹, D.G. Soares ² (¹ Araraquara School of Dentistry, São Paulo State University (Unesp), Araraquara, Brazil; ² Bauru School of Dentistry, University of São Paulo (Usp), Bauru, Brazil; ³ School of Dentistry, University of Michigan (Uofm), Ann Arbor, USA)
- P3.** Photoreactive Nanogels for Local Treatment of the Oral Cavity. **H. Escobedo**^{*}, J. W. Stansbury, D. P. Nair (University of Colorado Anschutz Medical Campus, Aurora, USA)
- P4.** Mini-Interfacial Fracture Toughness when Bonding Indirect Restorations with Light-Curable Composite. **C.M.F. Hardy**^{*}, V Landreau, M. Valassis, B. Mercelis, B. Van Meerbeek, **Leprince J.G T. Hill**^{*}, R. Fachko, G. Tysowsky (Ivoclar Vivadent, Inc, Amherst, USA)
- P5.** Rechargeable Dual Function Dental Sealant against Cariogenicity of Streptococcus Mutans. **M.S. Ibrahim** ^{1,2*}, A.S. Ibrahim ³, A.A. Balhaddad ^{1,2}, M.D. Weir ¹, T.W. Oates ¹, H.H.K. Xu ^{1,4}, M.A.S. Melo ¹ (¹ University of Maryland School of Dentistry, Baltimore, USA; ² College of Dentistry, Imam Abdulrahman Bin Faisal University, Dammam, Saudi Arabia; ³ Health Monitoring Centers, Ministry of Health, Jeddah Saudi Arabia; ⁴ University of Maryland School of Medicine, Baltimore, USA)
- P6.** Dark-Curing Photoinitiators that Extend the Cure Depth in Composite Materials. **K. Kim** ^{1*}, J. Sinha ¹, A. M. Salazar ¹, C. B. Musgrave ¹, J. W. Stansbury ^{1,2} (¹ University of Colorado, Boulder, Colorado, USA; ² School of Dental Medicine, Aurora, Colorado, USA)
- P7.** Development of Higher Substituted Thiols for Improved Thiol-Ene Dental Materials. **K. Long**^{*}, A. Ortego, M. Olin, C. Bowman (University of Colorado Boulder, USA)
- P8.** Residual Stresses in Bilayer Crowns: A VFEM Study. **C.S. Rodrigues**^{*1,2}, S. Dhital ³, L.G. May ², J. Kim³, Y. Zhang¹ (¹ New York University, USA; ² Federal University of Santa Maria, Brazil; ³ University of Connecticut, USA)

Marshalls Award Finalists

- M1.** Methacrylamide-Methacrylate Hybrid Monomers for Dental Applications. **A. Fugolin**^{*}, M.G. Logan, S. Lewis, J.L. Ferracane, C.S. Pfeifer (Oregon Health & Science University, Portland, USA)
- M2.** Antimicrobial Properties of PMMA Resin Containing Graphene. **A.C. Ionescu**^{*1}, S. Sauro ², P.M. Pires ³, A. López-Castellano ¹, A.M. Alambiaga-Caravaca ¹, E. Brambilla ¹ (¹ University of Milan, Department of Biomedical, Surgical and Dental Sciences, Milan, Italy; ² Universidad Cardenal Herrera-Ceu, Valencia, Spain; ³ Federal University of Rio De Janeiro, Rio De Janeiro, Brazil)
- M3.** Mechanical and Antimicrobial Properties of Novel Bioactive Dental Restorative Composites. **C.B. Tanaka**^{*1}, F. Gonçalves ², D.P. Lopes ², L.H. Catalani ³, R.R. Braga ³, J.J. Kruzic ¹ (¹ University of New South Wales, Australia; ² Ibirapuera University, Brazil; ³ University of São Paulo, Brazil)

List of Abstracts ADM 2019

THURSDAY 3RD OCTOBER

1. Chemical Characterization of Clay Material and Effects on Gingival Healing. **B. Akon-Laba**^{*1}, B.Doukouré ², Gt.Maroua ¹, Ap. Aké ³ (¹ Département de Biologie et Matières Fondamentales, Ufr Odonto-Stomatologie; ² Laboratoire D'Anatomie-Pathologie, Ufr Sciences Médicales; ³ Laboratoire de Chimie des Matériaux (Université Félix Houphouët Boigny, Abidjan, Côte D'Ivoire)
2. Influence of Dentin Biomodification on Bond Strength and MMP Activity. **M.A. Ferretti**^{*1}, K. Rischka ², G.F. Abuna ¹, M.C.A.J. Mainardi ¹, F.H.B. Aguiar ¹ (¹ Piracicaba Dental School, University of Campinas, Brazil; ² Fraunhofer Institute Ifam Bremen, Germany)
3. Two-Body Wear of Glass-Ceramics after Sliding Fatigue Using Three-Dimensional Inspection. **L.M.M. Alves**^{*1}, A.M.O. Dal Piva ¹, J.P.M. Tribst ¹, T.J.A. Paes-Junior ¹, A.L.S. Borges ¹, M.A. Bottino ¹, Y. Zhang ², R.M. Melo ¹ (¹ Sao Paulo State University (UNESP), Department of Dental Materials and Prosthodontics, Sao Jose Dos Campos, Br; ² New York University, Department of Biomaterials and Biomimetics, USA)
4. Curing Protocols' Effect on Micro-Flexural Strength Using Different Light-Curing Units. **A.O. Al-Zain**^{*1}, J.A. Platt ² (¹ Faculty of Dentistry, King Abdulaziz University, Jeddah, Kingdom of Saudi Arabia, ² Indiana University School of Dentistry, Indiana University Purdue University Indianapolis, USA).
5. Bone Regeneration with Extracellular Matrix Hydrogels from Porcine-Bladder and Bovine-Bone. **A.R. Ayala-Ham**^{*}, J.A. López-Gutierrez, G. Jiménez Gastélum, G.Y. Castro-Salazar, J.G. Romero-Quintana, E.L. Silva-Benitez, J.E. Soto-Sainz, E.M. Aguilar-Medina ¹, J. Sarmiento-Sanchez, R. Ramos-Payan (Autonomous University of Sinaloa, Culiacán, Sinaloa, México).
6. Dynamic Heat Profile Generated on Pulpal-Wall by Various Curing Lights. **F. Baabdullah**^{*}, E. Kilinc, C. Garcia-Godoy, S. A. Antonson (Nova Southeastern University, USA)
7. Anti-Biofilm and Mechanically Stable Bioactive Composite for Root Caries Restorations. **A.A. Balhaddad**^{*1,2}, M. Ibrahim ^{1,2}, M.D. Weir ¹, H.H.K. Xu ¹, M.A.S. Melo ¹ (¹ University of Maryland Dental School, Baltimore, USA; ² College of Dentistry, Imam Abdulrahman Bin Faisal University, Dammam, Saudi Arabia)
8. Dentin Matrix Stability and Gelatinolytic Activity with a Polyphenol-Enriched Extract. E.C. Bridi ¹, R.T. Basting ¹, F.M.G. França ¹, C.P. Turssi ¹, F.L.B. Amaral ¹, M.A. Foglio ², **R.T. Basting**^{*1} (¹ Dental School and Research Institute São Leopoldo Mandic, Brazil; ² University of Campinas, Brazil)
9. Wear Behavior of Translucent Zirconia after Chewing Simulation. **M. Borba**^{*1}, Y. Zhang ², T. Okamoto ², M. Zou ², M.R. Kaizer ³ (¹ University of Passo Fundo, Brazil; ² New York University, USA; ³ Positivo University, Brazil)
10. Adhesives Containing Calcium Phosphate: Bond Strength, Micro-Permeability and Collagen Degradation. M. D. S. Chiari ¹, Y.Alania ², A.K. Bedran-Russo ², **R. R. Braga**^{*1} (¹ University of São Paulo, São Paulo, Brazil; ² University of Illinois, Chicago, USA)
11. Comparative Research of Bacteria Gram-Negative and Positive on Ti-30Ta Alloy. **P. Capellato**^{*1}, D. Sachs ¹, A. P. R. A. Claro ², G. Silva ¹, C.A.C. Zavaglia ³ (¹ University of Itajuba , Brazil ; ² University Estadual Paulista, Brazil; ³ State University of Campinas, Brazil)
12. Proanthocyanidin Gel on Acquired Pellicle Enamel at Initial Erosion. **F Cardoso**^{*}, AP Boteon, GG Dallavilla, D Rios, HM Honório (University of São Paulo, Bauru, Brazil)
13. Azobenzene Hydrogels as Stimuli-Responsive, Antibacterial Oral Drug Delivery Networks. **C. Carpenter**^{*1}, G.M. Kehe ², D. Nair ², M. Schurr ² (¹ Metropolitan State University, Denver, USA; ² University of Colorado, Aurora, USA)
14. Analgesic-Loaded PVA Films for Tooth Extraction: Effect on Blood Coagulation. **B.I. Cerda-Cristerna**^{*1}, V.H. Flores-Valencia ¹, J.L. Suárez-Franco ¹, E.L. Galindo-Reyes ¹, J.C. Flores-Arriaga ² (¹ Universidad Veracruzana Región Orizaba Córdoba, México; ² Universidad Nacional Autónoma De México Enes León, México).
15. Effect of Surface Finishing on Flexural Strength of Translucent Y-TZPs. K.N. Monteiro, R.P. Nigro, **P.F. Cesar**^{*} (University of São Paulo, Brazil)
16. Shear Bond Strength Comparison of Self-Adhesive Resin Cements. L. Chen, **R. Wang**^{*}, B.I. Suh (Bisco, Schaumburg, USA)
17. Universal Adhesive Improved Bond Strengths of Self-Adhesive Resin Cements. **L. Chen**^{*}, B.I. Suh (Bisco, Schaumburg, USA)
18. Condition for a Valid Exposure Reciprocity Law in Dental Composites. S.V. Palagummi ¹, T. Hong ^{1,3}, Z. Wang ², C.K. Moon ³, **M.Y.M. Chiang**^{*1} (¹ Biosystems and Biomaterials Division, National Institute of Standards and Technology, Gaithersburg, USA; ² Department of Engineering Mechanics, Wuhan University, Wuhan, China; ³ Department of Materials Science and Engineering, Pukyong National University, Busan, Republic of Korea)
19. Additive Manufacturing of Photopolymerizable Thiol-Ene Thermoplastics. **K.K. Childress**^{*1}, M.D. Alim¹, J.J. Hernandez¹, J.W. Stansbury^{1,2}, C.N. Bowman¹ (¹ University of Colorado Boulder, Boulder, USA; ² University of Colorado Denver, Aurora, USA)
20. Study on Testing Methods for Efficacy of Tooth Manicure Products. **J.W. Choi**^{*}, S.Y. Yang, J.S. Kwon, S.B. Lee (Yonsei University College of Dentistry, Seoul, Korea)
21. Effect of an Experimental Etchant on Dentin Bond-Strength over Time. **A. Comba**^{*1}, T. Maravic ¹, E. Mancuso ¹, S. Ribeiro Cunha ^{1,2}, E. Mayer-Santos ^{1,2}, M. Cadenaro ⁴, A. Mazzoni ¹, L. Breschi ¹ (¹ University of Bologna, Italy; ² University of Sao Paolo, Brazil; ³ University of Trieste, Italy)
22. Effect of Er,Cr:YSGG Laser Conditions on Debonding YSZ Ceramic. **L.R. Corby**^{*}, D.S. Remley, D.M. Hutto, K.S. Jodha, J.A. Griggs, L. Contreras, S.M. Salazar Marocho (University of Mississippi Medical Center, Jackson, USA)

23. 3D Printed PBAT/BAGNb Scaffolds: In Vitro and In Vivo Analysis. **G. Balbinot***, L.M. Ulbrich, V.C.B. Leitune, D. Ponzoni, R.M.D. Soares, F.M. Collares (Universidade Federal do Rio Grande do Sul, Porto Alegre, Brazil)
24. Chemical Bonding and Micromechanical Interlocking to Dental Zirconia Substrate. N. Alsalem ¹, B. Hajhamid ², C. Lorenzetti ³, S. Barreto ⁴, **G.M. De Souza*²** (¹ Princess Nourah University, College of Dentistry, Riyadh, Saudi Arabia; ² Faculty of Dentistry, University of Toronto, Toronto, Canada; ³ State University of Sao Paulo, Araraquara School of Dentistry, Araraquara, Brazil; ⁴ State University of Campinas, Piracicaba School of Dentistry, Piracicaba, Brazil)
25. Color and Whiteness Stability of Composites after Bleaching and Aging. **A. Della Bona***, M.L. Vidal, J. Xavier, O.E. Pecho (University of Passo Fundo, Passo Fundo, Brazil)
26. Influence of Surface Treatments on Composite Resin Cores. **P.H. Dos Santos*¹**, J.B. Rossi ¹, H.B. Strazzi Sahyon ¹, A.T. Maluly-Próni ¹, B. Oliveira-Reis ¹, M.D. Moda ¹, T.Y.U. Suzuki ², S.B. Martins ¹, R.G. Fonseca ¹, A.L.F. Briso ¹. (¹ São Paulo State University, Brazil; ² Minas Gerais Federal University, Brazil)
27. Biomechanical Analysis of Zirconia Implant-Supported Crowns. N Kaur, HM Sherrill, **Y Duan*** (School of Dentistry, University of Mississippi Medical Center, Jackson, USA)
28. Dental Sealant Modified Biofilm Inhibitor: Effect on Streptococcus Mutans Growth. **J.F.B. Fonseca***, C.T.P. Araújo, A.B. Meireles, C.A. Santos, P.M. Alcântara, P.C.P. Paiva, M.H. Canuto (Federal University of the Jequitinhonha and Mucuri Valleys, Diamantina, Minas Gerais Brazil)
29. Effect of Mechanical Properties of Adhesives on Bond Strength. **K. Fujimori***, A. Arita, T. Kumagai (R&D Department, GC Corporation, Tokyo, Japan)
30. Effect of Hybrid Zinc-Based Particle with Ionic Liquid in Adhesive. **I.M. Garcia***, V.S. Souza, J.D. Souza, F. Visioli, J.D. Scholten, F.M. Collares (Federal University of Rio Grande Do Sul, Porto Alegre, Brazil)
31. Methacrylic Resin Compatibilization via Reactive and Inert Nanogels. **D. Gautam*¹**, J.W. Stansbury ^{1,2}, D.P. Nair ¹ (¹ Department of Craniofacial Biology, Anschutz Medical Campus, Aurora; ² Department of Chemical and Biological Engineering, University of Colorado, Boulder)
32. Mechanical Properties of 3D-Printed Dental Implant Guide by Sterilization Methods. **H.-B. Go*¹**, S.-Y. Im ¹, B.-S. Lim ², K.-M. Kim ¹, J.-S. Kwon ¹ (¹ Yonsei University College of Dentistry, Seoul, Korea; ² School of Dentistry, Seoul National University, Seoul, Korea)
33. Efficacy of PILP-Method for Remineralization of Artificial and Natural Lesions. M. Bacino ¹, E. Babaie ¹, G. W. Marshal ¹, L. Gower ², **S. Habelitz*¹** (¹ University of California, San Francisco, USA; ² University of Florida, Gainesville, USA)
34. Fluoride Ion Release/Recharge Behavior of Ion-Releasing Restorative Materials. Y.Hokii ¹, C. Carey ², **M. Heiss*¹**, G. Joshi ¹ (¹ GC America, Alsip, USA; ² University of Colorado, Aurora, USA)
35. SEPB Fracture Toughness of Six Dental Zirconias. **T. Hill***, R. Fachko, G. Tysowsky (Ivoclar Vivadent, Inc, Amherst, USA)
36. In Vitro Biocompatibility of Extracellular Matrix Scaffolds with Stem Cells. **GR Jiménez Gastélum*¹**, AR Ayala-Ham ¹, JA López-Gutierrez ¹, R Ramos-Payan ¹, GY Castro-Salazar ¹, JG Romero-Quintana ¹, JE Soto-Sainz ¹, EM Aguilar-Medina ¹, LF Espinoza-Cristobal ², EL Silva-Benitez ¹. (¹ Autonomous University of Sinaloa, Culiacán, México; ² Autonomous University of Ciudad Juárez, Chihuahua, México)
37. Monolithic Zirconia Structural Degradation Induced by Aging and Surface Treatments. **M.R. Kaizer*¹**, R.C. Hintz ¹, C.E.P. Borges ¹, A.B.F. Fernandes ¹, G. Serpa ¹, C. Rodrigues ², L. Wambier ¹, G.M. Correr ¹, Y. Zhang ², C.C. Gonzaga ¹ (¹ Positivo University, Brazil; ² New York University, USA)
38. Osteogenic and Mechanical Effect of ZrO₂-Bioactive Glasses Bone Graft Substitute. **T.Y.Kang***, J.H. Ryu, J.Y. Seo, K.M. Kim, J.S. Kwon (Yonsei University College of Dentistry, Seoul, Korea)
39. Photocontrollable Viscosity and Hydrophilicity of Nanogel Based Antibacterial Dental Adhesives. **G. Kehe***, R. Trivedi, K. Patel, D. Nair (University of Colorado Anschutz Medical Campus, Aurora, USA)
40. Contrast Ratio of Bulk Fill Composite Resins with Different Thicknesses. **P.V. Manozzo Kunz***, M.R. Kaizer, G.M. Correr, L.F. Cunha, C.C. Gonzaga (Universidade Positivo, Curitiba, Brazil)
41. Evaluation of Bond Strength to Dentin of Universal Adhesive Systems. **M.C.A. Lago***, C.L. Mendes, H. Anníbal, C.P.P. Assis, L.J.R. Oliveira, M.S. Albuquerque, V.L. Nascimento, A. Nascimento, P.M. Alcantara, R. Braz (Faculty of Dentistry, University of Pernambuco, Recife, Brazil)

FRIDAY 4TH OCTOBER

42. Influence of Biosilicate and Propolis on Adhesive Bond Strength. **R. Geng-Vivanco***, R. Tonani-Torrieri, A.B. Silva, F.M. Oliveira, F.C.P. Pires-De-Souza (Ribeirão Preto School of Dentistry, University of São Paulo, Ribeirão Preto, Brazil)
43. Characterization of a New Dental Resin Composite Containing Nano-MgO. J.Fu ^{1,3}, **B.S.H. Tonin*^{2,3}** (¹ Qingdao University, China; ² University of Sao Paulo, Brazil; ³ University of Minnesota, USA)
44. Effect of Shockwave on Desensitizer Penetration into Dentinal Tubules. **I.B. Lee***, C.H. Lee (School of Dentistry, Seoul National University, Seoul, Korea)
45. Influence of Water Storage Periods on Properties of Resin Materials. **A.F. Lima***, M.V. Salvador, C.H. Saraceni (Paulista University, Jundai, Brazil)

46. Biocompatibility of Endodontic Repair Cements with Pulp Cells. **JA López-Gutierrez***, M Bermúdez, AR Ayala-Ham, G Jiménez Gastélum, GY Castro-Salazar, R Ramos-Payan, JG Romero-Quintana, JE Soto-Sainz, EL Silva-Benitez, EM Aguilar-Medina (Autonomous University of Sinaloa, Culiacán, México)
47. Water Sorption Property of Experimental Nanocomposite. **H.Y. Marghalani*** (Faculty of Dentistry, King Abdulaziz University, Jeddah, Saudi Arabia)
48. Increased Cariogenic Biofilm Formation on under-Cured Bulk Fill Composites. **M.A.S. Melo***¹, H. Maktabi ¹, M. Ibrahim ¹, A. Balhaddad ², Q. Alkhubaizi ¹, A.P.P. Fugolin ², C.S. Pfeifer ², H. Strassler ¹ (¹ University of Maryland School of Dentistry, Baltimore, USA; ² School of Dentistry, Oregon Health & Science University, Portland, USA)
49. Microstructure of New Lithium-Disilicate CAD/CAM Block. **T. Miyake***, K. Kato, S. Akiyama, T. Azuma, K. Yamamoto, K. Kojima, K. Nagaoka, K. Shiraki, A. Fujimoto, T. Sato, T. Kumagai (Research & Development Dept., GC Corporation, Tokyo, Japan)
50. Inhibition of Streptococcus Mutans Biofilms on Azopolymer Composite Restorations. **D.I. Mori***, G.M. Kehe, M.J. Schurr, D.P. Nair (University of Colorado Anschutz Medical Campus, Aurora, USA)
51. Effect of Experimental S-PRG Giomer®-Based Toothpastes on Dentin Hydraulic Conductance. **V. Mosquim***¹, G.S. Zabeu ^{1,2}, G.A. Foratori-Junior ^{2,3}, L.S. Condi ¹, R.A. Caracho ¹, D. Rios ², L. Wang ¹ (¹ Bauru School of Dentistry, University of São Paulo, Bauru, Brazil; ² School of Dentistry, Sagrado Coração University, Bauru, Brazil; ³ University of Integrated Faculties of Ourinhos, Ourinhos, Brazil)
52. Antimicrobial Effects of Zinc-Fluoride Releasable Glass-Ionomer Cement on Fusobacterium Nucleatum. **Y. Nagano***, D. Mori, T. Kumagai (GC Corporation, Research & Development, Tokyo, Japan)
53. Effect of Zirconia Decontamination Protocols on Bond Strength. **M. D. Noronha***¹, B. M. Fronza ¹, C. B. Andre ¹, E. F. De Castro ¹, R. B. Price ², M. Giannini ¹ (¹ Piracicaba Dental School, University of Campinas, Piracicaba, Brazil; ² Dalhousie University, Halifax, Canada)
54. Effect of Ceramic on Degree of Conversion of Cements. **Q.N. Sonza***, G. Pizzolatto, A.D. Bona, M. Borba (University of Passo Fundo, Brazil)
55. Design Optimization of All-Ceramic Crowns. **R Ottoni***¹, JA Griggs ², PH Corazza ¹, M Borba ¹ (¹ Dental School, University of Passo Fundo, Brasil; ² Department of Biomedical Materials Science, University of Mississippi Medical Center, Jackson, USA)
56. Effect of Light Tip Optical Design on Dental Radiometer Accuracy. **W.M. Palin***, M. Hadis, A.C. Shortall (University of Birmingham, UK)
57. Evaluation of Bone Regeneration at Socket-Filled Extraction Sites with PRF. **G. Park***¹, G. Kurgansky ¹, A. Torroni ², L.F. Gil ³, R. Neiva ⁴, L. Witek ¹, P. Coelho ^{1,2} (¹ New York University College of Dentistry, New York, USA; ² NYU Langone Medical Center, New York, USA; ³ Department of Dentistry, Universidade Federal De Santa Catarina, Br; ⁴ University of Florida College of Dentistry, Gainesville, USA)
58. Stress Relaxation Behavior in Glassy Methacrylate Networks Containing Thiourethane-Based Oligomers. S.H. Lewis, A.P.P. Fugolin, J.L. Ferracane, **C.S. Pfeifer*** (Oregon Health & Science University, Portland, USA)
59. Dentin Adhesives Modified with DMSO: Cell Viability and Produced Cytokines. **C.T.A. Pimenta***, A.B. Meireles, I. M. Ottoni, I. D'angelis, P. Barroso, B. Avelar-Freitas, G. E. Brito-Melo (PRPPG, Federal University, Diamantina, Brazil)
60. Effectiveness of a Universal Adhesive used as Silane-Coupling Agent. **T.S. Porto***¹, A.J. Faddoul ¹, S.Y. Park ¹, F.F. Faddoul ¹, M.F. De Goes ² (¹ Case Western Reserve University, USA; ² Campinas State University, Brazil)
61. Effect of Preheating on Rheological Properties of Resin Composites. **D.L.N. Poubel***, S.J.L. Sousa, I.D.O. Pereira, F.C. Cunha, A.P.D. Ribeiro, P. Pereira, F.C.P. Garcia (University of Brasília, Brasília, Brazil)
62. Resin Cements Light-Cured Through Different Hybrid CAD/CAM Materials. **J. Pucci De Moraes***, L.O. Brasil, M.Z.D. Picolo, M. Giannini, V. Cavalli (Piracicaba Dental School, University of Campinas, Brazil)
63. Microstructure and Mechanical Properties of Stabilized Zirconia Ceramics. **S. Rada*** ^{1,2}, E. Culea ², M. Rada ¹ (¹ National Institute for Research Development of Isotopic and Molecular Technologies, Cluj-Napoca, Romania; ² Department of Physics & Chemistry, Technical University of Cluj-Napoca, Romania)
64. Improvement of Resin-Based Composites Physico-Mechanical Characteristics after Thermal Post-Cure. **C.M. Hardy** ^{1,2}, D. Dive ², J.G. Leprince ^{1,2}, **L.D. Randolph***¹ (¹ Louvain Drug Research Institute, Uclouvain, Belgium; ² School of Dental Medicine and Stomatology, Uclouvain, Belgium)
65. Physico-Mechanical Properties of 3D-Printed Resin used as Temporary Crown/Bridge Restoration. **F.A.P. Rizzante***¹, T.L. Bueno ², G.M.F. Guimarães ², G.F. Moura ³, R. Roperto ¹, T.S. Porto ¹, F. Faddoul ¹, A.Y. Furuse ², G. Mendonça ³ (¹ Case Western Reserve University, School of Dental Medicine, USA; ² Bauru School of Dentistry, University of São Paulo, Brazil; ³ University of Michigan School of Dentistry, USA)
66. Effect of Chemical Catalysis on Hydrogen Peroxide Bleaching Efficacy. **C.R.G. Torres***, L. F. Cornelio, A.B. Borges (Institute of Science and Technology, Sao Paulo State University, Sao Jose Dos Campos, Brazil)
67. Physico-Chemical Properties and Cytocompatibility of 36 Commercially Available “Graphene” Materials. **V. Rosa*** ^{1,2,3}, R. Melhotra ¹ (¹ Faculty of Dentistry, National University of Singapore, Singapore; ² Department of Materials Science and Engineering, National University of Singapore, Singapore; ³ Centre for Advanced 2D Materials and Graphene Research Centre, National University of Singapore, Singapore)
68. Bulk-Fill Composites Based on an Elastomeric Methacrylate Monomer. M.G Rocha ^{1,2}, **J.F. Roulet***², Oliveira D.C.R.S ^{1,2}, Sinhoreti M.A.C. ¹, Correr A.B. ¹ (¹ Piracicaba Dental School, State University of Campinas, Brazil; ² College of Dentistry, University of Florida, USA)

- 69.** Monomer Combination's for Bulkfill Applications. L.D. Pereira ¹, M.P.C. Neto ¹, L.M. Cavalcante ^{1,2}, **L.F. Schneider*** (¹ Veiga De Almeida University, Brazil; ² Federal Fluminense University, Brazil)
- 70.** RCT Papers in Prosthesis - Compliance with Consort Guidelines – A SR N. Meckelburg, A. Reis, A. Loguercio, **M. Schroeder*** (Universidade Federal do Rio de Janeiro, Rio de Janeiro, Brazil)
- 71.** Interfacial Gap and Fracture Resistance of Indirect CAD-CAM Restorations. **N. Scotti***¹, E.A. Vergano ¹, A. Baldi ¹, G. Zoppetto ¹, R. Michelotto Tempesta ¹, M. Alovisei ¹, D. Pasqualini ¹, A. Comba ², E. Berutti ¹ (¹ University of Turin, Dental School Lingotto, Italy; ² University of Bologna, Dibinem, Italy)
- 72.** Bond Strengths of Universal Adhesives Achieved by Different Dentin-Etching Approaches. **M. Sebold***, C.B. André, M. Giannini (Piracicaba Dental School, University of Campinas, Piracicaba, Brazil)
- 73.** Effect of Surface Treatments on Bond of CAD/CAM Composite Block. L. Chen, **T. Sedlacek***, B.I. Suh (Bisco Inc, Schaumburg, USA)
- 74.** Control of Dynamic Material Property Development in Photopolymers Using Photochromism. **P.K. Shah** ^{1*}, J. W. Stansbury ^{1,2} (¹ Department of Chemical & Biological Engineering, University of Colorado Boulder, USA; ² Department of Craniofacial Biology, University of Colorado Anschutz Medical Campus, USA)
- 75.** Effect of Tooth-Brushing with Microcurrent on Dentinal Tubule Occlusion. **G. Kim, Y. Shin*** (Yonsei University, South Korea)
- 76.** Ultrasonic Activation of Different Solutions on Root Canal Dentin. **J.E. Soto-Sainz***¹, J.A. Espinoza-Rodriguez, C. Samano-Valencia ², A.R. Ayala-Ham ¹, G.Y. Castro-Salazar ¹, N.V. Zavala-Alonso ³, R. Ramos-Payan ¹, E.M. Aguilar-Medina ¹, E.L. Silva-Benitez ¹, J.G. Romero-Quintana ¹ (¹ Universidad Autónoma De Sinaloa, México; ² Benemérita Universidad Autónoma De Puebla, México; ³ Universidad Autónoma De San Luis Potosí, México)
- 77.** Resin Property Control Throughout Conversion Based on Nanogel Functionalization. **M. Barros***¹, J. Vigil ¹, J. Stansbury ^{1,2} (¹ University of Colorado School of Dental Medicine, USA; ² Chemical Engineering, University of Colorado Boulder, USA)
- 78.** Physicochemical Study of Biodentine™-Dentine Tissue Interphase. **J.L. Suárez-Franco***, B.I. Cerda-Cristerna, A. Suárez-Porras, R.E. Flores-Ventura, M. Trujillo-Hernández, R. Trueba-García (Facultad De Odontología, Universidad Veracruzana, Orizaba, México)
- 79.** Reinforcement of Dental Adhesives with Bio-Inspired Monomers. **C. Szczepanski***¹, C. Ligo ² (¹ Michigan State University, Michigan, USA; ² Northwestern University, Evanston, USA)
- 80.** Inhibitory Effects of Various Ions Released from Surface Active Fillers. I. Salim ¹, R. Seseogullari-Dirihan ¹, S. Imazato ², **A. Tezvergil-Mutluay***^{1,3} (¹ University of Turku, Finland; ² University of Osaka, Japan; ³ Turku University Hospital, Finland)
- 81.** Fracture Resistance of Short-Fiber Resin Composite Bilayers. **J. Tiu***, R. Belli, U. Lohbauer (University of Erlangen-Nuremberg, Erlangen, Germany)
- 82.** Dentin Changes Associated with Patient Age and Cavity Site. **A.T. Weerakoon***¹, I.A. Meyers ¹, S. Roy ², C. Cooper ³, T.R. Cox ⁴, N.D. Condon ⁵, C. Sexton ¹, D.H. Thomson ¹, P.J. Ford ¹, A.L. Symons ¹ (¹ School of Dentistry, University of Queensland, Queensland, Australia; ² University of Queensland Centre for Microscopy and Microanalysis, Queensland, Australia; ³ Queensland University of Technology, Queensland, Australia; ⁴ Faculty of Medicine, UNSW Sydney, Australia; ⁵ Institute for Molecular Biosciences, University of Queensland, Queensland, Australia)
- 83.** Structural and Mechanical Effects of Ionizing Radiation on Human Enamel. **M. Wendler***¹, G. Jerez ², I. Luque-Martinez ², M. Lopez ³, A. Bedran-Russo ⁴, M. Muñoz ² (¹ Faculty of Dentistry, University of Concepcion, Chile; ² Faculty of Dentistry, Universidad De Valparaíso, Chile; ³ Faculty of Engineering, University of Concepcion, Chile; ⁴ College of Dentistry, University of Illinois at Chicago, Chicago, USA)
- 84.** Endocrown Luting procedures: analysis of dual luting cements conversion rate. **S. Chirico***^{1,2}, A. Ionescu ¹, L. Breschi ², E. Brambilla ¹, M.M. Gagliani ¹ (¹ Department of Biomedical, Surgical and Dental Sciences, University of Milan, Italy; ² DIBINEM, University of Bologna, Italy)
- 85.** Stress relaxation via covalent dynamic bonds in nanogel containing resins. **G. Gao***, X. Han, N. Swan, X. Zhang, C. Bowman, J. Stansbury (Chemical and Biological Engineering, University of Colorado Boulder, USA)

Aims and Scope

The principal aim of *Dental Materials* is to promote rapid communication of scientific information between academia, industry, and the dental practitioner. Original manuscripts on clinical and laboratory research of basic and applied character which focus on the properties or performance of dental materials or the reaction of host tissues to materials are given priority for publication. Other acceptable topics include: application technology in clinical dentistry and dental laboratory technology. Comprehensive reviews and editorial commentaries on pertinent subjects will be considered. Only manuscripts that adhere to the highest scientific standards will be accepted.

The Academy's objectives are: (1) to provide a forum for the exchange of information on all aspects of dental materials; (2) to enhance communication between industry, researchers and practising dentists; and (3) to promote dental materials through its activities.

Annual meetings and scientific sessions are held in conjunction with other dental organizations. The Academy sponsors symposia and scientific programs in international meetings; recognizes scholarship at all levels from students to senior scholars; and elects Fellows in the Academy.

For a full and complete Guide for Authors, please go to <http://www.elsevier.com/locate/dema>

USA mailing notice: *Dental Materials* (ISSN 0109-5641) is published monthly by Elsevier Ltd. (The Boulevard, Langford Lane, Kidlington, Oxford OX5 1GB, UK). Periodicals postage paid at Jamaica, NY 11431 and additional mailing offices.

USA POSTMASTER: Send change of address to *Dental Materials*, Elsevier Customer Service Department, 3251 Riverport Lane, Maryland Heights, MO 63043, USA.

AIRFREIGHT AND MAILING in USA by Air Business Ltd., c/o Worldnet Shipping Inc., 156-15, 146th Avenue, 2nd Floor, Jamaica, NY 11434, USA.

Publication information: *Dental Materials* (ISSN 0109- 5641). For 2019, volume 35 is scheduled for publication. Subscription prices are available on request from the Publisher or from the Elsevier Customer Service Department nearest you or from this journal's website (<http://www.intl.elsevierhealth.com/journals/dema>). Further information is available on this journal and other Elsevier products through Elsevier's website: (<http://www.elsevier.com>). Subscriptions are accepted on a prepaid basis only and are entered on a calendar year basis. Issues are sent by standard mail (surface within Europe, air delivery outside Europe). Priority rates are available upon request. Claims for missing issues should be made within six months of the date of dispatch.

Advertising Information: Advertising orders and enquiries can be sent to: **USA, Canada and South America:** Elsevier Inc., 360 Park Avenue South, New York, NY 10010-1710, USA: phone: (+1) (212) 633 3974. **Europe and ROW:** Sarah Ellis, Advertising Sales Executive, Elsevier Ltd, 32 Jamestown Road, London NW1 7BY, UK. Phone: +44 (0) 207 424 4538; fax: +44 (0) 207 424 4433; e-mail: s.ellis@elsevier.com

Orders, claims, and journal enquiries: Please visit our Support Hub page <https://service.elsevier.com> for assistance.

Photocopying. Single photocopies of single articles may be made for personal use as allowed by national copyright laws. Permission of the Publisher and payment of a fee is required for all other photocopying, including multiple or systematic copying, copying for advertising or promotional purposes, resale, and all forms of document delivery. Special rates are available for educational institutions that wish to make photocopies for non-profit educational classroom use.

For information on how to seek permission visit www.elsevier.com/permissions or call: (+44) 1865 843830 (UK) / (+1) 215 239 3804 (USA).

Derivative Works. Subscribers may reproduce tables of contents or prepare lists of articles including abstracts for internal circulation within their institutions. Permission of the Publisher is required for resale or distribution outside the institution. Permission of the Publisher is required for all other derivative works, including compilations and translations (please consult www.elsevier.com/permissions).

Electronic Storage or Usage. Permission of the Publisher is required to store or use electronically any material contained in this journal, including any article or part of an article (please consult www.elsevier.com/permissions). Except as outlined above, no part of this publication may be reproduced, stored in a retrieval system or transmitted in any form or by any means, electronic, mechanical, photocopying, recording or otherwise, without prior written permission of the Publisher.

Notice. No responsibility is assumed by the Publisher for any injury and/or damage to persons or property as a matter of products liability, negligence or otherwise, or from any use or operation of any methods, products, instructions or ideas contained in the material herein. Because of rapid advances in the medical sciences, in particular, independent verification of diagnoses and drug dosages should be made.

Although all advertising material is expected to conform to ethical (medical) standards, inclusion in this publication does not constitute a guarantee or endorsement of the quality or value of such product or of the claims made of it by its manufacturer.

Author inquiries: You can track your submitted article at <http://www.elsevier.com/track-submission>. You can track your accepted article at <http://www.elsevier.com/trackarticle>. You are also welcome to contact Customer Support via <http://support.elsevier.com>

Funding body agreements and policies

Elsevier has established agreements and developed policies to allow authors whose articles appear in journals published by Elsevier, to comply with potential manuscript archiving requirements as specified as conditions of their grant awards. To learn more about existing agreements and policies please visit <http://www.elsevier.com/fundingbodies>

Illustration services

Elsevier's WebShop (<http://webshop.elsevier.com/illustrationservices>) offers Illustration Services to authors preparing to submit a manuscript but concerned about the quality of the images accompanying their article. Elsevier's expert illustrators can produce scientific, technical and medical-style images, as well as a full range of charts, tables and graphs. Image 'polishing' is also available, where our illustrators take your image(s) and improve them to a professional standard. Please visit the website to find out more.

For a full and complete Guide for Authors, please go to: <http://www.elsevier.com/locate/dental>

Ⓢ The paper used in this publication meets the requirements of ANSI/NISO Z39.48-1992 (Permanence of Paper)

The item fee code for this publication is 0109-6641/ \$36.00

Printed by Henry Ling Ltd, The Dorset Press, Dorchester, UK.

Available online at www.sciencedirect.com

ScienceDirect

journal homepage: www.intl.elsevierhealth.com/journals/dema

Abstracts of the Academy of Dental Materials Annual Meeting, 3–5 October 2019 – Jackson Hole, USA

1

Chemical characterization of clay material and effects on gingival healing

B. Akon-Laba^{1,*}, B. Doukouré², Gt. Maroua¹, Ap. Aké³

¹ Département de Biologie et Matières Fondamentales, Ufr Odonto-Stomatologie

² Laboratoire D'Anatomie-Pathologie, Ufr Sciences Médicales

³ Laboratoire de Chimie des Matériaux (Université Félix Houphouët Boigny, Abidjan, Côte D'Ivoire)



Purpose/Aim: The objective of this study was to determine the chemical and mineralogical characteristics of green clay, in order to determine its healing properties on the gum.

Materials and Methods: Our study focused on green clay from the Anyama region in the south of the Ivory Coast. X-ray diffractometry and fluorescence spectrometry were used for mineralogical and chemical characterization. The mineral structure was observed by scanning electron microscopy (SEM). After application of clay to gingival wounds in wistar rats, an anatomo-pathological study was performed at D0, D3, D7 and D14.

Results: The results showed that the green clay in our study is an alumina silicate, polycrystalline with a predominance of hexagonal crystals (Fig. 1). Our green clay includes chlorite, illite, smectite, quartz and rutile with a predominance of chlorite and illite. From the 3rd day, an early healing is observed in rats treated with clay, which is not the case with untreated rats. In these untreated rats, healing began on day 7.

Conclusions: The chemical characterization of Anyama's green clay showed a complex material with a fine grain size and a neutral pH, with a predominance of chlorite and illite. These characteristics have promoted rapid healing of the gum wound.

<https://doi.org/10.1016/j.dental.2019.08.002>

2

Influence of dentin biomodification on bond strength and MMP activity

M.A. Ferretti^{1,*}, K. Rischka², G.F. Abuna¹, M.C.A.J. Mainardi¹, F.H.B. Aguiar¹

¹ Piracicaba Dental School, University of Campinas, Brazil

² Fraunhofer Institute Ifam Bremen, Germany



Purpose/aim: This study aimed to evaluate composite restoration microtensile bond strength to dentin, after dentin surface treatment with natural biomodifiers: DOPA, dopamine, and phytic acid.

Materials and methods: Sixty dentin blocks from human third molars were randomly divided into 6 groups ($n=10$): AFosf-Phosphoric acid etched dentin; AF-phytic acid etched dentin; AFosf+DOPA- etched dentin with phosphoric acid and DOPA treatment; AFosf+ Dopamina- etched dentin with phosphoric acid and dopamine treatment; AF + DOPA- etched dentin with phytic acid and DOPA treatment; AF + Dopamina- etched dentin with phytic acid and dopamine. Silicon carbide paper was used to remove the occlusal portion of the specimens, and each group received its corresponding treatment. All specimens were restored with a 4-mm high microhybrid composite block, and each resin increment was light-cured

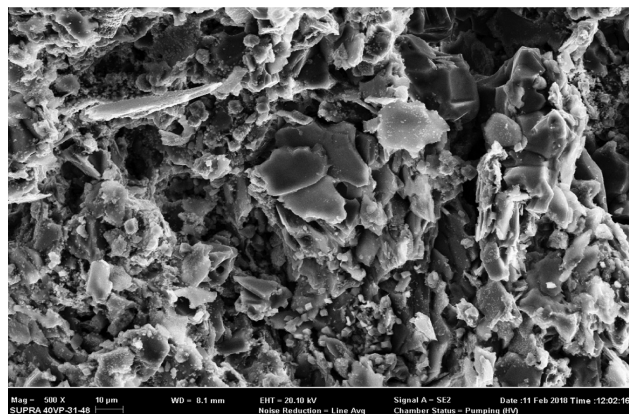


Figure 1 – SEM photomicrograph showing Morphology of clay platelets.

separately for 20 s. Then, stick-shaped specimens were obtained for the microtensile bond strength test. The fractured specimens were evaluated regarding failure mode by scanning electron microscopy (SEM). Three 1 mm-thick slices were obtained from the same specimens above mentioned in order to perform in situ zymography by confocal laser scanning microscopy (CLSM) 7 days after restoration. Bond strength data were evaluated by the Tukey-Kramer test ($\alpha=0.05$), and the chi-square test was used for failure mode analysis. For in situ zymography, a descriptive analysis was carried out, describing and comparing the structures observed among groups.

Results: AFosf and AF groups presented significantly higher mean bond strength (BS) values than all the other groups at 24 hours (Table 1). The groups in which DOPA was used as a surface biomodifier showed lower BS compared to dopamine, regardless of the acid used. The groups with phosphoric acid showed significantly higher BS than the groups in which phytic acid was used, regardless of the type of treatment. The AFosf group presented higher fluorescence in the hybrid layer than all the other groups. Among the groups without treatment, AF presented lower fluorescence than the AFosf. When biomodifiers were associated with phosphoric acid-etching, they led to lower fluorescence in the hybrid layer. The AF + DOPA and AF + dopamine groups presented lower fluorescence than the AF group.

Table 1 – Mean (standard deviation) dentin bond strength (in MPa) according to surface treatment and acid conditioner.

Surface Treatment	Phosphoric Acid	Phytic Acid
No Treatment	67.84 (17.76) Aa	57.70 (22.16) Ba
DOPA	21.03 (11.43) Ac	13.09 (6.04) Bc
Dopamine	44.18 (15.30) Ab	36.74 (19.41) Bb

Means followed by the same letters did not differ statistically ($p > 0.05$). Uppercase letters compare different acid conditioners for the same surface treatment (rows), while lowercase letters compare different surface treatments for the same acid conditioner (columns).

Conclusions: The biomodifiers used in this study were able to inhibit MMPs activity after 7 days of storage, but did not result in any increase in microtensile bond strength.

<https://doi.org/10.1016/j.dental.2019.08.003>

3

Two-body wear of glass-ceramics after sliding fatigue using three-dimensional inspection

L.M.M. Alves^{1,*}, A.M.O. Dal Piva¹,
J.P.M. Tribst¹, T.J.A. Paes-Junior¹,
A.L.S. Borges¹, M.A. Bottino¹, Y. Zhang²,
R.M. Melo¹

¹ Sao Paulo State University (Unesp), Department of Dental Materials and Prosthodontics, Sao Jose Dos Campos, Br

² New York University, Department of Biomaterials and Biomimetics, USA

Purpose/aim: Zirconia lithium silicate is a glass-ceramic possessing crystal different from lithium disilicate despite

being indicated for the same clinical applications. Are both of these materials capable of maintaining their integrity after “two-body wear” with sliding contact fatigue test? The aim was to investigate the three-dimensional wear and volumetric loss after sliding contact fatigue of two glass-ceramic materials against steatite.

Materials and methods: Lithium disilicate (LD, e.max CAD, Ivoclar) and Zirconia reinforced lithium silicate (ZLS, Vita Suprinity, Vita Zahnfabrik) discs ($n=20/\text{gr}$) were made and scanned to obtain a baseline stereolithography (STL) file for each sample. All discs were subjected to sliding contact fatigue (30 N, 300,000 cycles at 1.7 Hz, horizontal movement of 6 mm) using a steatite antagonist, in water. The samples were then scanned again and the volume loss was measured by overlapping the final scan with its respective baseline scan using 3D digital parametric inspection software (GOM Inspect, Braunschweig, Germany). The roughness was measured with a contact profilometer in Ra and Rz parameters. The ceramic volume loss (mm^3), wear crater depth (in micrometers) and roughness were analyzed by descriptive statistics and One-way analysis of variance (ANOVA) ($\alpha = 0.5\%$).

Results: One-way ANOVA showed statistically significant differences among the groups. Considering the ceramic volume loss (mm^3) and wear crater depth (μm), LD (-4.41 ± 1.11 ; $0.80 \pm 0.06 \mu\text{m}$) showed higher mean values than ZLS (-3.13 ± 0.90 ; $0.56 \pm 0.09 \mu\text{m}$). For the roughness analysis, only Rz was significantly different with higher values for LD (3.08 ± 1.02) than ZLS (1.51 ± 0.90). All discs exhibited surface scratches in the same direction of sliding with chipping, while large cracks were observed on wear tracks. These areas could be identified in blue by the overlapping of the STL files before and after wear in the inspection software. The linear reduction generated by sliding contact showed a sagittal graph with a similar wear pattern to SEM cross section.

Conclusions: Zirconia reinforced lithium silicate was more resistant to wear under sliding contact fatigue than lithium disilicate, with less volume loss and shallower surface wear craters.

<https://doi.org/10.1016/j.dental.2019.08.004>

4

Curing protocols' effect on micro-flexural strength using different light-curing units

A.O. Al-Zain^{1,*}, J.A. Platt²

¹ Faculty of Dentistry, King Abdulaziz University, Jeddah, Kingdom of Saudi Arabia

² Indiana University School of Dentistry, Indiana University Purdue University Indianapolis, USA

Purpose/aim: To investigate the influence of curing distance on μ -flexural strength of a resin composite when cured using the manufacturer curing time (MCT) compared to using a consistent radiant exposure (CRE) with three different light-curing units.

Materials and methods: Rectangular specimens were prepared using a dual photoinitiator system nano-hybrid composite (Tetric EvoCeram Bleaching shade XL, Ivoclar Vivadent). Specimens were divided into two curing protocol



groups; cured using the MCT and using a CRE. Curing times, irradiance and RE were measured using a Managing Accurate Resin Curing-Resin Calibrator (MARC-RC) spectrometer. Specimens were cured using three different light-curing-units (LCUs); a quartz-tungsten-halogen (QTH), a single emission peak light-emitting-diode (LED) (SLED), and a multiple emission peak LED (MLED) ($n=10$ /curing protocol/distance/LCU). Specimens were cured at 0–2–or 8–mm distances and the irradiance and RE passing through the specimen were collected in real-time from the bottom MARC-RC sensor. Specimens were finished and stored wet at 37 °C for 24 h. The μ -flexural strength test was performed using a universal testing machine at a crosshead speed of 1 mm/min. Data were analyzed using two-way analysis of variance followed by Tukey multiple comparison post-hoc test ($\alpha=0.05$).

Results: The mean irradiance received on the bottom surface at different distances ranged from 32.3–55.9 (QTH), 25.4–99.7 (SLED), and 27.9–72.5 mW/cm² (MLED). The mean RE at the different distances ranged from 0.7–1.1 (QTH), 0.3–1 (SLED), and 0.3–0.7 J/cm² (MLED). Irradiance and RE received on the bottom sensor significantly decreased compared to the top. The μ -flexural strength ranged from 422.1–516.6 MPa (MCT), and from 440.4–490.4 MPa (CRE). The μ -flexural strength significantly decreased when specimens were cured using a CRE at 2–mm distance with the QTH or cured using the MCT at 2–and 8–mm distances with the SLED. For the MLED, μ -flexural strength was significantly lower at 8–mm than 0–mm.

Conclusions: When using a CRE instead of the MCT, the μ -flexural strength was significantly reduced when curing at 2–mm with a QTH but increased at 2–and 8–mm with a SLED. In addition, for the MLED, curing at an 8–mm distance with the MCT significantly reduced μ -flexural strength.

<https://doi.org/10.1016/j.dental.2019.08.005>

5

Bone Regeneration with Extracellular Matrix Hydrogels from Porcine-Bladder and Bovine-Bone



A.R. Ayala-Ham*, J.A. López-Gutierrez,
G. Jiménez Gastélum, G.Y. Castro-Salazar,
J.G. Romero-Quintana, E.L. Silva-Benitez,
J.E. Soto-Sainz, E.M. Aguilar-Medina,
J. Sarmiento-Sanchez, R. Ramos-Payan

Autonomous University of Sinaloa, Culiacán,
Sinaloa, México

Purpose/Aim: The loss of bone tissue is a frequent problem worldwide, as result of illnesses or injuries, and is necessary to place synthetic or biological substitutes to restore it. However, no substitute has fulfilled the function and quality expected to achieve an efficient regeneration. Due to this problem, tissue engineering has a main objective the regeneration or replacement of tissues or organs through 3D constructions linked to biomolecules. Currently it has been reported that biomaterials in hydrogel have a consistency more similar to the natural tissue, allowing a better cell colonization and therefore a faster and more efficient regeneration. Within

these hydrogels the most recent analyzed are the extracellular matrix of urinary porcine bladder (hUBM) and demineralized bone matrix (hDBM), in addition to some synthetic or natural substitutes such as hydroxyapatite (HP). Therefore, the aim of this study was to evaluate the in vivo bone regeneration using hUBM, hUBM+HP and hDBM for future clinical trials.

Materials and Methods: A critical defect (8 mm) was made in the calvaria of 16 male Wistar adult rats using a dental trephine, in the following groups: porcine bladder hydrogel (hUBM) ($n=4$), hydrogel of porcine bladder plus hydroxyapatite (hUBM+HP) ($n=4$) and bone matrix hydrogel (hDBM) ($n=4$), positive control ($n=2$) granulated autograft was placed and negative control without placement of material ($n=2$). After 4 and 6 months rats were sacrificed and regeneration was evaluated macroscopically and histologically with H & E staining and alizarin red.

Results: The hUBM induced a vascularized and innervated connective tissue, with the presence of abundant fibroblasts. The hUBM+HP showed a hard consistency with soft tissue gaps, corresponding to areas of bone tissue formation, presence of osteoblast and osteocytes. The hDBM showed a hard consistency in the whole new tissue, with the presence of osteocytes and formation of bone tissue. The positive control showed irregular hard consistency and formation of irregular bone tissue. The negative control showed soft tissue, without mineralization.

Conclusions: The hUBM promotes angiogenesis and connective tissue formation in Wistar rats, without formation of mineralized tissue. Hydroxyapatite as an adjuvant of hUBM partially stimulates connective tissue mineralization. The hDBM achieved biomineralization and efficient regeneration. The hydrogel allowed a fast and better cellular colonization.

<https://doi.org/10.1016/j.dental.2019.08.006>

6

Dynamic heat profile generated on pulpal-wall by various curing lights



F. Baabdullah*, E. Kilinc, C. Garcia-Godoy,
S.A. Antonson

Nova Southeastern University, USA

Purpose/aim: Thermal damage to dental pulp is one of the factors to consider during restorative procedures. One of the potential thermal damage sources is the light curing units (LCUs) during resin-based composite (RBC) application. Kinetic energy is produced during the polymerization process to convert resin monomers to polymers. Heat is the by-product of this energy, transmitted from the LCUs through the RBC to dentin and pulp. This may lead to an adverse inflammatory effect on the pulp tissue. Polywave LCUs have been introduced to convert broad spectrum photo initiators in opposed to monowave. However, their thermal effect has not been studied in the literature. The aim was to evaluate the difference in heat generation profile between polywave and monowave LCUs at the pulpal wall (PW) when using bulk-fill RBC.

Materials and methods: Single sound extracted human molar was utilized to measure the heat generation from LCUs through the RBCs and dentin to the PW. Tooth was prepared to have an access window on the lingual aspect to visualize the buccal PW. On the buccal aspect, a 3x3x3 mm box was prepared leaving a 1 mm of remaining dentin thickness. Two groups of LCUs, one polywave (Valo[®], Ultradent), with average irradiance of 1,216 mW/cm², and one monowave (DemiTM Ultra, Kerr), with average irradiance of 1,392 mW/cm², were used with a bulk-fill RBC (Tetric EvoCeram[®] Bulk-Fill, Ivoclar Vivadent) without bonding agent. Temperatures on the PW and RBC during the full curing cycle of 20 s were recorded simultaneously utilizing thermal infrared camera (Thermovision-A320; FLIR Systems) and minimal-energy-loss mirror (λ/4 First Surface Mirror, NT99-456; Edmund Industrial Optics). The whole process was recorded for 90 s. RBC was removed and tooth was cleaned after each application. A total of 10 measurements were conducted for each LCU group. General linear model was employed to measure temperature increase above 5.5 °C as a function of time to reach to maximum temperature, duration above 5.5 °C, and LCU.

Results: Monowave LCU ($M=10.04^{\circ}\text{C}$, $SD=0.43$) had significantly lower temperature change (Fig. 1) on the PW than polywave LCU ($M=13.1^{\circ}\text{C}$, $SD=0.54$), $t(14.7)=14.39$, $p<0.001$. In addition, monowave LCU ($M=30.0\text{s}$, $SD=19.8$) had significantly lower duration for temperature above 5.5 °C than polywave LCU ($M=37.4\text{s}$, $SD=2.07$), $t(14.7)=9.69$, $p<0.001$. There was no difference in time to reach maximum temperature between monowave LCU ($M=19.8\text{s}$, $SD=0.42$) and polywave LCU ($M=20.0\text{s}$, $SD=0.47$), $t(17.78)=1$, $p=0.330$.

Conclusions: Polywave LCU induces higher temperature rise to PW compared to monowave LCU. However, results may vary for shorter duration of polymerization that is indicated for this RBC.

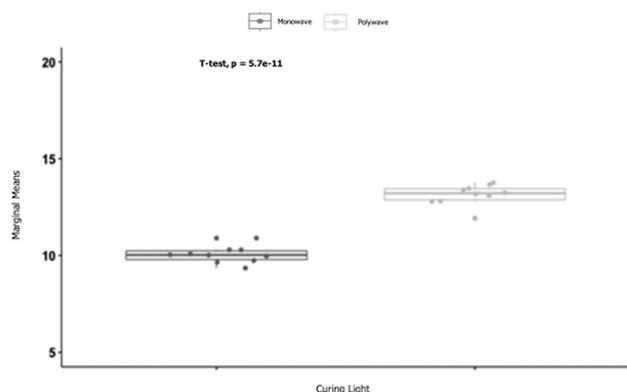


Fig. 1

<https://doi.org/10.1016/j.dental.2019.08.007>

7

Anti-Biofilm and Mechanically Stable Bioactive Composite for Root Caries Restorations



A.A. Balhaddad^{1,2,*}, M. Ibrahim^{1,2},
M.D. Weir¹, H.H.K. Xu¹, M.A.S. Melo¹

¹ University of Maryland Dental School, Baltimore, USA

² College of Dentistry, Imam Abdulrahman Bin Faisal University, Dammam, Saudi Arabia

Purpose/aim: The most significant driver of root caries process is biofilm formation over the surface of root dentin and dental materials. Based on dimethylaminohexadecyl methacrylate (DMAHDM) and nano-sized amorphous calcium phosphate (NACP), the design of bioactive composite for root caries restorations entails a high anti-biofilm performance to overcome the in vivo challenge of recurrent caries, especially at the cervical areas. However, the incorporation and increasing the content of bioactive agents may impart poor mechanical stability limiting the application of such promising materials. Towards this problem, we aimed to: (1) develop and optimize the proportion of composite formulations, meant for class V restorations, containing both DMAHDM and NACP at their maximum content; (2) maximize the anti-biofilm action of these formulations by increasing the DMAHDM concentration; and (3) access the effect of the dual DMAHDM/NACP composite formulations on the mechanical properties and surface roughness (Ra).

Materials and methods: NACP was synthesized by atomizing/spraying of a Ca/P suspension. DMAHDM was synthesized via a modified Menshutkin reaction method. A factorial design of experiments was applied to develop five formulations. The effect of 20 % NACP in two levels (presence/absence) and DMAHDM concentration in three levels (0, 3 and 5 wt%), as independent variables, were evaluated. The impact of these variables on human saliva microcosm biofilm response was evaluated by surface charge density, Live/dead assay, metabolic activity (MTT), colony-forming unit counts (CFU), and lactic acid (LA) production, as dependent variables. Mechanical properties and Ra were measured via three-point flexure and profilometry, respectively.

Results: Increasing the DMAHDM concentration affects the overall biofilm response with and without the NACP fillers. The design revealed a positive correlation between DMAHDM concentration and surface charge with increasing detrimental effect on biofilm viability. All the investigated formulations revealed higher antibacterial properties, and the greatest antibacterial action was observed with 5 %DMAHDM–20 %NACP. 5 %DMAHDM–20 %NACP reduced the metabolic activities and LA production by 90% and 99%, respectively ($p<0.01$). 5 %DMAHDM–20 %NACP also reduced the growth of total microorganisms, total streptococci, Mutans Streptococci, and Lactobacilli by 4–5 log compared to control, and 2–3 log compared to 3 %DMAHDM–20 %NACP group. Biofilms on 5 %DMAHDM–20 %NACP composites had noticeably more compromised bacteria compared to the other

groups. Mechanical properties and Ra were not detrimentally affected by 5 % DMAHDM and 20 %NACP.

Conclusions: The hybrid DMAHDM/NACP composite showed acceptable mechanical properties, strong positive surface charge, and high bacterial reduction. DMAHDM-NACP composites are promising to inhibit the bacterial invasion at the restoration margins, thereby inhibiting root caries.

<https://doi.org/10.1016/j.dental.2019.08.008>

8

Dentin Matrix Stability and Gelatinolytic Activity with a Polyphenol-Enriched Extract



E.C. Bridi¹, R.T. Basting¹, F.M.G. França¹, C.P. Turssi¹, F.L.B. Amaral¹, M.A. Foglio², R.T. Basting^{1,*}

¹ Dental School and Research Institute São Leopoldo Mandic, Brazil

² University of Campinas, Brazil

Purpose/Aim: The objective of this study was to investigate the immediate effect of dentin pretreatment with a polyphenol-enriched extract of *Arrabidaea chica* (Ac) on dentin matrix stability (DMS) and on gelatinolytic activity, using a total-etch adhesive system (Adper Scotchbond Multipurpose/ 3 M ESPE/SB).

Materials and Methods: Specimens were assigned to six groups to determine DMS: control groups [water (W) and ethanol (E)], 1%, 2.5% or 5% Ac in aqueous solution, and 2.5% Ac in ethanolic solution. Apparent modulus of elasticity (ME) and dentin matrix mass loss were determined following treatments for 1 hour. Dentin-resin interfaces were prepared according to groups: SB; W (dentin pretreatment with water + SB); ACSB (dentin pretreatment with 2.5% AC aqueous solution + SB); ACA (AC incorporated into the phosphoric acid of SB); ACP (AC incorporated into the primer of SB). After 24 hours, the dentin-interface was assessed under fluorescence microscopy to perform in situ zymography tests on different layers (hybrid layer, underlying dentin and dentin).

Results: The mixed model method for repeated measures showed an increase in ME after the treatments ($p=0.0380$). There were no significant differences among the treatments regarding ME ($p=0.9320$). Kruskal-Wallis showed mass gain for the groups treated with Ac (1%, 2.5% and 5%) in aqueous solution, and mass loss for the other groups, with significant differences among the groups ($p<0.0001$). Enzymatic activity showed no differences among the groups ($p=0.6710$), although the hybrid layer presented mean values lower than those for the underlying dentin and the dentin layers ($p<0.0001$) (ANOVA and Tukey tests).

Conclusions: AC in aqueous or ethanolic solutions for dentin pretreatment did not influence ME, although Ac in aqueous solutions at different concentrations provided a mass gain for dentin slabs. Ac did not reduce enzymatic activity when applied as a dentin pretreatment or incorporated into the primer of the SB after treatment.

<https://doi.org/10.1016/j.dental.2019.08.009>

9

Wear Behavior of Translucent Zirconia after Chewing Simulation



M. Borba^{1,*}, Y. Zhang², T. Okamoto², M. Zou², M.R. Kaizer³

¹ University of Passo Fundo, Brazil

² New York University, USA

³ Positivo University, Brazil

Purpose/Aim: To evaluate the volume loss and sub-surface damage of a translucent zirconia subjected to a mouth-motion simulation.

Materials and Methods: A translucent 5 mol.% yttria-partially-stabilized-zirconia (5Y-PSZ, Zpex Smile, Tosoh Corporation) and a control 3 mol.% yttria-partially-stabilized tetragonal zirconia (3Y-PSZ, Zpex, Tosoh Corporation) were evaluated. Twenty zirconia discs (1.2 mm thickness and 13.9 mm diameter) were produced for each material by cutting pre-sintered CAD-CAM blocks, sintering and polishing to a 1 μ m finish. Discs were adhesively bonded onto a dentin analogue substrate (G10) with a resin cement (Panavia F 2.0, Kuraray). Specimens were subjected to a sliding-contact mouth-motion fatigue test. The test was performed using an electrodynamic fatigue testing machine, in distilled water, with 2 Hz frequency. A 200 N off-axis (30°) load was applied to the center of the ceramic disc through a zirconia spherical antagonist ($r=3.15$ mm) for five different lifetimes ($n=4$): 100; 1,000; 10,000; 100,000; 1,000,000 cycles. After the mouth-motion simulation, the ceramic surface was scanned using a 3D Laser Scanner and images were analyzed with an image processing software in order to measure the volume loss (mm³). Data were analyzed with two-way ANOVA and Tukey tests ($\alpha=0.05$). SEM was used to characterize the surface and sub-surface damage.

Results: There was statistical significance for the 2 factors examined: material ($p<0.001$) and number of cycles ($p<0.001$), and for the interaction between factors ($p<0.001$). For 100 and 1,000 cycles, the volume loss was similar among materials. For lifetimes above 10,000 cycles, 5Y-PSZ showed higher volume loss than 3Y-PSZ. Additionally, for 5Y-PSZ, the volume loss increased over time, while for 3Y-PSZ the number of cycles had no significant effect. The surface and sub-surface analysis of 5Y-PSZ subjected to the mouth-motion simulation revealed a larger density of cracks, leading to the dislodgement of zirconia grains and thus a rougher surface than 3Y-PSZ.

Conclusions: The mouth-motion simulation induces higher wear and damage to the translucent 5Y-PSZ zirconia relative to 3Y-PSZ.

Acknowledgments: Funding was provided by NIH/NIDCR (Grant Nos. R01DE026772 and R01DE026279).

<https://doi.org/10.1016/j.dental.2019.08.010>

10

Adhesives containing calcium phosphate: bond strength, micro-permeability and collagen degradation

M.D.S. Chiari¹, Y. Alania²,
A.K. Bedran-Russo², R.R. Braga^{1,*}

¹ University of São Paulo, São Paulo, Brazil

² University of Illinois, Chicago, USA



Purpose/aim: Calcium and phosphate ions released by calcium silicates or bioactive glass particles were shown to reduce host enzyme-mediated collagen degradation. The purpose of this study was to evaluate the effect of dicalcium phosphate dihydrate (DCPD) or mineral trioxide aggregate particles (MTA) on microtensile bond strength (μ TBS), micro-permeability and enzymatic activity at the dentin–adhesive interface of experimental dental adhesives.

Materials and methods: Four experimental dental adhesives containing the same matrix (41.25 wt% BisGMA, 12 wt% TEGDMA, 6 wt% HEMA, 40 wt% EtOH, 0.15 wt% of camphorquinone and 0.6 wt% EDMAB) with prepared with 10 wt% of DCPD particles (functionalized with DEGDMA or citric acid/CA) or MTA. An unfilled adhesive was used as control. After acid etching, the adhesives were applied on flat occlusal dentin surfaces of human molars and received a 3-mm thick layer of Filtek Supreme Ultra (3M ESPE, MN, USA). The μ TBS and micro-permeability were determined with beam-size specimens ($0.8 \times 0.8 \text{ mm}^2$) sectioned from restored teeth ($n=7$). The μ TBS after storage for 24 h or 2 months in artificial saliva at 37 °C ($n=5$) on a microtensile testing machine (Bisco Inc., IL, USA). Six specimens (half stored 24 h and half stored 2 months in AS/37 °C) had the adhesive–dentin interface polished and infiltrated with Rhodamine B solution for micro-permeability assessment. Gelatinolytic activity at the adhesive interfaces was assessed by in situ zymography at 24 h and 2 m in AS/37 °C) using quenched fluorescein-conjugated gelatin as MMPs substrate. The substrate hydrolysis was assessed with fluorescence microscopy. μ TBS data were analyzed by ANOVA/Games–Howell test. Data from micropermeability and in situ zymography were analyzed by Kruskal–Wallis/Mann–Whitney test ($\alpha=5\%$).

Results: Statistically significant differences in the μ TBS was found among adhesives (control = MTA > citric acid > DEGDMA, $p < 0.001$), but not effect of storage time/. Micro-permeability and in situ zymography results are shown in the Table. For micro-permeability/24 h, the control group showed the lowest permeability. Except for CA group, no significant differences were shown the micro-permeability over time. For in situ zymography/24 h, only DEGDMA group presented statistically lower RFU than the control ($p < 0.01$). After storage, all groups presented significant reductions in RFU values.

Conclusions: DCPD particles reduced μ TBS compared to the control. The storage period did not affect the μ TBS. Micro-permeability did not change upon storage, except for CA. The presence of particles in the adhesive reduced gelatinolytic activity at 24 h (FAPESP 2018/02403-9).

Groups	Micro-permeability (% of area stained with Rhodamine B)		In situ zymography (RFU)	
	24 hours	2 months	24 hours	2 months
Unfilled	0.7 Ac (0.2)	0.7 Ab (0.3)	9.6 Aa (3.7)	3.0 Ba (1.28)
DEGDMA_DCPD	1.5 Aa (0.8)	1.4 Aa (0.7)	5.5 Ab (3.9)	1.6 Bab (1.1)
Citric Acid_DCPD	1.0 Ab (0.4)	1.3 Ba (0.4)	5.9 Aab (2.3)	1.9 Bab (1.3)
MTA	1.3 Ab (1.0)	1.2 Aa (0.6)	5.9 Aab (3.4)	1.5 Bb (1.0)

<https://doi.org/10.1016/j.dental.2019.08.011>

11

Comparative research of bacteria gram-negative and positive on ti-30ta alloy



P. Capellato^{1,*}, D. Sachs¹, A.P.R.A. Claro²,
G. Silva¹, C.A.C. Zavaglia³

¹ University of Itajuba, Br

² University Estadual Paulista, Br

³ State Uni. of Campinas

Purpose/aim: The aim of this study was comparative research of response to bacteria Gram-negative and Gram-positive on Ti-30Ta alloy and Ti cp for dental implant application. Nowadays, the most used way to replace teeth lost is a dental implant. The common material used in dentistry is Titanium due to the high strength, durability, and biocompatibility. However, the elastic modulus of Ti Cp is 105 GPa and the bone around 15–25 GPa its results in a stress shielding problem. Titanium with 30% tantalum results to alloy with an elastic modulus at 45 GPa. It is near to the spot bone. Studies have been shown the most failure of implantation is caused by infections. Staphylococcus aureus (S. aureus) and Escherichia coli are the most frequent bacterial strains found on the sources of infections. Thus, we investigated two gram-positive (S aureus and S. epidermidis) and gram-negative bacteria (Escherichia coli and P. aeruginosa) on Ti cp and Ti-30Ta alloy surface. So, the ideal material to dental implant must have properties to prevent and reduce bacterial-associated implant failure.

Materials and methods: The Ti-30Ta alloy was fabricated by mixing Ti cp and Tantalum. S. aureus, S. epidermidis, Escherichia coli and P. aeruginosa were selected to investigate the antimicrobial activity. The number of colony-forming units per milliliter (CFU/mL) was determined and analyzed statistically (ANOVA, Tukey test, $p < 0.05$). Characterization techniques such as scanning electron microscopy (SEM) were used in order to investigate the surface of samples.

Results: The results demonstrate the influence of Ti-30Ta alloy surface on bacterial adhesion on gram-positive strains. Significant statistical differences for bacterial adhesion of S epidermidis ($p < 0.05$) and S aureus ($p < 0.001$) were observed Ti-30Ta surface compared to Ti cp [Figure 1]. SEM images show Ti-30Ta alloy surface after the biofilms have been grown by incubated at 37 °C for 48 h. The surface of Ti-30Ta decreases bacterial adhesion of S epidermidis and S aureus. Gram-positive bacteria showed a decrease of adhesion because of the cell walls thicker and harder, absence of

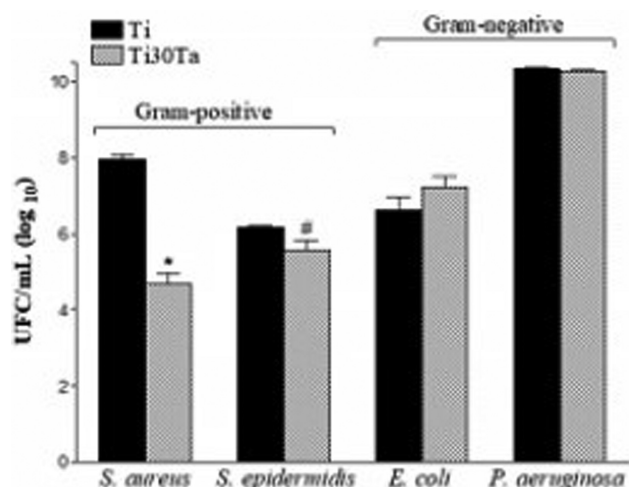


Figure 1

outer membrane and presence of proteins, lipids and teichoic acid.

Conclusions: The novel Ti-30Ta alloy has an influence on Gram-positive bacterial adhesion as you can see the number of colony-forming units per millimeter has been decreasing. Thus, Ti-30Ta alloy can be promising in the dental implant field because of the potential to prevent implant infection and the elastic modulus near to the bone.

<https://doi.org/10.1016/j.dental.2019.08.012>

12

Proanthocyanidin Gel on Acquired Pellicle Enamel at Initial Erosion

F. Cardoso*, A.P. Boteon, G.G. Dallavilla,
D. Rios, H.M. Honório

University of São Paulo, Bauru, Brazil



Purpose/Aim: Due to the high prevalence of dental erosion found in recent years, it's necessary to search for preventive therapies for this alteration. Proanthocyanidin is an agent currently studied because of its properties, which include, among others, remineralization, reduction of demineralization and biomodification of dentin. Thus, it may be a new alternative to prevent enamel erosion and / or potentiate natural protective factors, such as acquired pellicle. Therefore, the objective of this study was to evaluate the effect of Proanthocyanidin on the acquired enamel pellicle in the initial erosion.

Materials and Methods: The acquired pellicle was formed in situ by the use of intraoral palatal device by two volunteers for 2h. The enamel blocks of each study group (n=16) were treated in vitro according to the following groups: G1- Proanthocyanidin Gel at 6.5% + acquired pellicle formed in situ; G2- Proanthocyanidin Gel only at 6.5%; G3- Acquired pellicle only formed in situ. The gels were applied for 1 min. Then the enamel blocks were immersed in citric acid to promote a short erosive challenge. The response variable used was surface hardness (percentage of hardness loss).

Results: Data were analyzed by the Kruskal-Wallis test followed by the Dunn's test ($p < 0.05$). Data [Median (25% – 75%)] showed that G1 [7.70a (4.72 – 10.35)] had lower values of hardness loss presenting statistical difference when compared to G2 [17.67b (10.75 – 23.36)] and G3 [19.09b (11.10 – 21.11)]. G2 and G3 presented higher values of hardness loss, but with no statistical difference between them.

Conclusions: Therefore, this study suggests that 6.5% Proanthocyanidin Gel + acquired pellicle may be a good strategy to reduce the progression of enamel wear submitted to erosion.

<https://doi.org/10.1016/j.dental.2019.08.013>

13

Azobenzene Hydrogels as Stimuli-Responsive, Antibacterial Oral Drug Delivery Networks



C. Carpenter^{1,*}, G.M. Kehe², D. Nair²,
M. Schurr²

¹ Metropolitan State University, Denver, USA

² University of Colorado, Aurora, USA

Purpose/aim: The aim of this study is to evaluate azobenzene hydrogels as stimuli-responsive, antibacterial networks for oral drug delivery.

Materials and methods: Soft hydrogels discs (370 μ m height x 6.55 mm diameter) were fabricated using a polymer formulation of (Hydroxyethyl)methacrylate (HEMA) with Ebecryl 230 ($M_w = 5,000$ g/mol) as a crosslinker and characterized. Acrylated/Methacrylated azobenzenes including concentrations of AZO-acrylate and Bis-AZO (Disperse Yellow 7 methacrylate) were incorporated either as a coating or within the bulk of the network and polymerized with a thermal initiator (AIBN, 80 °C for 4 hours). Once cured, the soft materials are seeded with *Pseudomonas aeruginosa* in a brain-heart infusion (BHI) broth and cultured for 20 hours at 37 °C to promote biofilm formation on the substrates. A robust biofilm is established on the surface of the material before it will undergo irradiations from a 3M Elipar TM Dental Curing Lamp (700 mW/cm²) at a wavelength of 430-480 nm.

Results: Surface coating with azobenzene concentrations of 20.6 μ g/mm², initiated a 4-log reduction in biofilm growth compared to uncoated samples. The irradiations used at this frequency induce the trans-cis-trans isomerization (photoisomerization) of the AZO-acrylate compound. Two-Way ANOVA analysis indicates a statistical significance in the effect of irradiations on an AZO-coated sample (p -value = 0.0195). The Bis-Azo and AZO-acrylate samples at 20.6 μ g/mm², 2.06 μ g/mm², and 0.206 μ g/mm² concentration showed a 4-log reduction in biofilm removal after irradiation.

Conclusions: The photoisomerization effect is capable of disrupting mature biofilms on the surface of the soft materials without the assistance of antibiotics. Preliminary data indicates that azobenzene-hydrogel networks have a significant effect on the growth of bacterial biofilms, especially when exposed to light. The ability of these antibacterial hydrogels to control the delivery of a therapeutic in response to different

wavelengths of light exposure as a stimulus will be further studied.

<https://doi.org/10.1016/j.dental.2019.08.014>

14

Analgesic-loaded pva films for tooth extraction: effect on blood coagulation



B.I. Cerda-Cristerna^{1,*}, V.H. Flores-Valencia¹,
J.L. Suárez-Franco¹, E.L. Galindo-Reyes¹,
J.C. Flores-Arriaga²

¹ Universidad Veracruzana Región Orizaba
Córdoba, México

² Universidad Nacional Autónoma De México Enes
León, México

Purpose/aim: Sustained release of analgesic drugs is a strategy of great interest to apply after a tooth extraction. We have produced poly (vinyl alcohol) (PVA) based films loaded with tramadol (TR) and dextetopofen (DX) for inducing sustained release of those two drugs in a socket after a tooth extraction. Because the films will be applied in the socket after the tooth extraction, our purpose was to evaluate the in vitro effect of the PVA films on the prothrombin time (PT) as well as on the activated partial thromboplastin time (APTT). The PT test evaluates the extrinsic pathway of the blood coagulation while the APTT evaluates the intrinsic pathway of the blood coagulation.

Materials and methods: We produced 9 groups (G) of PVA films: PVA Mw 13-23 (G1), PVA Mw 13-23 with TRDX (G2), PVA Mw 13-23 crosslinked with citric acid with TRDX (G3), PVA Mw 31-50 with (G4), PVA Mw 31-50 with TRDX (G5), PVA Mw 31-50 crosslinked with citric acid with TRDX (G6), PVA Mw 85-124 (G7), PVA Mw 85-124 with TRDX (G8), PVA Mw 85-124 crosslinked with citric acid with TRDX (9). Ten milligrams of a film were incubated with blood for 15 min at 37 °C and 50 rpm of oscillatory stirring. After that, the PT and APTT were measured with a coagulometer. Blood from a healthy donor was used as a control. Samples were evaluated by triplicate.

Results: For PT, the results were: G1, 13.43 seconds (s) 0.8; G2, 12.97 sec. 0.15; G3, 12.93 sec. 0.06; G4, 11.93 sec. 0.21; G5, 12.85 sec. 0.35; G6, 13.97 sec. 0.40; G7, 12.6 sec. 1.14; G8, 13.87 sec. 0.25; G9, 11.73 sec. 0.21; Control 12.03 sec. 0.12. For APTT, the results were: G1, 22.7 sec. 1.93; G2, 21.70 sec. 0.917; G3, 22.83 sec. 0.12; G4, 23.07 sec. 0.5; G5, 22.93 sec. 0.84; G6, 23.60 sec. 0.79; G7, 23.03 sec. 0.72; G8, 23.57 sec. 0.75; G9, 22.83 sec. 1.0; Control: 23.17 sec. 1.15. A no parametric Kruskal-Wallis test showed no significant statistical differences between groups and the control for PT and APTT.

Conclusions: The PVA films showed a PT and APTT similar to the PT and APTT induced by the control. Hence, in the in vitro conditions the PVA films did not impacted negatively the intrinsic pathway and the extrinsic pathway of the blood coagulation.

<https://doi.org/10.1016/j.dental.2019.08.015>

15

Effect of surface finishing on flexural strength of translucent y-tzps



K.N. Monteiro, R.P. Nigro, P.F. Cesar*

University of São Paulo, Brazil

Purpose/aim: The aim was to determine the effect of the surface finishing (polished versus glazed) on the flexural strength of two translucent Y-TZPs.

Materials and methods: Disks (1.0 mm-thick and 12 mm in diameter) were obtained by slicing pre-sintered translucent Y-TZP blocks (Prettau Anterior, Zirkonzahn, and Lava Plus, 3 M). After sintering according to manufacturers' instructions, the specimens were mirror polished (only tensile surfaces) in a semi-automatic polishing machine using diamond suspensions down to 1 µm. The following properties were analyzed (n = 10): fracture toughness (FT, indentation fracture), and Vickers hardness (H), both using 15 kg and 20s dwell time. For biaxial flexural strength testing (BFS) (0.5 mm/min, piston-on-three balls/immersed in water at 37 °C/ASTM F 394-78), polished and glazed specimens were compared (n = 10). The glazed surface was created by applying Stain Glaze Plus (Zirkonzahn) with subsequent sintering at 750 °C for 5 min. Data were analyzed by either one-way (FT and H) or two-way (BFS) ANOVA and Tukey's test with a global significance level of 5%.

Results: Table 1 indicates that the fracture toughness of Lava was significantly higher than that obtained for Prettau, whereas the hardness measured for both materials was statistically similar. There was a significant effect of the surface finishing on the BFS for Lava, as for this material the mean strength was significantly higher for the polished specimen in comparison to that obtained for the glazed ones. For Prettau, polishing and glazing resulted in similar BFS mean values. When the same surface state is considered, Lava shows significantly higher strength values in comparison to those obtained for Prettau.

Table 1 – Mean values (and SD) for Fracture Toughness, Hardness and Flexural strength with two surface finishings.

Material	Surface finishing	Fracture toughness (MPa m ^{1/2})	Hardness (GPa)	Flexural strength (MPa)
Lava Plus	Glaze	-	-	554.1 ± 66.8 ^B
	Polished	4.7 ± 0.4 ^A	13.4 ± 0.4 ^A	753.9 ± 163.9 ^A
Prettau Anterior	Glaze	-	-	314.3 ± 11.8 ^C
	Polished	3.2 ± 0.3 ^B	13.2 ± 0.3 ^A	419.5 ± 121.7 ^{B,C}

Conclusions: The effect of the surface finishing on the flexural strength depended on the translucent zirconia tested. Polished specimens resulted in higher strength values than glazed specimens for Lava, whereas for Prettau, no effect of the surface finish on strength was noted.

<https://doi.org/10.1016/j.dental.2019.08.016>

16

Shear bond strength comparison of self-adhesive resin cements

L. Chen, R. Wang*, B.I. Suh

Bisco, Schaumburg, USA



Purpose/aim: The purpose of this study was to compare the bond strengths of current self-adhesive resin cements and new alkaline calcium-silicate-based self-adhesive resin cement, TheraCem (Bisco).

Materials and methods: Human dentin and dental zirconia specimens were randomly divided into 5 groups ($n=5$). Dentin was polished with 320-grit SiC paper, rinsed and dried. Zirconia was sandblasted with alumina sand, rinsed and dried. Shear bond strength was tested using the notched-edge shear bond strength test method (zirconia bonding, surface area 4.4 mm^2 , crosshead speed 1 mm/min) or using gel-cap test method (dentin bonding, surface area 15 mm^2 , crosshead speed 5 mm/min). Resin cement was placed on the dentin or zirconia surface and light-polymerized (40s, 500 mw/cm^2). The specimens were then stored in water at 37°C for 24 hours and tested by universal testing machine (Instron). The data were analyzed statistically by one-way ANOVA and Student-t Test.

Results: Mean shear bond strengths in MPa (standard deviation) are shown in Table 1. Means with different letters are statistically different ($p < 0.05$).

Table 1 – Mean shear bond strengths in MPa (SD).

Cement	Dentin	Zirconia
TheraCem (Bisco)	6.0 (1.6) ab	32.5 (10.1) a
Unicem 2 (3M Oral)	6.6 (2.1) ab	23.7 (7.8) ab
MaxCem Elite Chroma (Kerr)	2.3 (3.9) b	20.3 (8.2) ab
Calibra Universal (Dentsply)	0.4 (0.6) c	17.9 (5.5) b
Panavia SA Plus Cement (Kuraray)	6.7 (1.7) a	16.5 (3.2) b

Conclusions: The new alkaline calcium-silicate-based self-adhesive resin cement, TheraCem, had comparable or better strengths for zirconia and dentin bonding than other current self-adhesive resin cements.

<https://doi.org/10.1016/j.dental.2019.08.017>

17

Universal adhesive improved bond strengths of self-adhesive resin cements

L. Chen*, B.I. Suh

Bisco, Schaumburg, USA



Purpose/aim: The purpose of this study was to investigate whether universal adhesives could improve the dentin bond strengths of new alkaline calcium-silicate-based self-adhesive resin cement, TheraCem (Bisco).

Materials and methods: Human dentin specimens were randomly divided into 7 groups ($n=5$). Dentin was polished with 320-grit SiC paper, rinsed and dried. Dentin (except for the control group) was treated with a Universal Adhesive. The adhesive was then air dried, and light-cured at

Table 1 – Mean shear bond strengths in MPa (SD).

Adhesive	Dentin Bond Strength
No Adhesive	7.1 (4.3) a
All Bond Universal (Bisco)	32.0 (5.6) b
Adhese Universal (Ivoclar Vivadent)	24.2 (12.3) b
Clearfil Universal Quick (Kuraray)	29.1 (2.9)b
Optibond Universal (Kerr)	30.1 (9.4)b
Prime & Bond Elect (Dentsply)	27.5 (4.2)b
Scotchbond Universal (3M Oral)	24.2 (7.1)b

500 mw/cm^2 for 10 s. Shear bond strength was tested using the notched-edge shear bond strength test method (surface area 4.4 mm^2 , crosshead speed 1 mm/min). Resin cement (TheraCem) was placed on the dentin surface and self-polymerized (15 min at 37°C). The specimens were then stored in water at 37°C for 24 h and tested by universal testing machine (Instron). The data were analyzed statistically by one-way ANOVA and Student-t Test.

Results: Mean shear bond strengths in MPa (standard deviation) are shown in Table 1. Means with different letters are statistically different ($p < 0.05$).

Conclusions: All of the Universal Adhesives improved the dentin bond strength of the new alkaline calcium-silicate-based self-adhesive resin cement, TheraCem.

<https://doi.org/10.1016/j.dental.2019.08.018>

18

Condition for a valid exposure reciprocity law in dental composites

S.V. Palagummi¹, T. Hong^{1,3}, Z. Wang², C.K. Moon³, M.Y.M. Chiang^{1,*}

¹ Biosystems and Biomaterials Division, National Institute of Standards and Technology, Gaithersburg, USA

² Department of Engineering Mechanics, Wuhan University, Wuhan, China

³ Department of Materials Science and Engineering, Pukyong National University, Busan, Republic of Korea

Purpose/aim: In restorative dentistry, the replacement of quartz tungsten halogen lamps with light-emitting diodes (LEDs) for photocuring dental composites has been a trend due to their narrow bandwidth of operation that closely overlaps with the absorption profile of the photoinitiator, lower heat generation, and better power efficiency. These advancements along with the ever-increasing demand from dentists for reducing the exposure time has led to high irradiance LED curing units (e.g., $>2 \text{ W/cm}^2$). The justification of using high irradiance and short exposure time springs from the Bunsen-Roscoe reciprocity law in photochemistry, termed as the exposure reciprocity law (ERL). The ERL states that for a given radiant exposure (=irradiance \times exposure time), the photopolymerization (the degree of conversion) of the dental resin/composite does not change with any combination of irradiance and exposure time. However, studies in the literature have debated rather inconclusively about the validity

of the ERL in dentistry. The results of these studies depended on the combination of the photocuring conditions (irradiance and radiant exposures) and the materials (model and commercial composites) used. The objective of this work is to provide clarity on the validity debate and, hence, give guidance on the applicability of ERL as it pertains to resin based dental composites.

Materials and methods: Composites made from different mass ratios of resin blends (Bis-GMA/TEGDMA and UDMA/TEGDMA) and micro-sized glass fillers were used. All the composites used camphorquinone and ethyl 4-dimethylaminobenzoate as the photo initiator system. A cantilever beam-based instrument (NIST SRI 6005) coupled with NIR spectroscopy was used to simultaneously measure the degree of conversion, polymerization stress due to shrinkage, and temperature change in real time during the photocuring process. The instrument had an integrated LED light curing unit providing irradiances ranging from 0.01 W/cm² to 4 W/cm² at the wavelength of 460 nm (blue light).

Results: For the composites studied, there exists a minimum radiant exposure above which the exposure reciprocity law is valid. This minimum predominantly depends on the resin viscosity of composite (i.e., independent of the filler content), and an analytical model has been established based on the viscosity to estimate the minimum radiant exposure.

Conclusions: The study clarifies the applicability of the exposure reciprocity law for dental composites and enables the clinician to determine the radiant exposure, with the available light-curing unit, needed to sufficiently cure the dental composite in question. More importantly, a high irradiance curing should be adopted only when the associated temperature change is clinically acceptable.

<https://doi.org/10.1016/j.dental.2019.08.019>

19

Additive manufacturing of photopolymerizable thiol-ene thermoplastics

K.K. Childress^{1,*}, M.D. Alim¹, J.J. Hernandez¹, J.W. Stansbury^{1,2}, C.N. Bowman¹

¹ University of Colorado Boulder, Boulder, USA

² University of Colorado Denver, Aurora, USA

Purpose/aim: Thermoplastic materials produced from photopolymerization processes are notoriously difficult to produce efficiently and typically lack robust mechanical properties. These attributes tend to make them impractical for light-based additive manufacturing (3D printing) techniques such as stereolithography (SLA). Here, a systematically varied structural library of linear thiol-ene photopolymer systems demonstrating rapid reaction kinetics and high conversions were produced and characterized specifically for application as printable materials.

Materials and methods: Thiol-ene systems with stoichiometric 1,6-hexanedithiol (HDT) and diallyl terephthalate (DAT) were prepared with diphenyl(2,4,6-trimethylbenzoyl)phosphine oxide (TPO). Polymerization and crystallization kinetics were monitored with real-time Fourier transform infrared spectroscopy (FTIR) and photo-rheology.

Molecular weight was determined using size exclusion chromatography with multi-angle light scattering (SEC-MALS), and crystallization and melting temperatures were found using differential scanning calorimetry (DSC). Polarized optical microscopy (POM) was used to monitor crystal development with time, and 3D printing was achieved using a Solus DLP 3D printer.

Results: Bulk polymers were formed in seconds at low irradiation intensities and exhibited remarkable mechanical properties such as high elongations to break (800%) and toughness (24 J m⁻³). A representative system that exhibited well-controlled polymerization-induced crystallization was implemented for SLA additive manufacturing using commercial 3D printers. A series of complex structures were successfully printed ranging from narrow pillar structures (diameter: 200 μm) to overhanging features (model Marvin test print) using typical printing parameters. Because of the plasticity of the printed structures, these prints were easily melted and reprocessed at 80 °C in a matter of minutes.

Conclusions: Photopolymerizable thermoplastic thiol-enes composed of commercially available materials demonstrated rapid polymerization kinetics and excellent mechanical properties and were used to print complex structures that could be melted. This demonstrates their applicability for recyclable printable materials and investment casting forms that allow for melt processing rather than polymer burnout treatments.

<https://doi.org/10.1016/j.dental.2019.08.020>

20

Study on testing methods for efficacy of tooth manicure products



J.W. Choi*, S.Y. Yang, J.S. Kwon, S.B. Lee

Yonsei University College of Dentistry, Seoul, Korea

Purpose/aim: Recently, liquids without hydrogen peroxide that can be applied on teeth for tooth whitening have been developed, and commonly known as tooth manicure. Despite growing market, there has been no study on efficacy of these materials in terms immediate and temporary tooth color alteration. In this study, we explored the testing method for efficacy testing of tooth manicure product.

Materials and methods: Total of six tooth manicures (A, B, C, D, E and F) without hydrogen peroxide were selected as the test materials. The drop of tooth manicures was placed on the cover glass and the original colors were measured using the spectrophotometer. Color change and gloss were observed on C4 shade surface of shade guide and enamel surface of bovine tooth covered with the tooth manicure, respectively. Color alteration was evaluated based on the CIE Lab parameters. Gloss level was measured using the gloss meter at 60° angle before and after coating on polished bovine tooth. The setting time was tested with the 1/4 lb Gillmore needle on the slide glass. The retention rate of tooth manicure was measured by weight change before and after the storage in distilled water of 37 °C for 24 h. Also, the detachability of tooth manicure from the bovine tooth surface was measured using the cross-brushing machine.

Table 1 – The results of color and gloss.

Group	Color on coated glass		Color on shade guide (C4)		Color on coated shade guide		Difference before and after application on coated shade guide			Gloss (ΔGU)
	L	b	L	b	L	b	ΔL	Δb	ΔE	
A	77.59 ± 0.43 ^a	7.85 ± 0.65 ^a			75.8 ± 2.20 ^a	9.21 ± 2.83 ^a	32.43 ± 2.20 ^{a*}	1.60 ± 2.83 ^a	32.84 ± 2.29 ^a	0.7 ± 0.5 ^a
B	68.85 ± 0.39 ^b	6.56 ± 0.57 ^a			68.35 ± 0.75 ^b	8.63 ± 0.60 ^{a*}	14.13 ± 8.37 ^{b*}	1.02 ± 0.60 ^a	25.63 ± 0.72 ^{bc}	5.1 ± 1.1 ^{bc}
C	75.31 ± 0.40 ^c	6.46 ± 0.47 ^a			76.11 ± 0.57 ^a	9.47 ± 1.17 ^{a*}	32.65 ± 0.57 ^{a*}	1.86 ± 1.17 ^a	33.27 ± 0.62 ^a	2.8 ± 0.9 ^{acd}
D	66.16 ± 0.78 ^d	2.21 ± 0.80 ^b			70.81 ± 0.39 ^{b*}	6.83 ± 0.57 ^{a*}	27.35 ± 0.39 ^{a*}	-0.77 ± 0.56 ^a	27.82 ± 0.40 ^{bd}	4.5 ± 0.5 ^{bde*}
E	89.78 ± 0.86 ^e	8.64 ± 0.54 ^c	43.46	7.61	76.88 ± 1.57 ^{a*}	16.24 ± 0.42 ^{b*}	33.43 ± 1.58 ^{a*}	8.64 ± 0.42 ^{b*}	34.54 ± 1.62 ^a	2.4 ± 0.2 ^{adf*}
F	68.60 ± 0.27 ^b	-13.20 ± 0.23 ^d			67.83 ± 0.16 ^{b*}	-8.51 ± 0.73 ^{c*}	24.37 ± 0.15 ^{ab*}	-16.12 ± 0.73 ^{c*}	29.27 ± 0.30 ^{acd}	4.6 ± 0.6 ^{bdf*}

Asterisk marks mean statistical significance between before and after application on coated specimen within each group ($p < 0.05$). And the same lowercase letter indicates no differences among the groups ($p > 0.05$).

Results: L values of A, C and E group ranged from 75.31 to 89.78, gloss values ranged from 0.7 to 2.8. Otherwise, L values of B, D and F group ranged from 66.16 to 70.81, gloss values exhibited between 4.5 and 5.1. It was high values when compared with before. L value after applied tooth manicure was significantly increased in all groups and b values differed the most in the between E and F group. Also, ΔE values ranged from 25.63 to 34.54. The setting time was within in the one minute in all groups. The retention rate was ranged from 99.54 to 99.69%. Tooth manicure applied on the tooth surface was not removed after 3 minutes under 150 g pressure. It needs to modify for removing tooth manicure remained on the tooth surface Table 1.

Conclusions: In this study, we tried to evaluate the variable efficacy of tooth manicure. It is expected the baseline data of evaluation method and safety of consumers can be established by suggesting the guideline of the tooth manicure efficacy testing. Also, these results will be used as a good tool of the tooth manicure efficacy testing.

<https://doi.org/10.1016/j.dental.2019.08.021>

21

Effect of an experimental etchant on dentin bond-strength over time



A. Comba^{1,*}, T. Maravic¹, E. Mancuso¹,
S. Ribeiro Cunha^{1,2}, E. Mayer-Santos^{1,2},
M. Cadernaro³, A. Mazzoni¹, L. Breschi¹

¹ University of Bologna

² University of Sao Paolo, Brazil

³ University of Trieste

Purpose/aim: Dentin demineralization with phosphoric acid greatly depends on its concentration and contact time. To address this issue, a novel, self-limiting etchant has been developed. The aim of this study was to investigate, using micro-tensile bond strength test (μTBS) and nanoleakage the performance of an experimental etchant as an alternative to conventional etching of the dentin immediately and over time.

Materials and methods: Non-carious teeth (N = 8 per group) were cut to expose middle/deep dentin, assigned to 4 groups and treated according to the manufacturers' (Ivoclar Vivadent) instructions: G1: dentin was etched with the experimental etching gel and bonded with Adhese Universal (AU); G2: dentin

was etched with phosphoric acid gel and bonded with AU (AU control); G3: dentin was etched with the experimental etching gel and bonded with ExciTE F (ExF). G4: dentin was etched with phosphoric acid gel and bonded with ExF (ExF control). Half of the specimens were further subjected to μTBS and stressed until failure at baseline, while the second half was aged for 12 months in artificial saliva at 37° and then stressed until failure. Additional 3 teeth per group were prepared for nanoleakage analysis and the amount of silver-nitrate within the hybrid layer was evaluated using light microscopy both at T = 0 and T = 12.

Results: The tree-way Anova test showed that the adhesive system, and the etchant, as well as time significantly influenced the results ($p < 0.05$). Bond strength was significantly higher with the experimental etching gel compared to the control group when AU bond was used. AU showed significantly higher bond strength than the ExF when associated with the experimental etchant. Finally, independently from the adhesive procedures, time negatively affected bond strength. There were no differences in the nanoleakage expression between the tested groups.

Conclusions: The experimental etchant seems to have a positive influence on resin-dentin bond strength immediately and over time. Hence, the experimental etchant could be recommended as a novel, safe and efficient demineralization technique in the every-day clinical practice. However, further studies on long-term influence of the novel etchant on bond strength are required.

<https://doi.org/10.1016/j.dental.2019.08.022>

22

Effect of Er,Cr:YSGG laser conditions on debonding ysz ceramic



L.R. Corby*, D.S. Remley, D.M. Hutto,
K.S. Jodha, J.A. Griggs, L. Contreras,
S.M. Salazar Marochio

University of Mississippi Medical Center, Jackson,
USA

Purpose/aim: High-speed diamond burs are traditionally used for crown removal, but the polycrystalline nature of yttrium-stabilized zirconia (YSZ) ceramics makes this process time-consuming, expensive and uncomfortable for patients.

The erbium:chromium:yttrium–scandium–gallium–garnet (Er,Cr:YSGG) laser could serve as a fast and non-destructive alternative for debonding YSZ restorations. The aim was to determine the effect of different laser conditions of the Er,Cr:YSGG laser on the debonding strength between an YSZ ceramic and a resin cement.

Materials and methods: Slices (~1 mm thick) from an YSZ block (IPS e.max ZirCAD, Ivoclar Vivadent) were treated using 30 µm silica-coated aluminum oxide particles (Cojet Sand, 3 M) and silane (Monobond Plus, Ivoclar Vivadent). Resin composite cylinders (Ø = ~4.0 mm) were cemented to the YSZ slices using a dual-cure resin cement (Multilink Automix, Ivoclar Vivadent). The samples were randomized and divided into groups according to the condition of the Er,Cr:YSGG laser (Waterlase MD, Biolase) application: the control group had no laser irradiation, the wet group consisted in laser irradiation with 1% water and 1% air and the dry group was irradiated without water/air irrigation. The samples were irradiated for 2 min each using a line scanning method at a distance of 1 mm, perpendicular to the surface. The sapphire tip (Ø = 1 mm, MG6; Biolase) was used at 1 W and 20 pulses per second. After laser irradiation, samples immediately underwent shear bond strength testing (ElectroForce 3200, Bose) using a custom clamp with a 0.5 mm orthodontic stainless steel wire at a loading rate of 1 mm/min until failure. Failure analysis was performed using an optical microscope to assess adhesive (YSZ/cement interface) and mixed failure (adhesive + cohesive of resin cement) in each group.

Results: The data passed the normality test (S–W, $p = 0.303$) and had a statistical power of 0.943. Tukey's test ($\alpha = 0.05$) showed similar bond strength values (Table 1) when the laser was used in either dry or wet conditions ($p = 0.529$). However, significant differences were found between the control and both wet ($p < 0.001$) and dry ($p = 0.008$) groups. All of the groups had predominately mixed failure; however, there was an increase in adhesive failure when the laser was applied in dry condition.

Table 1 – Mean bond strength (SD) and type of failure.

Group	n	Mean ± Std. Dev. (MPa)	Failure Classification	
			Adhesive	Mixed
Control	8	9.5 ± 2.7 ^A	1 (12.5%)	7 (87.5%)
Dry	12	5.1 ± 2.1 ^B	1 (8.3%)	11 (91.7%)
Wet	12	6.1 ± 2.1 ^B	4 (33.3%)	8 (66.7%)

Conclusions: Laser irradiation using a low power setting of 1 W in either wet or dry conditions significantly decreases the bond strength between the YSZ ceramic and the resin cement. The fracture surface of the samples tested in dry condition suggests laser irradiation had a thermal effect on the resin cement, decreasing the bond strength to the YSZ surface.

<https://doi.org/10.1016/j.dental.2019.08.023>

23

3D Printed PBAT/BAGNb scaffolds: in vitro and in vivo analysis



G. Balbinot*, L.M. Ulbrich, V.C.B. Leitune,
D. Ponzoni, R.M.D. Soares, F.M. Collares

Universidade Federal do Rio Grande do Sul, Porto Alegre, Brazil

Purpose/aim: The aim of this study was to produce 3D printed composite scaffolds of polybutylene adipate terephthalate (PBAT) and niobium-containing bioactive glasses (BAGNb).

Materials and methods: The composite filaments were produced by melt–extrusion in a twin–screw extruder with the addition of 10wt% of BAGNb (BAGNb10%). Filaments without BAGNb were produced as the control group (CG). The produced filaments were characterized by Fourier Transformed Infrared Spectroscopy (FTIR) and thermogravimetric analysis (TGA). The produced composites were used to produce the scaffolds in a 3D printer using the fusion filament fabrication. The scaffolds were evaluated in vitro by microcomputed tomography (MicroCT) and by the contact angle. Cell culture was performed using MC3T3–E1 cells. Cell viability was assessed by Sulphorhodamine B and mineralization was analyzed by Alizarin S Red. The BAGNb10% group was analyzed in vivo. Scaffolds were tested in a rat femur model ($n = 10$) and the new bone formation was assessed after 15, 30 and 60 postoperative days. For this analysis, deproteinized bovine bone marrow and autogenous bone were used as control.

Results: The characterization of developed composite filaments showed the presence of Si–O–Si (1050 cm^{-1} and 450 cm^{-1}) bonds from BAGNb and C=O (1700 cm^{-1}) and C–H (1105 cm^{-1} , 1270 cm^{-1} , 2960 cm^{-1}) bonds from PBAT. TGA curves showed reduced temperature for degradation when BAGNb was added. The printed structures presented porosity of 69.8% for BAGNb10% group and 74.5% for PBAT group in MicroCT analysis. No statistically significant difference was found between BAGNb10% and CG in contact angle measurements. Higher cell viability ($105.2\% \pm 0.9$) was observed for BAGNb10% group when compared to CG ($93.1\% \pm 1.2$). Mineralization was higher for BAGNb10% after 7 and 14 d of culture. In the in vivo analysis, no postoperative complications were observed and all materials presented the formation of new bone in the defect after 60 d. Increased bone was observed from 15 to 60 d.

Conclusions: The PBAT/BAGNb scaffolds were successfully produced by 3D printing and the in vitro analysis showed suitable properties for application in vivo. The implantation of materials in the animal model showed that developed materials were safe and able to promote bone formation.

<https://doi.org/10.1016/j.dental.2019.08.024>

24

Chemical bonding and micromechanical interlocking to dental zirconia substrate

N. Alsalem¹, B. Hajhamid², C. Lorenzetti³,
S. Barreto⁴, G.M. De Souza^{2,*}

¹ Princess Nourah University, College of Dentistry,
Riyadh, Saudi Arabia

² Faculty of Dentistry/University of Toronto,
Toronto, Canada

³ State University of Sao Paulo, Araraquara School
of Dentistry, Araraquara, Brazil

⁴ State University of Campinas, Piracicaba School
of Dentistry, Piracicaba, Brazil

Purpose/aim: Yttria-stabilized tetragonal zirconia (Y-TZP) has been used in dentistry to replace missing/severely damaged teeth. However, the absence of a glass phase makes Y-TZP bonding to luting systems very challenging. 10-methacryloyloxydecyl dihydrogen phosphate (MDP) is the most promising molecule to bond to the Y-TZP oxide surface. Alumina blasting is also used in an attempt to develop a surface micromechanical interlocking that will lock the resin cement in place. This study investigated the effect of MDP-containing materials and alumina blasting on the bonding to Y-TZP.

Materials and methods: Forty Y-TZP samples were cut, sintered and polished to a final dimension of 10x8x4 mm³. Specimens were distributed in 2 surface treatments ($n=20$): as sintered (CT-control) or alumina blasting (AB): 45 μm Al_2O_3 particles with 3.5 bar pressure at 10 mm standoff distance. Then, Y-TZP blocks were cemented to composite resin blocks of same dimensions with either a MDP-containing adhesive (Scotchbond Universal, 3M) and resin cement (RelyX Ultimate, 3M) or a MDP containing primer (Clearfil Ceramic primer plus, Kuraray) and resin cement (Panavia V5, Kuraray). Microtensile slabs were cut after 24 hour-water storage, counted and tested after 24 hours or 3 months. Microtensile results were analyzed by two-way Analysis of Variance (ANOVA) and Tukey HSD test. Independent variables were material and surface treatment. Number of slabs/sample were analyzed by one-way ANOVA ($P=0.05$).

Results: Both, material ($p<0.001$) and treatment ($p=0.002$) had a significant effect on bond strength at 24 hours. After 3 months, only treatment ($p=0.004$) and the interaction material*treatment ($p<0.001$) were significant. AB/MDP-adhesive resulted in the highest bond strength values at both storage times (24 h– 26.34 ± 3.15 MPa; 3m – 22.24 ± 3.64 MPa) while CT samples had the lowest values at both storage times: 24 h/MDP-primer– 15.93 ± 5.70 MPa; 3m/MDP-adhesive – 13.69 ± 3.17 MPa. There was no effect of surface treatment ($p=0.70$), material ($p=0.41$) or the interaction treatment*material ($p=0.29$) on number of slabs produced by each experimental block.

Conclusions: In spite of the reported effective bonding between MDP molecule and Y-TZP oxide layer, higher bond strength results are still associated with alumina-blasting of the surface. This study further indicates that there is no

correlation between number of microtensile slabs obtained and bond strength results.

<https://doi.org/10.1016/j.dental.2019.08.025>

25

Color and whiteness stability of composites after bleaching and aging

A. Della Bona*, M.L. Vidal, J. Xavier,
O.E. Pecho

University of Passo Fundo, Passo Fundo, Brazil

Purpose/aim: To evaluate color stability and whiteness variations of resin-based composites (RBC) after different bleaching, light activation distance and aging procedures.

Materials and methods: 60 disc-shaped specimens (10 mm in diameter and 1 mm thick) of shade A2 were fabricated from two RBCs (Z2- Filtek Z250 XT; and Z3- Filtek Z350 XT) and light-activated in two different distances (0- 0 mm, and 8- 8 mm). A dental spectrophotometer (VITA Easshade, Vita Zahnfabrik) was used to obtain CIELAB color coordinates after 24 hours of fabrication (T-0), one day after bleaching (T-1), and six months after bleaching (T-6). Specimens were always stored in 37 °C distilled water. After the first color measurement (T-0), bleaching treatments were performed as follows: HB- at-home bleaching using 6% hydrogen peroxide (White Class 6%, FGM; 2 hour/day, for 21 days); OB- in-office bleaching using 35% hydrogen peroxide (Whiteness HP Blue 35%, FGM; 15 min/day for 3 days); and C- no bleaching (control). Thus, 30 specimens ($n=5$) were fabricated from each RBC and divided into six experimental treatments. CIEDE2000 color difference ($\Delta E-00$) and variations of whiteness index for dentistry ($\Delta WI-D$) were used to evaluate color stability with aging (T-0, T-1 and T-6). $\Delta E-00$ and $\Delta WI-D$ data were analyzed considering the 50:50% perceptibility ($PT=0.81$) and acceptability ($AT=1.77$) thresholds; and 50:50% whiteness perceptibility ($WPT=0.72$) and whiteness acceptability ($WAT=2.63$) thresholds, respectively. Analysis of variance and Tukey tests ($\alpha=0.05$) were used to statistically analyze the data.

Results: After bleaching (T-1-T-0), Z2-8 with HB (2.47), and Z3-8 with HB (2.46) and OB (1.91) showed $\Delta E.00$ values above AT. In addition, Z2-0 (-4.10), Z2-8 (-4.83), Z3-0 (-3.79), and Z3-8 (-3.99) showed $\Delta WI-D$ values above WAT but only for HB groups. After aging (T-6-T-0), both RBCs showed similar $\Delta E-00$ and $\Delta WI-D$ values for all groups ($p>0.05$). Both RBCs showed the lowest $\Delta WI-D$ values after six months of aging.

Conclusions: Color changes of RBCs that were light activated at 8 mm of distance and whiteness variations after at-home bleaching were not clinically acceptable. Aging produced the greatest color changes, which were clinically perceptible.

<https://doi.org/10.1016/j.dental.2019.08.026>



26

Withdrawn

27

Biomechanical analysis of zirconia implant-supported crowns

N Kaur, HM Sherrill, Y Duan*

School of Dentistry, University of Mississippi
Medical Center, Jackson, USA



Purpose/aim: To investigate the effect of various restorative materials on the stress distribution of posterior dental crowns supported by a one-piece regular-diameter zirconia dental implant using three-dimensional finite element analysis (FEA).

Materials and methods: FEA model of a full-coverage molar crown supported by a commercially available one-piece zirconia dental implant (Z-Systems Z5m, Ø=4.0 mm) was created using X-ray micro-CT scanning data. Three commonly-used restorative crown materials were simulated using elastic constants determined by literature: monolithic zirconia (MZ), polymer-infiltrated-ceramic network (PICN), and glass-ceramic (GC). Axial and oblique loadings of 100N were applied respectively to simulate the physiological occlusal loading. Stress distribution was plotted and analyzed in commercial FEA software ABAQUS.

Results: The oblique loadings resulted in higher stress values compared to the axial loadings for all three groups. GC group showed the highest maximum first principal stress value in the crown under axial loading among three groups, while there was no significant difference between PICN and MZ groups. MZ group has the highest maximum stress value in the crown under oblique loading, while PICN group has lowest stress value. MZ group showed the lowest stress value in the cementation layer while PICN group showed the highest value. There is no significant difference in the stress values of zirconia implants among three groups.

Conclusions: All three restorative materials are resistant to the fracture under given physiological loading amplitude for dental crowns supported by the one-piece zirconia implant. Monolithic zirconia generates lowest stress concentration in both crown and cementation layer under axial loading, while PICN material generates least stress concentration in the crown under oblique loading.

<https://doi.org/10.1016/j.dental.2019.08.028>

28

Dental sealant modified biofilm inhibitor: effect on streptococcus mutans growth

J.F.B. Fonseca*, C.T.P Araújo, A.B. Meireles, C.A.Santos, P.M. Alcântara, P.C.P Paiva, M.H. Canuto

Federal University of the Jequitinhonha and
Mucuri Valleys, Diamantina, Minas Gerais, Brazil



Purpose/aim: The development of protein-repellent materials able to reduce protein adsorption and bacterial adhesion related to the formation of dental biofilm is a promising strategy against caries disease. Thus, the incorporation of a biofilm inhibitor component into dental materials formulations as resinous sealant can be highly desirable for the control of carious lesions, specially on occlusal surfaces of posterior teeth since their anatomy details as pits and fissures put them in group of more vulnerable to caries. The objective of this work was to modify a commercially available resin sealant (Defense-Chroma - ANGELUS) with the biofilm inhibitor, 2-methacryloyloxyethylphosphorylcholine (MPC) and to evaluate the ability to inhibit adhesion of *Streptococcus mutans* (*S. mutans*) determined according to colony forming units (CFU/ml).

Materials and methods: 09 blocks of bovine teeth distributed in 3 groups and each group received one type of treatment namely: Control group received no type of sealing; the second group received treatment with the commercial sealant and the 3rd group was treated with the MPC modified sealant. The sealant was applied according to the manufacturer's instructions. The response variable was the count of CFU/ml produced on the enamel surface after 48 h of inoculation and with microscope images.

Results: The results (Table 1) revealed a significant difference between the treatment of the control group vs. the conventional sealant group ($p=0.001$), between the control group vs. the inhibitor sealant group ($p=0.352$) and between the conventional sealing group vs. the sealing group with inhibitor ($p=0.001$). Microscope images demonstrated the presence exclusively of Gram-positive cocci.

Table 1 – Result of counting Colony Forming Units per milliliter (CFU/mL)*

Treatment groups	Control (G1)	Sealant without biofilm inhibitor (G2)	Sealant with biofilm inhibitor (G3)
CFU/mL	12.3 (77.0)a	126.4 (129.3)b	9.4 (12.4)a

* edian values. Same letter at the same line are not significantly different from each other (significance test with Mann Whitney U tests, $p < 0,05$).

Conclusions: It was observed that in the incubation period for 48 hours, the modified sealant was strongly effective in inhibiting *S. mutans* adhesion.

Acknowledgment: PRPPG/UFVJM; CAPES

<https://doi.org/10.1016/j.dental.2019.08.029>

29

Effect of mechanical properties of adhesives on bond strength



K. Fujimori*, A. Arita, T. Kumagai

R&D Department, GC Corporation, Tokyo, Japan

Purpose/aim: The aim of this study was to evaluate the effect of mechanical properties of adhesives on bond strength.

Materials and methods: Shear bond strength test; bovine enamel and dentin surfaces were ground with 320-grit SiC paper and divided into two groups ($n=5$ each): New 2-step type adhesives (GC) (BZF); CLEARFIL SE BOND 2 (Kuraray) (SE2). Adhesives were applied to the tooth surface according to manufactures' instructions. Adhesives were light cured via the ultradent mold ($\varphi=2.38$ mm), and composite resin was applied via the mold and light cured. The bonded specimens were subjected to shear bond strength (SBS) test at 1 mm/min after stored in water at 37 °C for 24 h. Data were analyzed using t-test ($p<0.05$). Flexural strength test; flexural strength and elastic modulus of each material were measured according to ISO 4049($N=5$). Results were analyzed using t-test ($p<0.05$). Compressive strength test; Adhesives was filled in a mold (diameter 4 mm \times height 6 mm) and light was irradiated to obtain test samples. The specimens were subjected to compressive strength test at 1 mm/min after stored in water at 37 °C for 24 h. Data were analyzed using t-test ($p<0.05$).

Results: Means (\pm SD) of the shear bond strength, flexural strength and compressive strength were shown in Table 1. SBS of enamel and dentin of BZF were significantly higher than

SE2. There was no significant difference between BZF and SE2 in flexural strength, but there was a significant difference in elastic modulus. There was no significant difference between BZF and SE2 in compressive strength, but there was a significant difference in elastic modulus. It was found that the flexural and compressive strength of adhesives does not affect the bond strength, but the elastic modulus affects the bond strength.

Conclusions: If the elastic modulus of the material is low, the shear stress applied to the bonded surface becomes uneven and the shear stress is localized. It may lead low bond strength. MDP and HEMA, which are often contained in bonds, are monofunctional and hard to polymerize, and HEMA is easy to absorb water. BZF has high elastic modulus and high bond strength because it does not contain them.

<https://doi.org/10.1016/j.dental.2019.08.030>

30

Effect of hybrid zinc-based particle with ionic liquid in adhesive



I.M. Garcia*, V.S. Souza, J.D. Souza, F. Visioli, J.D. Scholten, F.M. Collares

Federal University of Rio Grande Do Sul, Porto Alegre, Brazil

Purpose/aim: The aim of this study is to synthesize a hybrid zinc-based particle with ionic liquid and evaluate the effect of its addition in an experimental adhesive resin.

Materials and methods: The ionic liquid 1-n-butyl-3-methylimidazolium chloride (BMI.Cl) and zinc chloride ($ZnCl_2$) were used to synthesize the particles of simonkolleite (SKT). These hybrid particles (SKT) were evaluated by transmission electron microscopy (TEM). An experimental adhesive resin was formulated with 66.66 wt.% of bisphenol A-glycidyl methacrylate and 33.33 wt.% of hydroxyethylmethacrylate with a photoinitiator system. The particles of SKT were incorporated at 1 (G1%); 2.5 (G2.5%) and 5 (G5%) wt.% in the experimental adhesive resin and one group remained without SKT to be used as control (GCtrl). The adhesive resins were evaluated for degree of conversion (DC), ultimate tensile strength (UTS), softening in solvent, microtensile bond strength (μ -TBS), contact angle with water or α -bromonaphthalene, surface free energy (SFE), antibacterial activity against *Streptococcus mutans* and cytotoxicity against pulp fibroblasts.

Results: SKT presented a hexagonal shape with a dimension of up to 1 micrometer. The DC ranged from 62.18 (± 0.83)% for GCtrl to 64.44 (± 1.55)% for G2.5% ($p>0.05$). There was no statistically significant difference among groups for UTS ($p>0.05$), μ -TBS ($p>0.05$), nor softening in solvent ($p>0.05$). The addition of SKT did not influence the contact angle ($p>0.05$), nor the SFE ($p>0.05$). There was statistically significant difference among groups for antibacterial activity, with lower biofilm formation from 1 wt.% of SKT addition compared to GCtrl ($p<0.05$). There was statistically significant difference among groups for antibacterial activity against planktonic bacteria ($p<0.05$). The cell viability tested in the cytotoxicity

Table 1 – Mean and standard deviation of share bond strength test, flexural strength test and compressive strength test.

		BZF	SE2
Share bond strength test	Enamel (MPa)	37.2(± 8.0) A	29.3(± 6.2) B
	Dentin (MPa)	41.8(± 8.8) a	34.8(± 7.1) b
Flexural strength test	Flexural strength (MPa)	123.0(± 4.3)	119.9(± 2.4)
	Elastic modulus (GPa)	5.3(± 0.6)	4.2(± 0.6)
Compressive strength test	Compressive strength (MPa)	131.1(± 8.0)	133.5(± 1.0)
	Elastic modulus (GPa)	2.19(± 0.2)	1.8(± 0.1)

Different letters indicate significant statistical differences between BZF and SE2 ($p<0.05$).

assay showed values over 80% for all groups, without statistically significant difference ($p > 0.05$).

Conclusions: The addition of hybrid zinc-based particles with ionic liquid in an experimental adhesive resin did not affect the physico-chemical properties of the adhesive resin and provided antibacterial activity without cytotoxic effect.

<https://doi.org/10.1016/j.dental.2019.08.031>

31

Methacrylic resin compatibilization via reactive and inert nanogels



D. Gautam^{1,*}, J.W. Stansbury^{1,2}, D.P. Nair¹

¹ Department of Craniofacial Biology, Anschutz Medical Campus, Aurora

² Department of Chemical and Biological Engineering, University of Colorado, Boulder

Purpose/aim: The aim of this study is to synthesize tailored reactive and inert nanogels as compatibilizers for hydrophobic/hydrophilic/amphiphilic blends of monomers photopolymerized in the presence of a solvent to formulate homogenous, polymer networks for composite restorations.

Materials and methods: Nanogels were synthesized via a solution polymerization reaction with either 70:30 mol per cent of a commercial aliphatic urethane diacrylate, Ebecryl270, ($M_w = 1500$ g/mol): UDMA ($M_w = 470.5$ g/mol) or with 100 mol per cent UDMA. Both nanogels used 1wt% of the thermal initiator 2,2'-Azobis(2-methylpropionitrile) and 20 mol% of the chain transfer agent 2-mercaptoethanol and were stirred at 80 °C using methyl ethyl ketone (4x) as a solvent. The nanogels were monitored via FTIR spectroscopy until vinyl conversion was at 50% and then end-capped with either a 50:50 mol% mix of Mercaptosuccinic acid and Thioglycerol, with 20% unreacted acrylic/methacrylic functionality or a 50:50 mol% mix of the reagents with no residual acrylic/methacrylic functionality. Compatibility was studied with hydrophobic/hydrophilic/amphiphilic monomer blends in the presence of ethanol with Irgacure 2959 as the photoinitiator (1wt%). The optical clarity of the polymer was quantified via UV Spectroscopy (Synergy HTX Multi-Mode Microplate reader).

Results: The molecular weight and hydrodynamic radii of the Ebecryl 270/UDMA and UDMA nanogels was 52,000 kDa, 3.73 nm and 80,600 kDa and 10.56 nm respectively.

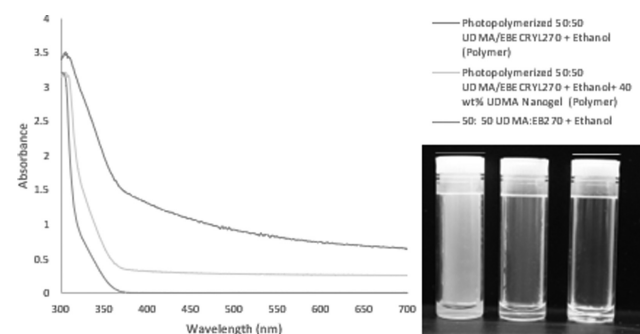


Fig. 1

It is observed that the presence of reactive functionality was necessary to prevent solvent induced phase separation during photopolymerization. The incorporation of the reactive nanogels within networks altered the opacity of the blends as shown in Fig. 1. Networks with reactive nanogels showed up to a 3X reduction in absorbance after polymerization.

Conclusions: Nanogels can be successfully implemented as network compatibilizers for hydrophobic/hydrophilic/amphiphilic blends of monomers. The presence of reactive functionality within the nanogels were critical to preventing solvent induced phase separation. The presence of the acid groups and the relative ratio of hydrophilic vs hydrophobic monomers within the nanogel can be altered to optimize compatibilization.

<https://doi.org/10.1016/j.dental.2019.08.032>

32

Mechanical properties of 3d-printed dental implant guide by sterilization methods



H.B Go^{1,*}, S.Y Im¹, B.S Lim², K.M Kim¹, J.S Kwon¹

¹ Yonsei University College of Dentistry, Seoul, Korea

² School of Dentistry, Seoul National University, Seoul, Korea

Purpose/aim: Dental implant guide is a medical device that is used during the implant surgery, and recently produced by 3D printing technology. As dental implant guide is placed in the patient's mouth and to be in direct contact with the mucosa and blood, sterilization is essential. Sterilization refers to the complete destruction of microorganisms which the methods include autoclave sterilization and E.O. gas sterilization, etc. Additionally, dental implant guide should have adequate mechanical properties for the effective use in the clinic. Despite some recent studies on 3D printed dental implant guide, mechanical properties according to the sterilization method have not yet been investigated. Therefore, the purpose of this study was to evaluate the mechanical properties of 3D printed dental implant guide according to the sterilization method.

Materials and methods: In this study, photopolymer resin for 3D printing dental implant guide (SG, Nextdent) and DLP type 3D printer (ND5100, Nextdent) were used. The rectangular (flexural test) and cylinder-shaped (shore test) specimens were printed. After printing specimens, post-treatment and post-curing process was performed according to the manufacturer's instructions. The samples were then undergone either the autoclave sterilization (AC) or E.O. gas sterilization (EO), while no sterilization process was applied on the control group. The sizes of the sterilized specimens were measured using a digital Vernier caliper and 3-point bending test was carried out by a universal testing machine (5942, Instron) according to ISO 20795-1. Also, the specimens were assessed by scanning electron microscopy (SEM) and energy dispersive spectroscopy (EDS) and Fourier transform infrared (FT-IR) spectroscopy. The hardness values of samples were tested by Shore D-type hardness instrument (HPSD, SCHMIDT). The

data were analyzed with one-way ANOVA with post-hoc analysis using Tukey's test ($p < 0.05$).

Results: The flexural strength was highest in EO group compare to others ($p < 0.05$) while the values for the control was the lowest. In terms of the flexural modulus, the EO group was significantly higher than two other groups ($p < 0.05$), but there was no significant difference between the control group and the AC group. Finally, various sterilization techniques affected the microstructure of the photopolymer resin. The hardness values were in order of EO, AC and control group.

Conclusions: Different sterilization methods result in mechanical and chemical changes in 3D printed dental implant guide. Thus, it is recommended that sterilization is carried out by the E.O gas sterilization method for the proper mechanical properties of the 3D printed dental implant guide.

<https://doi.org/10.1016/j.dental.2019.08.033>

33

Efficacy of PILP-method for remineralization of artificial and natural lesions



M. Bacino¹, E. Babaie¹, G.W. Marshal¹,
L.L. Gower², S. Habelitz^{1,*}

¹ University of California, San Francisco, USA

² University of Florida, Gainesville, USA

Purpose/aim: The Polymer-Induced Liquid Precursor (PILP) process has been recognized as a method to reintroduce apatite mineral into collagen fibrils that is able to remineralize artificial carious lesions in dentin facilitating a substantial recovery of its properties. In this study, a series of PILP-releasing cements was tested for their ability to restore mineral content and elastic properties and compared to commercial glass-ionomers (GIC) and to the conventional PILP-method in solution.

Materials and methods: Three kinds of dentin substrates were used: 1) artificial lesions of 140 μm depth; 2) artificial lesions with a depth of 700 μm and 3) natural lesions in dentin of extracted teeth which were treated minimal invasively by selective removal of the infected portion of the dentin using carbide burs. Specimens were either restored with GICs, with or without PILP placement of a PILP-releasing cement as a liner or the use of PILP-conditioning solutions and exposed to saturated calcium phosphate solutions with or without 0.1 mg/ml poly-aspartic acid. Changes in the elastic modulus of the artificial lesions were evaluated by nanoindentation and changes in mineral density were determined by micro-CT at periods of up to 6 months of treatment.

Results: In shallow lesions of 140 μm , there was substantially recovery of the elastic modulus for all specimens which were treated with poly-Asp, while control GIC did only show minimal improvements. At an increased lesion depth of 700 μm , immersion of specimens into PILP-solutions for one month produced significant recovery across the lesions with an average modulus of about 8 GPa. PILP-releasing cements and PILP-conditioning showed recovery from the bottom up to about 300 μm depth, while the outer portion of the lesion

did not improve in stiffness and remained at about 0.2 GPa. Commercial GIC showed only minor improvement in elastic modulus. Mineral density of natural lesions showed improvement in all treatment groups and volume of the lesion was reduced most when treated with PILP-conditioner (19.8%), followed by PILP-cements (10.9%) and GIC (6%). Image analysis showed the distribution of mineral was patchy with some areas recovering significantly while others did not.

Conclusions: This study suggests that PILP-treatments are beneficial for the remineralization of dental caries and highest efficacy is obtain when PILP is applied in form of an aqueous solution.

<https://doi.org/10.1016/j.dental.2019.08.034>

34

Fluoride ion release/recharge behavior of ion-releasing restorative materials



Y.Hokii¹, C. Carey², M. Heiss^{1,*}, G. Joshi¹

¹ GC America, Alsip, USA

² University of Colorado, Aurora, USA

Purpose/aim: To compare fluoride ion release and recharge behavior for ion-releasing restorative materials under neutral and acidic pH condition.

Materials and methods: Six restorative materials, GC Fuji Automix LC (FAM), EQUIA FORTE FIL (EQF), EQUIA FORTE COAT (EFC), GC Fuji Triage (FTR) (GC America), ACTIVA BioACTIVE-RESTORATIVE (ABA, Pulpdent), and BEAUTIFIL IILS (BF2, Shofu) were used. MI Paste ONE (1100 ppm F, 10% ACP-CPP, GC America) was used for recharge. Six test groups were compared by using above listed materials as follows; 1) FAM, 2) EQF + EFC, 3) EQF, 4) FTR, 5) ABA and 6) BF2. Restorative materials were filled into acrylic mold with a 7.0 mm diameter, 2 mm in depth hole ($n = 5$). Hardened specimen was immersed into 3.5 mL of 50 mM HEPES-NaOH buffer (pH 7.0) or 50 mM Lactic Acid Buffer (pH 4.6) at 32degC. Fluoride Ion was measured by the fluoride ion selective electrode (F-ISE) from start of immersion: day 1, 2, 7, 14, 21, 30. At day 30, after ion concentration measurement, surface of materials were treated using 1 mL of MI Paste ONE slurry (2:1 = deionized water: MI Paste ONE) for 2 min and washed with deionized water for 10 seconds for 3 times. After 8 hours, specimens were treated MI Paste ONE slurry again. Fluoride ion were analyzed after MI Paste ONE treatment: day 1 (= day 31), 2 (= day 32), 7 (= day 37). Obtained values by fluoride ion analysis were calculated and converted to amount of released fluoride ion per unit area ($\mu\text{g}/\text{mm}^2$). The data were compared by using 1-way ANOVA and Tukey's tests ($\alpha = 0.01$).

Results: Both pH4.6 and pH 7.0, FAM (pH 4.6: 636.29 ± 57.73 , pH 7.0: 115.63 ± 31.22), EQF (pH 4.6: 904.09 ± 33.92 , pH 7.0: 219.10 ± 10.43) and FTR (pH4.6: 979.34 ± 38.57 , pH7.0: 192.20 ± 5.84) showed significantly higher cumulative fluoride release than EQF + EFC (pH4.6: 49.91 ± 26.64 , pH7.0: 4.76 ± 2.36), ABA (pH4.6: 44.11 ± 10.38 , pH7.0: 19.47 ± 8.10) and BF2 (pH4.6: 32.05 ± 4.47 , pH7.0: 8.10 ± 1.23). Also, fluoride release of EFQ and FTR, which is conventional GIC, was higher than FAM. Under acidic condition, significant recharge

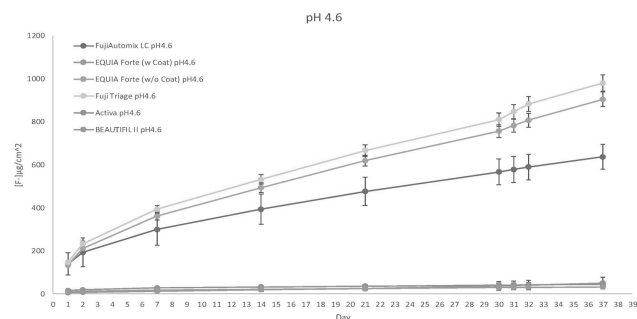


Figure 1

and release phenomena were observed at day 31 and 32 (Fig. 1).

Conclusions: GI (EQF and FTR) and RMGI (FAM) has significant higher fluoride release properties comparing to other 3 products. Under acidic condition, fluoride recharge was observed on the surface of GIC by using bioactive fluoride toothpaste.

<https://doi.org/10.1016/j.dental.2019.08.035>

35

SEPB fracture toughness of six dental zirconias



T. Hill*, R. Fachko, G. Tysowsky

Ivoclar Vivadent, Inc, Amherst, USA

Purpose/aim: The use of zirconia in dentistry is increasing at a rapid rate. There are over a 100 different brands on the market and growing. Because these zirconia brands include varying amounts of tetragonal and cubic phase, they can have very different mechanical and optical properties. One important property that is difficult to measure for zirconia is fracture toughness. In order to properly obtain accurate values of fracture toughness, the crack tip must be sharper than the microstructure of the material, meaning for zirconia less than 1 µm which precludes the use of the SEVN method. According to ISO6872, the SEPB method is a preferred method to obtain values. The purpose of this study was to measure the fracture toughness of 6 zirconia materials using the SEPB method.

Materials and methods: Six zirconias were tested: Sagemax NexxZr S (3Y), Sagemax NexxZr T (3Y), Sagemax NexxZr Plus (4Y), e.max ZirCAD LT (3Y), e.max ZirCAD MT (4Y) and Cubix2 (5Y). Ten Flexure bars (36 mm x 4 mm x 3 mm after sintering) per zirconia material in a disc were milled to obtain six specimens per group using a Wieland Zenotex Select milling with Zenotec CAM V3 3.4.029 software. Milled the bars were desprued and cleaned, they were sintered according to the manufacturer's instructions. The fully sintered bars were lined with 3 equally spaced indents across the center of the bar using 10 or 20 kg loads using a Marco Vickers Hardness Tester. The bars were then placed in bridge indentation pre-cracking fixture as described in ASTM Standard C 1421 and loaded in an Instron Universal testing machine (33R4204) at

Table 1 – Mean Fracture toughness (SD). Different capital letters indicate significance.

Table 1	KIC (MPa•m ^{1/2})
Sagemax NexxZr S (3Y)	5.45 (0.3) A
Sagemax NexxZr T (3Y)	5.55 (0.1) A
e.max ZirCAD LT (3Y)	5.12 (0.2) A
e.max ZirCAD MT (4Y)	3.81 (0.1) B
Cubix2 (5Y)	2.7 (0.3) C
Sagemax NexxZr Plus (4Y)	4.08 (0.2) B

a crosshead speed of 0.25 mm/min until a crack was heard or until 10kN were obtained. The specimen was then back-lit to examine for a crack. If no crack was observed, the specimen was loaded again and raised 2.5kN until a crack was observed. The specimens were then loaded in a 30 mm 3-point flexure loading fixture until failure at a cross-head speed of 1 mm/min. After fracture three equa-spaced measurements were made at 80x using an Olympus SZX12 optical microscope.

The fracture toughness was calculated using:

$$KIC = (PfS/bW^{3/2})f(a/W)$$

where

$$f(a/W) = (3/2)(a/W)^{1/2}(1.964 - 2.837a/W + 13.711a^2/W^2 - 23.250a^3/W^3 + 24.129a^4/W^4)$$

where

Pf = Failure load(N), S = Support span(m), B = Thickness(m), W = Width(m) and a = Precrack length

The averages were then calculated with standard deviations.

Results: The results are given in Table 1.

Conclusions: The SEPB method is a good method for determining fracture toughness values in dental zirconias.

<https://doi.org/10.1016/j.dental.2019.08.036>

36

In vitro biocompatibility of extracellular matrix scaffolds with stem cells



GR Jiménez Gastélum^{1,*}, AR Ayala-Ham¹, JA López-Gutierrez¹, R Ramos-Payan¹, GY Castro-Salazar¹, JG Romero-Quintana¹, JE Soto-Sainz¹, EM Aguilar-Medina¹, LF Espinoza-Cristobal², EL Silva-Benitez¹

¹ Autonomous University of Sinaloa, Culiacán, México

² Autonomous University of Ciudad Juarez, Chihuahua, México

Purpose/aim: The necessity to manufacture scaffolds with superior biocompatibility capabilities and biodegradability characteristics has led to the production of extracellular matrix scaffolds (ECM). Among their advantages is a better capacity to allow cell colonization, which enables its successful integration into the tissue surrounding the area to be repaired. The objective of this study is to evaluate biocompatibility of ECM scaffolds with mesenchymal stem cells (MSCs).

Materials and methods: ECM hydrogels were prepared from pig bladder submucosa by decellularization and enzymatic digestion methods; and a conditioned media were prepared by placing the hydrogels for 8 h in shaking. With biocompatibility assays were carried out placing 2,000 cells per well during 1 to 7 days evaluating their capacity to metabolize tetrazolium salts (MTT and LDH). All trials were performed in triplicate with their respective targets and controls. Also, a 24-well culture box was prepared by placing 1 ml of pregel and gelled at 37 °C for 1 hour. 25,000 MSCs were cultured, supplied with 1 ml of supplemented culture medium and incubated at 37 °C for 7 and 14 d. Adherence was evaluated by observing the surface by microscopy and penetration making histological sections with H & E staining.

Results: It was possible to obtain a bladder ECM in the form of a hydrogel of good consistency without cell debris. The biocompatibility tests indicate that the ECM hydrogels do not have cytotoxicity and not affect cell proliferation at the evaluated times. On the surface of the hydrogel it was possible to observe a large number of cells with fibroblastoid morphology at a confluence of 50% of the culture area. In addition, a part of the cells managed to penetrate approximately 500 µm inside the hydrogel maintaining the morphology.

Conclusions: The above results show that the hydrogel allows cell adhesion, penetration and proliferation, which indicates that it does not affect cellular metabolic activity or cause cytotoxic effects.

<https://doi.org/10.1016/j.dental.2019.08.037>

37

Monolithic zirconia structural degradation induced by aging and surface treatments



M.R. Kaizer^{1,*}, R.C. Hintz¹, C.E.P. Borges¹, A.B.F. Fernandes¹, G. Serpa¹, C. Rodrigues², L. Wambier¹, G.M. Correr¹, Y. Zhang², C.C. Gonzaga¹

¹ Positivo University, Brazil

² New York University, USA

Purpose/aim: To investigate the magnitude of structural degradation of a monolithic zirconia induced by clinically relevant grinding and polishing procedures, associated or not to low temperature degradation, caused by accelerated hydrothermal aging in autoclave or thermocycling.

Materials and methods: Ninety Y-TZP discs (Vipi Block Zirconn) were prepared (Ø12 × 1 mm). The specimens were divided into nine groups (n = 10): according to the surface treatment – as sintered (no surface treatment), grind (diamond bur), or grind + polish (diamond bur followed by polishing set); and according to the aging method – baseline (no aging), autoclave (134 °C, 2.2 kgf/cm², 5 h), or thermocycling (200,000 cycles of 5 and 55 °C). The average roughness (Ra – µm) was measured by using a contact roughness meter. The biaxial flexural strength (MPa) was measured in a universal testing machine, with a loading speed of 1 mm/min, using the piston on three balls method, with the specimens immersed in artificial saliva.

The quantification of the monoclinic-zirconia phase fraction was obtained based on X-ray diffraction spectra (XRD). Results were statistically analyzed by two-way ANOVA and Tukey test ($\alpha = 0.05$). The correlation between roughness and biaxial flexural strength was analyzed by Spearman correlation coefficient.

Results: With regards to surface treatment, grind resulted in an increase in roughness (As Sintered = 0.32 (0.10)C; Grind = 0.87 (0.16)A) and flexural strength (As Sintered = 775 (190)B; Grind = 1078 (235)A) compared to the group as sintered. Whereas grind + polish yielded intermediate roughness (0.55 (0.12)B) and flexural strength (1129 (139)A) similar to the group grind. Aging had little effect on roughness, yet it yielded a significant reduction in strength (Baseline = 1149 (232)A; Autoclave = 939 (211)B; Thermocycling = 916 (230)B). Phase transformation from tetragonal to monoclinic was observed in all groups, caused by either mechanical stresses (grind and polish) or by LTD.

Conclusions: Clinically relevant grinding and polishing procedures can potentially compromise the surface quality of monolithic zirconia restorations. Nonetheless, toughening by phase transformation was observed associated to such procedures in this study. However, when those treated zirconia surfaces are exposed to LTD, the strength of the material is compromised.

<https://doi.org/10.1016/j.dental.2019.08.038>

38

Osteogenic and mechanical effect of ZrO₂-bioactive glasses bone graft substitute



T.Y. Kang*, J.H. Ryu, J.Y. Seo, K.M. Kim, J.S. Kwon

Yonsei University College of Dentistry, Seoul, Korea

Purpose/aim: In dentistry, bone graft materials are frequently used in periodontics and oral and maxillofacial surgery. A variety of synthetic bone graft materials has been used over the centuries to heal bone defects. One of them is Bioactive glass (BAG), which possesses both osteoinduction and osteoconduction. However, success of the bone fill also depends on the mechanical properties, where BAG is known to have low fracture toughness in relation to cortical bone. ZrO₂ has been previously studied to enhance mechanical properties of various materials. The aim of this study was to investigate the osteogenic effects, bioactivity and mechanical properties of ZrO₂-BAGs as bone graft materials.

Materials and methods: To make the experimental BAGs, ZrO₂ was added to replace Na₂O on the 45S5 BAG; 1% (Zr1-BAG), 3% (Zr3-BAG), 6% (Zr6-BAG) and 12% (Zr12-BAG) of ZrO₂ was added and the samples were fabricated by the melt-quenching method. The characteristics of BAGs were analyzed using an XRD, SEM-EDS and Vicker's microhardness. For assessing the bioactivity of BAGs, the ability for apatite formation on surface of BAGs upon their immersion in SBF was checked using SEM. The biodegradation test was measured in accordance with ISO10993-14. In addition, ion

release was detected by ICP–OES. MC3T3–E1 cells were cultured in the presence of 1 mg/ml of the BAGs and assessed for cytotoxicity and proliferation. Also, to confirm the osteogenic differentiation, ALP activity after 7 d assessed the expression of the osteoblast phenotype. For the detection of bone formation, using Alizarin Red S assay (ARS) after 21 d. To evaluate cells morphology after 4 d with BAGs, stained with DAPI and rhodamine phalloidin and images were obtained using a fluorescence microscope. The results of each test were statistically analyzed with one-way ANOVA followed by Tukey's test ($P < 0.05$).

Results: Increased fracture toughness has been noted as increase in ZrO_2 contents. Also, ZrO_2 –BAG exhibited slower ion release rate. The presence of a newly formed apatite layer of all BAGs surface were confirmed by SEM. ALP activity and ARS of cells were significantly promoted by BAGs compared to control ($P < 0.05$).

Conclusions: ZrO_2 can improve mechanical properties and control the bioactivity of BAG with the increase of ZrO_2 amount. Also, these BAGs supported both preosteoblast cell proliferation and promoted cell differentiation into cells expressing the osteoblast phenotype. Therefore, it is possible to deduce that the solubility and mechanical properties of ZrO_2 –BAG is controllable through variation of the amount of ZrO_2 , considering the bone graft material's indications.

<https://doi.org/10.1016/j.dental.2019.08.039>

39

Photocontrollable viscosity and hydrophilicity of nanogel based antibacterial dental adhesives



G. Kehe*, R. Trivedi, K. Patel, D. Nair

University of Colorado Anschutz Medical Campus,
Aurora, USA

Purpose/aim: The aim of this study is to synthesize azobenzene nanogels as additives for BisGMA:HEMA dental adhesives and evaluate their impact on microtensile bond strength, viscosity, hydrophilicity, and antibacterial properties.

Materials and methods: Azobenzene nanogels were synthesized via an isocyanate–alcohol solution polymerization in 4X toluene with 4-phenylazophenol, 2-isocyanatoethyl methacrylate, glycerol, and hexamethylene diisocyanate. The nanogels were characterized with dynamic light scattering (Zetasizer Nano™) and triple-detector GPC (Viscotek™). Samples were photopolymerized with CQ/Amine and Elipar™ Dental Curing Lamp (1000 mW/cm²). The viscosity of the ethanol-solvated nanogels in the presence and absence of light was quantified with a Brookfield CAP 2000 + Viscometer at 22 °C. Microtensile Bond Tests were performed using 2 × 2 × 25 mm bar specimens with BisGMA/HEMA/Nanogel formulations with nanogels at concentrations 1, 2.5, and 5 weight percent. Antibacterial studies were performed using *Streptococcus mutans* biofilms grown on adhesive layers in a Brain Heart Infusion Broth (1% sucrose). Adhesives were removed from culture, sonicated in 1X PBS, serial diluted and seeded on BHI Agar plates to quantify the biofilms.

Results: The ability of the ethanol-solvated networks to stabilize the polar cis-isomer of Azobenzenes is observed in the enhanced photofluidization effect and increased viscosity upon irradiation of the samples (19.9 ± 5.1 mPa*s vs 71.2 ± 8.5 mPa*s at 40% nanogel concentration). The microtensile bond strength (μ TBS) of the different networks was assessed, with no statistical significance between test groups and the control, peak stress = 4.0 ± 1.4 , 4.8 ± 2.3 , and 3.45 ± 0.7 MPa for 1, 2.5, and 5% nanogel concentration respectively, and control peak stress = 3.5 ± 2.2 MPa (One-way ANOVA p-value > 0.05). Antibacterial assays indicate a significant reduction in the biofilms present on the BisGMA/HEMA/Nanogel networks after 10 hours of culturing (Control = $1.1 \times 10^9 \pm 1.5 \times 10^8$ CFUs, 1, 2.5, 5% nanogel concentration = $6.16 \times 10^8 \pm 1.8 \times 10^8$, $3.73 \times 10^8 \pm 1.4 \times 10^8$, and $3.9 \times 10^8 \pm 2.0 \times 10^8$ CFUs respectively, One-way ANOVA p-value < 0.0001 for all test groups).

Conclusions: The viscosity and polarity of azobenzene nanogels within BisGMA/HEMA formulations can be dynamically altered to penetrate the interfibrillar spaces on dentin during the application of the adhesive. The ability of the BisGMA/HEMA/Nanogel formulation to prevent *S. mutans* biofilm growth and proliferation is promising and will be investigated further.

<https://doi.org/10.1016/j.dental.2019.08.040>

40

Contrast ratio of bulk fill composite resins with different thicknesses



P.V. Manozzo Kunz*, M.R. Kaizer, G.M. Correr,
L.F. Cunha, C.C. Gonzaga

Universidade Positivo, Curitiba, Brazil

Purpose/aim: The aim of this study was to evaluate the contrast ratio (CR) of four bulk-fill composite resins with different thicknesses after 180 d of water storage.

Materials and methods: Disk specimens with 1 mm, 2 mm and 4 mm in thickness were prepared with four bulk-fill composite resin [Filtek One Bulk Fill (capsule), Filtek Posterior Bulk Fill, Filtek One Bulk Fill, Opus Bulk Fill and SonicFill] ($n = 05$). A spectrophotometer was used to determine color parameters at time periods of 24 hours, 7, 30, 90 and 180 d. CR was calculated as the ratio of reflectance when the specimens were placed on the black background (Yb) to that of the same specimen when it was placed over the white background (Yw): $CR = Yb/Yw$. Data were analyzed by three-way ANOVA and Tukey's test ($\alpha = 5\%$).

Results: The results (Table 1) indicated statistically significant differences for bulk fill resins ($p < 0.0001$), thickness ($p < 0.0001$) and time ($p < 0.0001$). In the double interactions only the resins x thickness interaction showed no statistically significant difference ($p = 0.117138$). All other double and triple interactions (resins x thickness x time) were statistically significant ($p < 0.0001$).

Conclusions: 4 mm specimens showed the higher CR values, compared to 2 mm and 1 mm specimens, after 180 days

Table 1 – Mean values for Contrast Ratio (SD) at different time intervals.

Composite resin	Thickness	CR				
		24 h	7 days	30 days	90 days	180 days
Filtek One Bulk Fill (capsule)	1 mm	0.81 ± 0.02 ^{abA}	0.82 ± 0.01 ^{abA}	0.81 ± 0.02 ^{aA}	0.81 ± 0.01 ^{aA}	0.81 ± 0.02 ^{aA}
	2 mm	0.88 ± 0.01 ^{abA}	0.88 ± 0.01 ^{abA}	0.89 ± 0.01 ^{abA}	0.86 ± 0.02 ^{aA}	0.90 ± 0.01 ^{bA}
	4 mm	0.98 ± 0.02 ^{dA}	0.97 ± 0.02 ^{cA}	0.98 ± 0.01 ^{bA}	0.94 ± 0.04 ^{bA}	0.99 ± 0.03 ^{cdA}
Filtek Posterior Bulk fill	1 mm	0.79 ± 0.01 ^{abA}	0.81 ± 0.03 ^{aA}	0.82 ± 0.02 ^{aA}	0.81 ± 0.01 ^{aA}	0.78 ± 0.03 ^{aA}
	2 mm	0.85 ± 0.02 ^{abA}	0.85 ± 0.02 ^{abA}	0.88 ± 0.02 ^{aA}	0.87 ± 0.02 ^{aA}	0.88 ± 0.02 ^{abA}
	4 mm	0.94 ± 0.03 ^{cdA}	0.99 ± 0.05 ^{cA}	0.96 ± 0.02 ^{bA}	0.99 ± 0.04 ^{cA}	1.03 ± 0.05 ^{cdA}
Filtek One Bulk Fill	1 mm	0.82 ± 0.04 ^{abA}	0.85 ± 0.07 ^{abA}	0.83 ± 0.04 ^{aA}	0.82 ± 0.04 ^{aA}	0.82 ± 0.05 ^{aA}
	2 mm	0.91 ± 0.03 ^{cdA}	0.90 ± 0.01 ^{bcA}	0.95 ± 0.02 ^{bA}	0.93 ± 0.04 ^{bA}	0.92 ± 0.04 ^{bA}
	4 mm	0.97 ± 0.03 ^{cdA}	0.98 ± 0.02 ^{cA}	0.97 ± 0.02 ^{bA}	1.00 ± 0.01 ^{cA}	1.01 ± 0.02 ^{cdA}
Opus Bulk Fill	1 mm	0.79 ± 0.05 ^{aA}	0.80 ± 0.02 ^{aA}	0.83 ± 0.02 ^{aA}	0.81 ± 0.08 ^{aA}	0.82 ± 0.04 ^{aA}
	2 mm	0.88 ± 0.05 ^{bcA}	0.85 ± 0.05 ^{abA}	0.85 ± 0.04 ^{aA}	0.88 ± 0.03 ^{abA}	1.05 ± 0.07 ^{dA}
	4 mm	0.94 ± 0.10 ^{dA}	0.97 ± 0.06 ^{cA}	0.95 ± 0.04 ^{bA}	0.98 ± 0.01 ^{cA}	0.96 ± 0.03 ^{bcA}
SonicFill	1 mm	0.85 ± 0.02 ^{abA}	0.84 ± 0.01 ^{abA}	0.83 ± 0.01 ^{aA}	0.82 ± 0.01 ^{aA}	0.83 ± 0.01 ^{aA}
	2 mm	0.93 ± 0.03 ^{cdA}	0.96 ± 0.05 ^{cA}	0.91 ± 0.06 ^{bA}	0.91 ± 0.05 ^{bA}	0.93 ± 0.07 ^{bA}
	4 mm	0.96 ± 0.02 ^{cdA}	0.97 ± 0.03 ^{cA}	0.98 ± 0.05 ^{bA}	1.00 ± 0.03 ^{cA}	0.98 ± 0.04 ^{cdA}

In each column (time), different small case superscripts indicate significant differences ($p < 0.05$). In each row (composite resin and thickness), different uppercase superscripts indicate significant differences ($p < 0.05$)

of water storage. Considering resins and thickness, for each group, CR values were similar in all evaluated times.

<https://doi.org/10.1016/j.dental.2019.08.041>

41

Evaluation of bond strength to dentin of universal adhesive systems



M.C.A. Lago*, C.L. Mendes, H. Anníbal,
C.P.P. Assis, L.J.R. Oliveira, M.S. Albuquerque,
V.L. Nascimento, A. Nascimento,
P.M. Alcantara, R. Braz

Faculty of Dentistry, University of Pernambuco,
Recife, Brazil

Purpose/aim: Evaluate the bond strength of the seven universal adhesive systems, ClearFil Universal, Universal Scotch Bond, Universal Amber, Ybond Universal, Universal Bond, Tetric N-Bond Universal, Prime & Bond Universal, through adhesive strategy self-conditioning.

Materials and methods: Sixteen healthy human permanent molar teeth were used, with no endodontic treatment, avulsed for therapeutic reasons, through donation of the UEPB

tooth bank, after submission to the Ethics Committee (CEP / UPE) for approval. Immediately after their surgical removal, the dental elements were stored in distilled water solution, then 0.2 % Thymol immersed for 24 h – for disinfection (ISO–TR 11405, 2015), then washed in running water, cleaned with periodontal curettes for posterior prophylaxis with Robson's brush (KG Sorensen) and pumice paste. Afterwards, the teeth were stored in distilled water, replaced weekly, at a temperature of 4 °C, for a maximum period of six months (ISO–TR 11405, 2015). The teeth were submitted to mechanical loading with a 20 kg load cell at a constant speed of 0.5 mm / min (ISO / TS11405, 2003). The initial results were in MPa.

Results: The highest average (Table 1) corresponded to the Scotch Bond Universal group (33.9 MPa), followed by the ClearFil Universal (31.6 MPa), Primer Bond (29.7 MPa) and Tetric–N Bond (29.6 MPa) groups. (20.8 MPa) and ranged from 24.7 to 26.1 MPa in the other two groups, which were found to be significant between groups ($p < 0.001$). The Kruskal–Wallis statistical test showed a significant difference between the Clearfil SE Bond control group and all the other groups of the universal adhesive systems. The Clearfil Universal, Scotch Bond Universal and Tetric N-Bond Universal groups did not present statistical differences, such as Ambar Universal, All-Bond Universal and Prime & Bond Universal, and the Tetric N-Bond Universal and Prime & Bond Universal groups. All universal adhesive systems were superior to the Clearfil SE Bond control group.

Conclusions: The universal adhesives did not present significant differences between the studied groups. The Scotch Bond Universal adhesive showed the best behavior among the other universal adhesives. All universal adhesive systems were superior to the Clearfil SE Bond (self-etching) control group.

<https://doi.org/10.1016/j.dental.2019.08.042>

Table 1 – Mean strength values (SD) in MPa. Different superscript letters indicate significance.

Group	Mean bond strength (SD) MPa
ClearFil Universal	31.7 ^(A) (0.7)
Scotch Bond Universal	33.9 ^(A) (5.2)
Ambar Universal	26.1 ^(B) (2.2)
All Bond Universal	24.7 ^(B) (1.4)
Tetric N-Bond	29.6 ^(AD) (3.4)
Clearfil SE BOND	20.8 ^(C) (2.0)
Primer Bond	29.7 ^(BD) (12.7)

Friday 4th October

42

Influence of biosilicate and propolis on adhesive bond strength



R. Geng-Vivanco*, R. Tonani-Torrieri,
A.B. Silva, F.M. Oliveira, F.C.P. Pires-De-Souza

Ribeirão Preto School of Dentistry, University of
São Paulo, Ribeirão Preto, Brazil

Purpose/aim: This study evaluated the effect of the use of Biosilicate solution associated with propolis on the bond strength (BS) of composite restorations to dentin.

Materials and methods: 320 healthy human molars were selected and flattened on occlusal surfaces. Cavities (5 mm × 4 mm × 4 mm) were prepared. Half of the teeth were submitted to Des-Re protocols for the development of artificial caries. All teeth were separated into eight groups (n = 20) according to the treatment received before the adhesive system (Adper Single Bond Universal, 3M ESPE): Control Group – Adhesive System; CHX Group – 0.12% Chlorhexidine (CHX); Bio Group – 10% Biosilicate solution (Bio); P16 Group – Propolis extract with low levels of polyphenols (P16); P45 Group – Propolis extract with high levels of polyphenols (P45); CHXBio Group – CHX + Bio; P16Bio Group – P16 + Bio; P45Bio Group – P45 + Bio. After restorative procedures, samples were sectioned into sticks in accordance with the “non-trimming” technique, separated and stored in distilled water at 37 °C for 24 h and 6 months. After the storage times, the sticks were submitted to microtensile test (0.5 mm/min). The fracture pattern was analyzed in digital microscope (VH-M100).

Results: According to the results (2-way ANOVA, Bonferroni's test, $p < .05$), there was higher BS ($p < .05$) when the caries-affected dentin (CAD) was treated with CHXBio, P16Bio and P45Bio and tested immediately after restoration, but the BS on this substrate was lower than the sound dentin ($p < .05$) for Control, CHX, Bio and P45 groups. After 6 months aging, the sound substrate presented higher BS ($p < .05$) than CAD for all groups, except for Control, Bio and P45 groups. Regarding the effect of the treatments, there was no difference on the BS ($p > .05$) immediately after restoration for any substrate. After 6 months aging, P16 demonstrated higher BS ($p < .05$) than Control group, with no difference ($p > .05$) among the other groups. Sound dentin presented adhesive and mixed fractures whereas the CAD showed more non-adhesive fractures. Sound groups tested immediately showed higher incidence of non-adhesives fractures when Propolis and/or Bio was applied. After 6 months aging, the non-adhesive fractures increased for all groups.

Conclusions: The pre-treatments with propolis and bioactive-glass can affect the BS of composite restoration to dentin.

<https://doi.org/10.1016/j.dental.2019.08.043>

43

Characterization of a new dental resin composite containing nano-MgO



J. Fu^{1,3,*}, B.S.H. Tonin^{2,3}

¹ Qingdao University, China

² University of Sao Paulo, Brazil

³ University of Minnesota, USA

Purpose/aim: The aim of this study is to incorporate nano-magnesia (nano-MgO) into a new photocurable dental resin to provide it with antibacterial activity.

Materials and methods: Bismethylene spiroorthocarbonate expanding monomer (BMSOC) and 3,4-epoxycyclohexylmethyl-3,4-epoxycyclohexane carboxylate (epoxy) were added into the matrix resin Bisphenol-A diglycidyl methacrylate (Bis-GMA). Camphorquinone (CQ, 1 wt%), N, N-dimethylaminoethyl methacrylate (DMAEMA, 2 wt%) and diphenyliodonium hexafluorophosphate (DPIHFP, 2 wt%) were used as a three-component photo-initiation system. Nano-MgO particles were mixed with micro silica particles at different ratios (2, 4, 6, and 8 wt%) to form fillers. The specimens were then divided into five groups according to Nano-MgO content: Control Group (0 wt%), Group A (2 wt%), Group B (4 wt%), Group C (6 wt%), and Group D (8 wt%). The microstructure and chemical composition of the specimens were analyzed by scanning electron microscopy (SEM) and X-ray energy dispersive spectroscopy (EDS), respectively. The antibacterial effect of the experimental resins on the growth of streptococcus mutans was determined by the film contact test. Wettability and Vickers hardness were also measured.

Results: According to the SEM and EDS analysis, the filler particles were generally well dispersed. However, as the content of nano-MgO increased, agglomeration of the nano particles increased. The water surface contact angle of the experimental groups was significantly higher than that of the control group (0 wt%) ($P < 0.05$). As nano-MgO increased, the antibacterial property of the resin composites gradually increased. However, the Vickers hardness decreased with increasing nano-MgO content (from 0% to 8%).

Conclusions: A new light-cured dental resin composite containing nano-MgO and BMSOC has been successfully formulated. Nano-MgO has shown strong antibacterial activity against Streptococcus mutans and increase the hydrophobicity of the new resin composites.

<https://doi.org/10.1016/j.dental.2019.08.044>

44

Effect of shockwave on desensitizer penetration into dentinal tubules



I.B. Lee*, C.H. Lee

School of Dentistry, Seoul National University,
Seoul, Korea

Purpose/aim: The purpose of this study was to develop a new instrument that can improve the effect of desensitizer using shockwave, and to verify its efficacy.

Materials and methods: A shockwave generation instrument was developed using a piezoelectric actuator (PIA1000, piezosystem jena GmbH, Jena, Germany) and a high voltage pulser (700 V, 100 μ s). The occlusal surface of twenty extracted human upper or lower third molars without caries or restoration was reduced to expose occlusal dentin, and the prepared occlusal surface was acid-etched with 32 % phosphoric acid to remove smear layer. The root apex was connected to a fluid flow measuring instrument (nanoFlow, IB SYSTEMS, Seoul, Korea) and dentinal fluid flow (DFF) was measured for 300 s under water pressure of 25 cm high (Baseline DFF). A desensitizer (SuperSeal, Phoenix Dental, Fenton, USA) was applied on the acid-etched occlusal dentin surface of randomly selected ten tooth specimens, left for 10 s, and rubbed with a microbrush for 30 s (Group 1). For the others, the desensitizer was applied, followed by applying shockwave (100 μ m stroke, 10,000 G) for 10 s (2 shots/s), and rubbed with a microbrush for 30 s (Group 2). DFF was continuously measured in real-time for 300 s before the desensitizer application, and for 600 s after the application procedure. Percent reduction in DFF after desensitizer application (+ shockwave) was calculated with respect to the baseline DFF. Data were analyzed with independent t-test ($\alpha = 0.05$).

Results: For all tooth specimens DFF was decreased after the desensitizer application irrespective of shockwave. Percent reduction in DFF of SuperSeal with shockwave group (Group 2) was $42.8 \pm 19.0\%$, which was significantly higher than that ($26.2 \pm 13.6\%$) of SuperSeal only group (Group 1) ($p < 0.05$).

Conclusions: It was verified by measuring DFF change in real-time that shockwave can help the reduction of dentin permeability by SuperSeal. Shockwave enhances the effect of desensitizer.

<https://doi.org/10.1016/j.dental.2019.08.045>

45

Influence of Water Storage Periods on Properties of Resin Materials



A.F. Lima*, M.V. Salvador, C.H. Saraceni

Paulista University, Jundai, Brazil

Purpose/aim: The aim of the present was to evaluate the effects of different periods of water storage on flexural strength and modulus, water sorption, solubility and mass variation of polymers with crescent hydrophilicity.

Materials and methods: Resins with different hydrophilicity (70–30 %wt BisGMA–UDMA; 70–30 %wt BisGMA–TEGDMA and 70–30 %wt BisGMA–HEMA) were prepared. The initiator system used was camphorquinone (0.4 %wt), dimethylamino ethyl benzoate (0.8 %wt) and bis(4-methyl phenyl)iodonium hexafluorophosphate (0.2 %wt%). The flexural strength and modulus of different formulations were evaluated using a 3-point bending test (25 mm length, 2 mm height, 2 mm thick), after different periods of water storage (0, 14, 30, 60, 180 days). The water sorption and solubility, as well as the mass variation along time (1, 2, 3, 4, 5, 6, 7, 8, 12, 24, 36 h, 7 days, 14 days, 21 days) were also analyzed. For flexural strength and modulus the results were analyzed by ANOVA two-way. For water sorption,

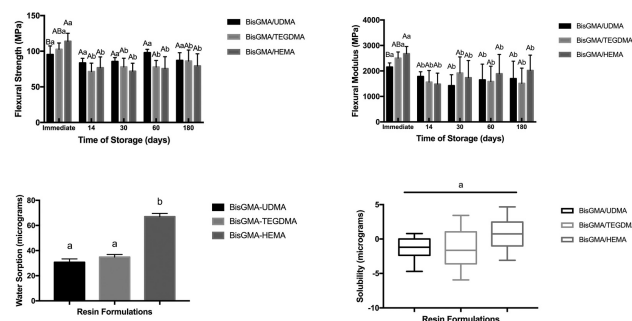


Figure 1

ANOVA one-way was used, and for solubility, Kruskal-Wallis and Dunn's Test.

Results: Bis-GMA-HEMA had the highest flexural strength, and BisGMA-UDMA formulations the lower one without water storage (Fig. 1). However, after water storage, only BisGMA-UDMA resin maintained the flexural strength, with the other formulations presenting a reduction just after 14 days of water storage. For the flexural modulus, BisGMA-HEMA had the highest result and UDMA containing resin the lowest one without water storage. However, for this property, all resins presented a reduction on the results after 14 days of water storage, maintaining the same parameters during all periods evaluated. Resins containing UDMA and TEGDMA had the lowest water sorption than BisGMA-HEMA resins and the solubility of the three formulations tested were statistically similar. Resins with UDMA and TEGDMA had similar mass variation along the periods evaluated. BisGMA-HEMA resin presented a remarkable increase in water uptake after 24 h, increasing along the periods cited.

Conclusions: It could be concluded that the water influenced the properties of the resin materials, however, the flexural modulus seems to be influenced initially, and then the flexural strength, according to the hydrophilic characteristics of the resins.

<https://doi.org/10.1016/j.dental.2019.08.046>

46

Biocompatibility of endodontic repair cements with pulp cells



J.A. López-Gutierrez*, M. Bermúdez, A.R. Ayala-Ham, G. Jiménez Gastélum, G.Y. Castro-Salazar, R. Ramos-Payan, J.G. Romero-Quintana, J.E. Soto-Sainz, E.L. Silva-Benitez, E.M. Aguilar-Medina

Autonomous University of Sinaloa, Culiacán, México

Purpose/aim: Root canal treatment is a complex procedure due to the great variation in the radicular anatomy, which increases the probability of accidents during the biomechanical procedure, whereby different materials have been developed to act as a barrier that promotes the repair of the zone. The aim of this study is to determine the biocompatibility of 3 repair cements in a pulp cells culture.

Materials and methods: A healthy third molar was extracted after obtaining informed consent and transported to the laboratory at 4°C in basic medium (DMEM supplemented with 10% FBS). In a laminar flow hood the crown was cut at the cement-enamel junction to reveal the pulp chamber. Pulp tissue was obtained, cut in small pieces and disintegrated with collagenase (12 mg/ml) and dispase (16 mg/ml). The suspension of dental pulp was seeded in a six well box and incubated at 37°C in 5% CO₂, the culture medium was changed every three days until the cell confluence was achieved. Conditioned media were prepared with different materials evaluated in this study (Biodentine, white MTA and gray MTA) in a concentration of 10 mg/ml during 8 h in agitation. Subsequently, cytotoxicity tests (quantification of released LDH) were performed at 24 h, placing 25 × 10³ cells per well and for proliferation tests (metabolic conversion of MTT to formazan) placing 10 × 10³ cells per well at 24, 48, 72 and 96 h with their respective controls in triplicate. The results were analyzed by one-way ANOVA with Bonferroni post-hoc analysis using the SPSS v20.0 program.

Results: When comparing cytotoxicity between groups ($p > 0.5$), more dead cells were observed in the presence of the cements with respect to the control, in increasing order: Control (1546.6), white MTA (3530.8), Biodentine (3823.2) and gray MTA (5177.9). In proliferation assay, it was very similar between the Biodentine and the control ($p > 0.5$). MTA cements show a delay in the growth kinetics ($p > 0.5$), despite this, gray MTA group obtain a greater number of cells at 96 h of exposure.

Conclusions: The results show that evaluated materials presents no high cytotoxicity, however, the MTA-based cements delayed proliferation at 48 and 72 h, suggesting alterations in the cell cycle, which will be evaluated in future investigations. It is concluded that Biodentine presented the best biocompatibility of the materials studied.

<https://doi.org/10.1016/j.dental.2019.08.047>

47

Water sorption property of experimental nanocomposite

H.Y. Marghalani

Faculty of Dentistry, King Abdulaziz University, Jeddah, Saudi Arabia

Purpose/aim: The aim of this in vitro study was to evaluate water sorption property [sorption (S), solubility (SL) and percentage of mass change (Mg%)] of an experimental nanocomposite following immersion in distilled water.

Materials and methods: A disc-shaped specimen of each composite material [experimental graphene-based nanocomposite (GnC) and Tetric® N-Flow (TNF)] were fabricated in a split-Teflon mold and irradiated by poly-wave LED light-curing unit (Bluephase 20i, Ivoclar/Vivadent) at 1000 mW/cm² for 20s covering eight overlapping sections on each side. The volume of each specimen was calculated and then placed inside a desiccator containing silica gel, thereafter, weighed on an analytical electronic balance until a

constant mass m1 obtained. The specimens were immersed in vials containing distilled water maintained at 37°C for different time intervals: 1, 24, 48 and 168 h, where the sorption (S) property (μg/mm³) was calculated after obtaining m2. The SL and Mg% were measured after 168 h of immersion. The data were statistically analyzed by independent sample t-test one-way ANOVA and post hoc Tukey's test ($p < 0.05$).

Results: Analysis of variance revealed highly significant differences between the different immersion times for water sorption values examined ($p < 0.05$). Independent samples T-test expressed high significant differences of all the sorption values between GnC and TNF composite materials ($p < 0.05$). The highest liquid's sorption was exhibited by TNF material after immersion in distilled water for 168 h period followed by GnC at the same time-interval (19.18 and 17.21 μg/mm³, respectively), while the lowest sorption was presented by GnC nanocomposite after 1 h immersion period in water (3.71 μg/mm³). The solubility (SL) value was higher for TNF than that for GnC after 168 h immersion period.

Conclusions: The low sorption and solubility values for GnC could be related to its higher filler load, inclusion of hydrophobic graphene nanofillers or presence of silanated hydroxyapatite nanofillers.

<https://doi.org/10.1016/j.dental.2019.08.048>

48

Increased cariogenic biofilm formation on under-cured bulk fill composites



M.A.S. Melo^{1,*}, H. Maktabi¹, M. Ibrahim¹, A. Balhaddad², Q. Alkhubaizi¹, A.P.P. Fugolin², C.S. Pfeifer², H. Strassler¹

¹ University of Maryland School of Dentistry, Baltimore, USA

² School of Dentistry, Oregon Health & Science University, Portland, USA

Purpose/aim: Bulk fill composites rely on optimal curing to ensure ideal material properties at the base of thick increments. In general dental practice, variations on the curing conditions can decrease adequate radiant exposure (RE) which may trigger potential deleterious effects on the restoration longevity. This study aims to assess the influence of inadequate RE on the degree of conversion (%DC), Streptococcus mutans biofilm formation of bulk-fill (BF) composites under different light curing conditions.

Materials and methods: A factorial design 2 × 4 was applied where two light curing units (LCUs) holding 600 and 1,000 mW/cm² were used on the simulation of four different clinical scenarios for curing of 4-mm bulk fill composite: (1) optimal- no light tip angulation and no separation between the tip and the surface of the specimen; (2) light tip 2 mm away from the surface of the specimen, (3) light tip angulation (θ = 20°); and (4) moderate tip angulation (θ = 35°). RE was recorded using the spectrometer. %DC was measured in the top and bottom of composites. After subject to an S. mutans biofilm model, colony-forming units (CFU), and surface rough-

ness were assessed. Two-way ANOVA and Tukey post-hoc test ($\alpha=0.05$) were used.

Results: The influence of RE expressed in J/cm² on *S. mutans* CFU values, and DC% are dependent on the curing conditions and radiant emittance ($p<0.05$). The influence of the underperformed conditions ($F=10.48$, $p<0.001$) and radiant emittance of LCU ($F=10.30$, $p=0.0024$) on the RE were significant. Moderate angulation reports a significantly reduced RE for both LCUs. For 600 mW/cm² –LCU increased biofilm formation, and reduced %DC were found for all tested scenarios. For 1000 mW/cm² –LCU, there was increased biofilm only in the condition of moderated angulation.

Conclusions: Inadequate curing of bulk fill composites could impart increasing bacterial colonization on the bottom surface of a bulk fill composite. The irradiance from LCUs has a significant influence on the biofilm. The use of LCU with 1000 mW/cm² was able to overcome the detrimental increasing of bacterial colonization on the bulk fill surface under light tip displacement and angulation. The use of optimal curing conditions and high irradiance LCU are preferred to avoid increased biofilm formation that may compromise the longevity of such restorations and accelerate the incidence of secondary caries.

<https://doi.org/10.1016/j.dental.2019.08.049>

49

Microstructure of new lithium-disilicate CAD/CAM block



T. Miyake*, K. Kato, S. Akiyama, T. Azuma, K. Yamamoto, K. Kojima, K. Nagaoka, K. Shiraki, A. Fujimoto, T. Sato, T. Kumagai

Research & Development Department, GC Corporation, Tokyo, Japan

Purpose/aim: In the dental clinics, lithium–disilicate (LDS) glass ceramic products are famous and useful because of advantage of aesthetic and physical property. These days, digital-dentistry is becoming mainstream and various products with LDS advantage are applied for CAD/CAM. Initial LiSi Block, LDS glass ceramic block for CAD/CAM, is developed with focusing on one-visit treatment (No heat treatment required) and long-term prognosis (good compatibility and durability) in addition to LDS advantage. The objective of this study was to evaluate the stability of the LDS glass ceramic block for CAD/CAM.

Materials and methods: After immersion in 5N NaOH (aq) at 60 °C for 5 d, the crystal structure on polished surface of Initial LiSi Block (LSB, GC), IPS e.max CAD (EMC, Ivoclar Vivadent) and CELTRA DUO (CED, DentsplySirona) was observed with SEM (SU-70, HITACHI) and relative crystalline surface area was measured by image analysis software (Image J, NIH). To evaluate edge-stability, the triangular prism shaped master model with an angle of 30° was scanned with CEREC Omnicam (DentsplySirona). And, each of materials was ground with CEREC MC XL (DentsplySirona) ($n=8$). After grinding, arithmetic mean line roughness (Ra) and maximum height (Rz) of the specimen's edge (Fig. 1, see arrow) were measured with 3D Measuring Microscope (VR-5000, Keyence).

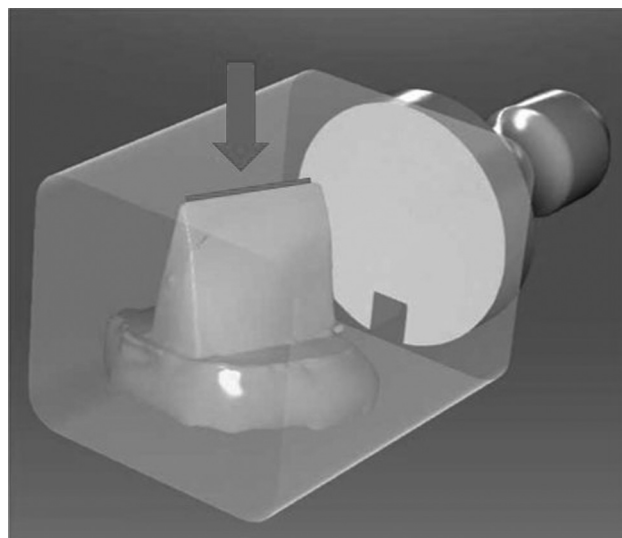


Figure 1

Results: After grinding test, LSB showed lower Ra ($9.1 \pm 6.6 \mu\text{m}$) and Rz ($61.3 \pm 26.8 \mu\text{m}$) compared to EMC (Ra: $37.1 \pm 11.7 \mu\text{m}$, Rz: $262.6 \pm 119.8 \mu\text{m}$) and CED (Ra: $32.2 \pm 25.1 \mu\text{m}$, Rz: $208.2 \pm 127.9 \mu\text{m}$). SEM observation confirmed high density and fine crystal precipitation in LSB glass matrix (relative crystalline surface area is 71.3%) and revealed that LDS crystal size of LSB were smaller than that of EMC and CED.

Conclusions: Thanks to high density and micronized crystal structure, it is suggested that Initial LiSi Block as a new LDS glass ceramic block has the accurate designed marginal edge and is expected to have long-term stability in clinical use.

<https://doi.org/10.1016/j.dental.2019.08.050>

50

Inhibition of streptococcus mutans biofilms on azopolymer composite restorations



D.I. Mori*, G.M. Kehe, M.J. Schurr, D.P. Nair

University of Colorado Anschutz Medical Campus, Aurora, USA

Purpose/aim: The aim of this study is to develop oral antibacterial polymeric coatings that can 1) inhibit the growth of *S. mutans* biofilms and 2) dynamically remove biofilms from the surface of resin restorations.

Materials and methods: Phenolic acrylic azobenzene monomers (OH-AAZO) were synthesized, characterized (via ¹H NMR), and polymerized as the ultimate layer of acrylic resin restorations. The polymerization was monitored via near Fourier-transformed infrared spectroscopy by observing the disappearance of the acrylate peak ($\sim 6167 \text{ cm}^{-1}$). The azobenzene-coated resins were characterized via Dynamic Mechanical Analysis (TA Q800) and cytotoxicity assays (ISO9993 using L929 mouse fibroblast cells). *S. mutans* biofilms were grown under sucrose-rich conditions on the surface of azobenzene-coated acrylic resins, removed after 24 h via

sonication, and serially diluted/plated to quantify the colony forming units (CFUs). The azobenzene concentration dependence on biofilm growth and proliferation was studied. The elimination and detachment of mature *S. mutans* biofilms for up to 72 h was initiated via intermittent light exposure (430–490 nm, FlashMax™ dental lamp, 3 s flashes) and washes in PBS. Biofilm growth and disruption were imaged via a Zeiss digital microscope.

Results: The presence of polymerized OH-AAZO coatings at concentrations of $>5 \mu\text{g}/\text{mm}^2$ were shown to successfully inhibit *S. mutans* biofilm formation (0 CFU's, $n>3$) relative to biofilms grown on uncoated substrates (10^8 CFU's, $n>3$) over a 24 h time period. The effectiveness of OH-AAZO to inhibit biofilm growth is concentration dependent, with $6 \mu\text{g}/\text{mm}^2$ coatings having higher antibacterial activity compared to $0.6 \mu\text{g}/\text{mm}^2$ coatings. The phenolic azobenzene monomers resulted in inhibiting the growth and proliferation of *S. mutans* biofilms (0 CFU's, $n>3$) compared to hydroxyl and phenolic groups with/without the presence of azobenzenes (1.68×10^8 CFU's, $n>3$). The OH-AAZO also demonstrated long-term inhibition (0 CFU's, $n=3$) in sucrose-dependent conditions over 48 h. Both the thermomechanical properties and cytocompatibility of the acrylic resin were not impacted by the presence of azopolymer coatings.

Conclusions: Preliminary results indicate that OH-AAZO can inhibit *S. mutans* biofilm formation on resin restorations for up to 24 h while being able to opto-mechanically disrupt mature biofilms at 48 h. Future work will focus on elucidating the biofilm elimination pathway via assays that quantify the inhibition of the electron transport chain (ETC) upon introducing an OH-AAZO coating. Future work will also focus on designing azobenzene molecules and polymers with the ability to selectively inhibit and detach *S. mutans* biofilms from the surface of composite restorations.

<https://doi.org/10.1016/j.dental.2019.08.051>

51

Effect of experimental S-PRG giomer®-based toothpastes on dentin hydraulic conductance



V. Mosquim^{1,*}, G.S. Zabeu^{1,2},
G.A. Foratori-Junior^{2,3}, L.S. Condi¹,
R.A. Caracho¹, D. Rios², L. Wang¹

¹ Bauru School of Dentistry, University of São Paulo, Bauru, Brazil

² School of Dentistry, Sagrado Coração University, Bauru, Brazil

³ University of Integrated Faculties of Ourinhos, Ourinhos, Brazil

Purpose/aim: Clinically, dentin hypersensitivity (DH) is related to dentin exposure and increase in its permeability. Therefore, one strategy to minimize this condition is by using fluoridated vehicles to obliterate exposed dentin tubules. As fluoridated toothpastes constitute a daily, low-cost and effective strategy to control dental caries, it could also promote some level of tubule obliteration and lead to the control of DH. Hence, this study aimed to analyze the effect of a new tech-

nology based on a multiple ion releasing system with S-PRG (surface pre-reacted glass) Giomer using experimental toothpastes containing 0%, 1%, 5%, 20% and 30% on reducing hydraulic conductance (Lp).

Materials and methods: The Lp of the dentin disks (1.0 ± 0.2 mm) was evaluated using Flodec. All specimens were etched in 37% phosphoric acid solution (15 s) to allow random allocation into 5 groups ($n=8$). The minimum (smear layer) and the maximum (after acid etching) Lp values were recorded. Treatments were performed using the designated toothpaste applied actively for 15 s, and left rest for 1 min as follows: 1) SPRG Giomer® 0 wt.%, 2) SPRG Giomer® 1 wt.%, 3) SPRG Giomer® 5 wt.%, 4) SPRG Giomer® 20 wt.%, and 5) SPRG Giomer® 30 wt.%. The Lp after each treatment was assessed. Samples were exposed to an erosive challenge (6% citric acid, pH 2.1, 1 minute), and the final Lp was recorded. Kruskal-Wallis for analysis between groups, and Friedman for comparisons between periods, followed by post-hoc Dunn were used ($p<0.05$).

Results: For comparisons between periods, at all groups, the lowest values of Lp were seen for minimum Lp, and it differed from all other Lp values, which did not differ from each other ($p<0.0001$). For comparisons between groups, all groups were similar for minimum and maximum Lp values ($p<0.039$). The optimal level of obliteration was noticed for the 5% group, which was similar to the 30% group and differed from 0%, 1% and 20%.

Conclusions: It can be concluded that the SPRG Giomer® at 5% seems to present a promising desensitizing potential, with perspective to offer stability overtime under erosive challenge.

<https://doi.org/10.1016/j.dental.2019.08.052>

52

Antimicrobial Effects of Zinc-Fluoride Releasable Glass-Ionomer Cement on Fusobacterium Nucleatum



Y. Nagano*, D. Mori, T. Kumagai

GC Corporation, Research & Development, Tokyo, Japan

Purpose/aim: CAREDYNE RESTORE is the next generation glass ionomer cement (GIC) for prevention and restoration. CAREDYNE RESTORE contains BioUnion Filler which releases Zn^{2+} , Ca^{2+} and F^- . Each ion has been reported to show several bioactive effects. We have presented inhibitory effect of root dentin demineralization at ADM 2018. *Fusobacterium nucleatum* is a gram-negative organism that is commonly found in the dental plaque. It's reported that *F. nucleatum* might have an indirect role in dental plaque maturation, contributing to the conditions necessary for the survival of *P. gingivalis* and possibly other anaerobes less tolerant to oxygen. The purpose of this study is to evaluate antimicrobial effects of CAREDYNE RESTORE on *F. nucleatum*.

Materials and methods: CAREDYNE RESTORE (CAR, GC, Tokyo, Japan), Fuji IXGP EXTRA (EX, GC), ACTIVA Bioactive-Restorative (AR, Pulpdent), Beautifil Flow Plus X (BF, Shofu) were used in this study. Sample extract solution was

made as below: Material was filled in acrylic mold (? 10 mm, d 2 mm) and stored at chamber (37 °C, 1 h). After removal, sample was immersed in BHI culture medium (1 mg/L Vitamin K1, 5 mg/L Hemin) and stored at chamber (37 °C, 24 h). Finally, sample was removed, and culture was filtered. Control was culture medium only. *F. nucleatum* suspension was made as below: 50 µL of *F. nucleatum* (ATCC10953) stock solution was added to culture medium (10 mL) and cultured under anaerobic condition (37 °C, 24 h). Suspension was diluted with culture medium to adjust absorbance (OD600=0.3). Suspension 10 µL and extract solution 90 µL was added to 96well plate (final value of absorbance was 0.03) and incubated under anaerobic condition for 24 hrs (37 °C, n = 3). Finally, absorbance was measured (OD600). Tukey–Kramer was used for statistical analysis ($p < 0.05$).

Results: The lowest value was observed in CAREDYNE RESTORE, and significant difference was observed to other material. Ion homeostasis affects the proliferation, communication, metabolism and survival of bacteria. F^- has been reported to acidify the cytoplasm and reduce proton gradient and enzyme activity of bacteria. On the other hand, when the concentration of extracellular Zn^{2+} increases, the bacteria will transport some cations, including Zn^{2+} , into the cell to maintain their membrane potential. It is known that intracellular cation accumulation could result in depolarization of membrane potential and ultimately destruction of cells. F^- was detected from all samples without control, however Zn^{2+} was only observed from CAREDYNE RESTORE extract solution.

Conclusions: CAREDYNE RESTORE has superior antimicrobial effects and it was shown to be useful as a preventive and restorative material.

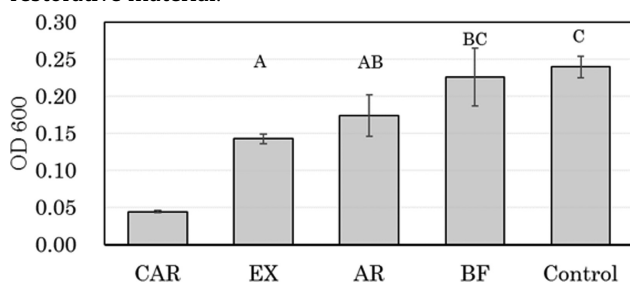


Fig. Results of absorbance after cultivation (same superscript indicates no significant difference).

<https://doi.org/10.1016/j.dental.2019.08.053>

53

Withdrawn

54

Effect of ceramic on degree of conversion of cements

Q.N. Sonza*, G. Pizzolatto, A.D. Bona, M. Borba

University of Passo Fundo, Brazil

Purpose/aim: Low-viscosity resin composite was proposed as a cementation material of all-ceramic restorations. The aim of this study was to evaluate the effect of a lithium disilicate

laminate on the degree of conversion (DC) of a low-viscosity resin composite.

Materials and methods: Two cementation materials were evaluated: RC– low-viscosity resin composite (Tetric N-Flow, Ivoclar Vivadent) and LC– light-cured resin cement (Variolink Esthetic LC, Ivoclar Vivadent). Specimens were produced using a matrix (5 mm diameter and 0.4 mm thickness) and they were light activated (Bluephase G2, Ivoclar; 800 mW/cm²) directly over the material or throughout a 0.5 mm thick lithium disilicate laminate (n=5), for the time recommended by the manufacturer. FTIR spectra (Agilent Technologies Cary 630) was recorded for the materials immediately (10 min) and after 24 h of light curing and the degree of conversion was calculated (DC%). Data were statistically analyzed with ANOVA and Tukey tests ($\alpha = 0.05$).

Results: When DC was measured immediately, RC was similar to LC; and the presence of the ceramic laminate resulted in lower DC in both materials ($p < 0.001$). Yet, when the DC was measured after 24 h, there was no effect of the ceramic laminate ($p = 0.089$). The DC of RC and LC cured throughout the ceramic laminate increased after 24 hours.

Conclusions: Lithium disilicate-based ceramic laminate affected the immediate DC of luting materials, which increased after 24 hours. The DC of low-viscosity resin composite is similar to the light-cured resin cement.

<https://doi.org/10.1016/j.dental.2019.08.055>

55

Design optimization of all-ceramic crowns

R. Ottoni^{1,*}, J.A. Griggs², P.H. Corazza¹, M. Borba¹

¹ Dental School, University of Passo Fundo, Brasil

² Department of Biomedical Materials Science, University of Mississippi Medical Center, Jackson, USA

Purpose/aim: To estimate the combination of factors involved in the design of all-ceramic crowns (abutment preparation, ceramic processing, and scanning method) that provide the best mechanical behavior and adaptation.

Materials and methods: Two types of abutment preparations chamfer (C) and round angle (A), were produced with a dentin analogue material (G10). For extra-oral scanning (E), an impression of the abutments was obtained, and a plaster model was produced. For intraoral scanning (I), abutments were directly scanned. Captured images were processed using CAD software, and the design of a second upper premolar was used to produce the crowns. Blocks of lithium disilicate glass-ceramic (Cad, e-max CAD) were milled using CAD/CAM system and subjected to a crystallization cycle. For the heat-pressing method (Press, e-max PRESS), crowns were first 3D-printed using a polymeric material and the heat-pressing protocol was performed according to the manufacturer instructions. Design of experiments (DOE) was used to estimate the experimental groups and sample size for adaptation and fracture load analysis. To evaluate the inner and marginal adaptation, the replica technique was used. Then, crowns were adhesively cemented to the respective abutments

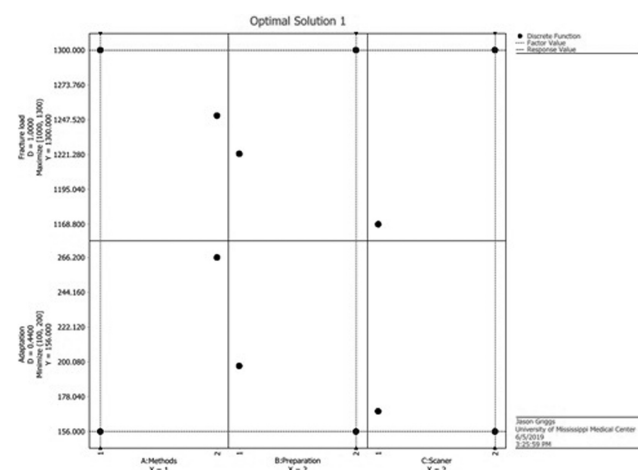


Figure 1 – Graph showing the optimal design parameters of the study, combining the chamfer abutment preparation (Preparation 2), extra-oral scanning (Scanner 2) and heat-pressing method (Method 1). The fracture load and mean gap thickness chosen as target were 1300 N (minimum 1000 N) and 100 µm (maximum 200 µm), respectively.

and loaded to fracture using a universal testing machine (0.5 mm/min, 37° distilled water). ANOVA and multiple linear regression statistical tests were used to investigate the significant effects for each dependent variable. In addition, the best combination of factors to achieve an optimum value of both adaptation and fracture load was estimated (optimization).

Results: For fracture load, only the scanning method was significant. Crowns produced with the extra-oral scanning showed the highest fracture load ($p=0.025$). For adaptation, only ceramic processing was significant, meaning that the gap thickness of crowns produced with the heat-pressing method was smaller ($p<0.001$). The optimum design parameters (Fig. 1) achieved 100% of the desired fracture load (above 1000 N) and 44% of the desired adaptation (below 200 µm).

Conclusions: The best combination of factors to achieve an optimum value of both adaptation and fracture load for the all-ceramic crowns was chamfer abutment preparation, extra-oral scanning and heat-pressing method.

<https://doi.org/10.1016/j.dental.2019.08.056>

56

Effect of Light Tip Optical Design on Dental Radiometer Accuracy



W.M. Palin*, M. Hadis, A.C. Shortall

University of Birmingham, UK

Purpose/aim: Studies have shown Dental Radiometers (DRs) vary widely in accuracy for some light curing units (LCUs) mainly because of sensor and aperture size, filters and spectral responsivity. A new hypothesis is that LCU tip design; Type I (fiber-bundle light guide) or Type II (light source at tip) can influence the accuracy of DRs. Consequently, a novel light measurement device checkUP (BlueLight Analytics Inc.) has

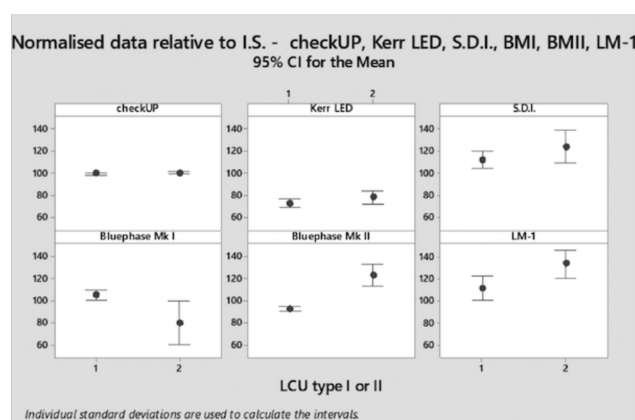


Fig. 1

been developed that relies on machine learning to calibrate a nonlinear spectral response sensor and light interaction effects between the light and meter. This study aims to compare this device to five commercially available DRs and to the “Gold Standard” (GS) spectrometer method as described in the ISO 10650 (2018).

Materials and methods: Irradiance was measured from nine Type I and five Type II LED LCU models using five commercial DRs and checkUP. GS irradiance values were derived from power measurements made with a laboratory grade integrating sphere and fiber-optic coupled spectrometer setup. Data sets were analysed with standard parametric (GLM ANOVA) and non-parametric (Kruskal-Wallis and Mann Whitney U) test methods ($p=0.05$). Irradiance results from the DRs and checkUP were normalised relative to GS data for comparison purposes.

Results: Substantial discrepancies were reported between the GS and commercial DRs (Fig. 1). Pooled normalised percentage differences (Type I & II combined) were >20% relative to mean GS data except for the Bluephase Meter II (Ivoclar-Vivadent; 15.9%) and checkUP (1.8%). Mean peak differences between the DR and individual LCU and LCU modes ranged from 5.5% (checkUP) to 100% (LED, SDI). The inaccuracy of the five commercially available DRs differed significantly ($p<0.001$) according to LCU Type (I or II) for the Bluephase Meters I&II, with better results for Type I units (<10% difference relative to GS) compared with Type II units (>20% of GS). No significant difference (Kruskal-Wallis test $P>0.05$) between the inaccuracy of the other 3 commercial DRs was found according to LCU type (Kerr LED, $P=0.09$; S.D.I., $P=0.356$; LM-1, $P=0.204$).

Conclusions: The inaccuracy for some DRs was significantly affected by LED LCU type ultimately impacting curing times required for light cured materials. checkUP offers a reliable way of determining LCU irradiance output across different LCU types and is comparable to the Gold Standard ISO 10650 (2018) spectrometer method. Further work with a wide range of LED LCUs and DRs is indicated to investigate this subject further.

<https://doi.org/10.1016/j.dental.2019.08.057>

57

Evaluation of bone regeneration at socket-filled extraction sites with PRF



G. Park^{1,*}, G. Kurgansky¹, A. Torroni²,
L.F. Gil³, R. Neiva⁴, L. Witek¹, P. Coelho^{1,2}

¹ New York University College of Dentistry, New York, USA

² NYU Langone Medical Center, New York, USA

³ Department of Dentistry, Universidade Federal De Santa Catarina, Br

⁴ University of Florida College of Dentistry, Gainesville, USA

Purpose/aim: Following tooth extraction, the alveolar ridge undergoes a remodeling process that may affect the integration of implants, their ability to properly function, and the esthetic results of prosthodontic therapy. To minimize alveolar bone loss, various treatments have been proposed such as alleviating extraction trauma, limiting flap elevation, and performing distraction osteogenesis, guided bone/tissue generation (GBR/GTR), and socket preservation. Socket preservation is intended to enable placement of stable dental implants and reduce alveolar bone loss and need for additional grafting procedures. The aim of this study was to compare the effects of PRF and grafting material in facilitating alveolar ridge preservation.

Materials and methods: The study utilized a 6 week in vivo canine model ($n=7$). The grafting material utilized was Geistlich Bio-Oss[®] (Geistlich Pharma Inc[®]) and autogenous PRF. The first molars were bilaterally extracted with the right side receiving no material (negative control) in one socket and the second receiving Bio-Oss (positive control). The left side adopted the same design in combination with PRF. Samples were harvested, histologically processed and evaluated for bone area fraction occupancy (BAFO). A linear mixed model (ANOVA Test, Confidence Interval 95%) analysis was conducted.

Results: Statistically significant differences in BAFO were detected for the defects which received grafts compared to the negative control ($p=0.041$). The empty defect had significantly less bone regeneration compared to the empty defect with PRF ($p=0.03$) Bio-Oss with and without PRF better maintained vertical ridge dimension compared to the empty defect ($p=0.016$ & $p=0.006$). A significant difference in the area of coronal soft tissue infiltration was noted for the empty defect with PRF and Bio-Oss with and without PRF compared to the empty defect. ($p=0.015$, $p=0.024$, $p=0.001$). Collapsed across all groups, PRF exhibited statistically greater means than the groups without PRF. ($p=0.038$) Furthermore, Bio-Oss better maintained the vertical ridge dimension and resulted in less area of coronal soft tissue infiltration compared to the empty defect. ($p=0.044$ & $p=0.046$)

Conclusions: No further bone healing was achieved by adding PRF to particulate xenograft, 6 weeks in vivo. PRF, when utilized alone, augments socket regeneration to levels comparable to xenografts, suggesting PRF as a viable material for socket preservation. Bio-Oss preserved the vertical ridge dimension and PRF resulted in comparable less area of cor-

nal soft tissue infiltration to Bio-Oss. No significant horizontal ridge augmentation was noted. Further investigation is warranted at different time points to fully assess early and late healing.

<https://doi.org/10.1016/j.dental.2019.08.058>

58

Stress relaxation behavior in glassy methacrylate networks containing thiourethane-based oligomers



S.H. Lewis, A.P.P. Fugolin, J.L. Ferracane,
C.S. Pfeifer*

Oregon Health & Science University, Portland, USA

Purpose/aim: Thiourethane oligomers have been shown to reduce stress development during polymerization when added to methacrylate networks. Other than delayed gelation afforded by pendant thiol groups, this study tested the hypothesis that stress relaxation via active strand behavior also contributed to lower stress results.

Materials and methods: Unfilled BisGMA/UDMA/TEGDMA (50/30/20 wt%) was mixed with 0 (control) or 20wt% of the following oligomers: thiourethane (TU = trithiol + diisocyanate), thiol-ene (TE = trithiol + trivinyl) or urethane (UMA = triol + diisocyanate, methacrylated with 2-isocyanateethyl methacrylate). The photoinitiator system was 0.2/0.8 wt% camphorquinone/ethyl 4-(dimethylamino)benzoate, and 0.5 wt% butyl hydroxytoluene was the inhibitor. Bar specimens (1 x 3 x 25 mm, $n=3$) were photopolymerized at 320–500 nm with 850 mW/cm² for 2 min on each side, then heat treated at 180 °C for 24 h (until conversion >90%). Bars were subjected to stress relaxation testing in a dynamic mechanical analyzer in tension mode (0.1% strain, 1 Hz, 30 min deformation time) at 25, 45, 65, 85, 105, 125, 145 °C. Characteristic stress relaxation times were calculated with the Arrhenius equation. Elastic/viscoelastic moduli (E_1/E_2) and viscosity (η) were calculated through fit to the standard linear viscoelastic model for each of the temperatures. Data were analyzed with one-way ANOVA/Tukey's test ($\alpha=5\%$).

Results: Results for stress relaxation as a function of temperature are shown in Fig. 1. None of the materials reached the Arrhenius threshold (37%) for stress relaxation at 25 °C. In general, the oligomer-containing materials presented faster relaxation times, and greater overall relaxation. The negative values of relaxation may be due to the relatively low strain used in the test, and this will be investigated further in the future. The elastic component is represented by E_1 , while the viscoelastic component of the relaxation is a combination of E_2 and η . The variation in E_2 and η (MPa and Pa*s, respectively) between 45 and 145 °C was greater for the oligomer containing materials (ΔE_2 – Control: $-145.0 \pm 95.0a$; TU: $+53.7 \pm 10.1d$; TE: $+20.5 \pm 9.0c$; UMA: $+76.4 \pm 22.3b$; $\Delta \eta$ – Control: $-8.0E3 \pm 4.8E3a$; TU: $-5.3E3 \pm 7.3E2a$; TE: $-7.6E2 \pm 2.2E2a$; UMA: $-4.4E3 \pm 3.6E2a$), indicating that the viscoelastic component contributed more markedly to the relaxation compared to the control, especially for the TU-containing material. No trend was observed

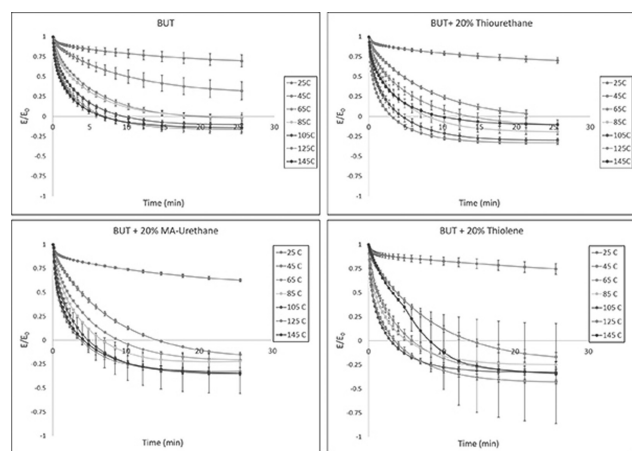


Figure 1: Stress relaxation profile for the BUT control material, and oligomer-containing materials.

Figure 1

in terms of E1 (in MPa): Control: $-44.9 \pm 19.0a$; TU: $-44.9 \pm 22.0a$; TE: $+28.6 \pm 0.3c$; UMA: $+4.0 \pm 0.4b$.

Conclusions: All oligomer-containing materials presented greater stress relaxation behavior compared to the control. The viscoelastic component played a major role in stress relaxation, particularly for the TU-containing material.

Support: NIH-NIDCR (U01-DE023756; R01-DE026113; K02-DE025280).

<https://doi.org/10.1016/j.dental.2019.08.059>

59

Dentin adhesives modified with DMSO: cell viability and produced cytokines

C.T.A. Pimenta*, A.B. Meireles, I.M. Ottoni, I. D'angellis, P. Barroso, B. Avelar-Freitas, G.E. Brito-Melo

PRPPG, Federal University, Diamantina, Brazil



Purpose/aim: This study was aimed at verify the toxicity of a comercial adhesive system modified with 3 different concentrations of DMSO. Cell viability and the expression of two cytokines: tumor necrosis factor- α (TNF- α) and interferon- γ (IFN- γ) by lymphocytes populations were evaluated.

Materials and methods: Adper Single Bond Adhesive (SB) was modified by the incorporation of 0, 1.25, 2.5 and 5% v/v of DMSO (SB, SB 1.25, SB 2.5 and SB 5, respectively) following previous studies. After homogenization, specimens of 1X2X8mm were made and photoactivated. For the viability analyses, cultures of human lymphocytes were isolated from approximately 10mL of human venous blood sample from volunteers ($n=5$). Lymphocytes were incubated for 24hours with adhesive (SB, SB 1.25, SB 2.5 and SB 5 groups) and without adhesive (control group) specimens. Then they were analyzed to determine cell viability by the trypan blue exclusion method. For cytokines analyses, non stimulated cultures (NC) and stimulated cultures ($n=3$) (with phorbol-12-myristate-13-acetate-PMA -PMA-, ionomycin and brefeldin-A). Cells were permeabilized and

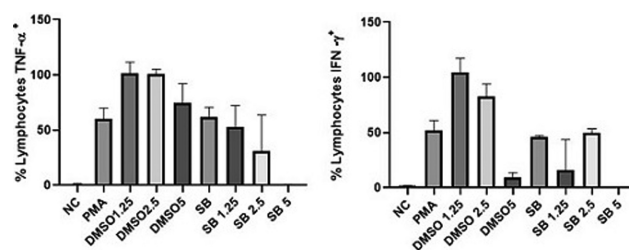


Figure 1

incubated with monoclonal antibodies conjugated with specific fluorochromes for cytokines IFN- γ (mAb-IFN- γ -PE-Cy7) and TNF- α (mAb-TNF- α -PE). The cytokines expression was evaluated for NC and PMA groups as well as for stimulated groups treated with DMSO at 1.25, 2.5 and 5% and cultures in direct contact with specimens of SB, SB 1.25, SB 2.5 and SB5 using a BD FACSCanto™ with 30,000 events recorded.

Results: There was no significant difference for the percentage values of live cells between the control group NC ($98\% \pm 0.82$) and the groups SB, SB 1.25, SB 2.5 and SB5 ($p < 0.05$) (One way Anova, post hoc of Tukey) demonstrating that the DMSO incorporated did not decreased lymphocytes viability. Figure 1 shows the tables for cytokines expression and it was possible to observe the potential of the incorporation of such solvent in a dental adhesive to provide a biomaterial with anti-inflammatory potential by the means values, in spite of no statistically significant differences.

Conclusions: The results suggested that the modified adhesive has potential to improve comercial dental adhesives since non-significant statistical differences were evident for lymphocytes viability. Cytokine expression results encourage further experiments increasing the number of individuals studied.

Acknowledgement: "The authors acknowledge the PRPPG/UFVJM and CAPES for the financial support."

<https://doi.org/10.1016/j.dental.2019.08.060>

60

Effectiveness of a universal adhesive used as silane-coupling agent

T.S. Porto^{1,*}, A.J. Faddoul¹, S.Y. Park¹, F.F. Faddoul¹, M.F. De Goes²

¹ Case Western Reserve University, USA

² Campinas State University, Brazil

Purpose/aim: The aim of this in vitro study is a comparison on the micro-shear bond strength between one universal adhesive and a silane ceramic primer application on the treated surface of lithium disilicate glass-ceramic.

Materials and methods: Forty-five slices of lithium disilicate glass-ceramic (IPS e.max CAD - Ivoclar Vivadent) were cut from the original pre-sintered block (LT A3.5/C14). The slices, measuring 2 mm thick with the width and length kept to original dimensions (12 mm and 14 mm, respectively), were poured with acrylic resin in order to be polished. After the polishing, three different surfaces were prepared as follows:



polished (PO); 9.6% hydrofluoric acid (HF) for 30 s (ET3); 9.6% hydrofluoric acid for 90 s (ET9). On each of the treated surfaces, RelyX Ceramic Primer (3M ESPE) (RLX), Scotchbond Universal Adhesive (3M ESPE) (SUA), and both were applied (RLA). After the different adhesive strategies, 4 composite pins measuring 2.38 mm in diameter and 4 mm in height were cemented onto the surfaces of each specimen. Then, 9 groups ($n=20$ pins) were submitted to non-accelerated and accelerated aging conditions between 5 °C and 55 °C (dwell time 55 s, 25 s in each bath) for 20,000 cycles. The specimens were then submitted to micro-shear bond strength (μ SBS; MPa) in the Ultratester machine (Ultradent Products). Separate groups of specimens were submitted to measurement of the contact angle using the sessile drop technique; subsequently, the surface free energy was calculated using the Young's formula. Results were statistically analyzed with two-way ANOVA and one-way ANOVA, respectively. Statistical significance was set to $\alpha=0.05$.

Results: The accelerated aging condition decreased the μ SBS for all groups tested ($\alpha=0.05$). The independent application of SUA did not increase μ SBS values in comparison with RLX; however, SUA showed effectiveness when used as adhesive after the application of RLX. In addition, the surface free energy was not statistically significant different between ET3 and ET9 ($p=0.997$). The same similarity for the surface free energy was found after the application of the RLX on the treated surfaces of ET3 and ET9 ($p=0.702$).

Conclusions: The application of universal adhesive system in replacement of regular silane does not seem reliable since that is not more effective than the use of regular silane-coupling agents. Even though longer etching times does not increase the surface free energy, that longer etching supports the μ SBS values at higher levels after accelerated aging.

<https://doi.org/10.1016/j.dental.2019.08.061>

61

Effect of preheating on rheological properties of resin composites



D.L.N. Poubel*, S.J.L. Sousa, I.D.O. Pereira,
F.C. Cunha, A.P.D. Ribeiro, P. Pereira,
F.C.P. Garcia

University of Brasilia, Brasilia, Brazil

Purpose/aim: The presence of inorganic fillers on composite resins can enhance its physical characteristics such as abrasion resistance, its mechanical strength, hardness and

reduces the polymerization shrinkage. Preheating of dental composites might be helpful in clinical practice to improve their flowability, facilitating successful cementation of indirect restorations. Purpose: In the present study, the effects of various temperature conditions upon the viscoelastic properties of three preheated dental composite were studied.

Materials and methods: Using a rotational rheometer, a permanent oscillatory shear test was undertaken at 25, 35, 50 and 60 °C of Z100 (3M ESPE), Beautifil II (Shofu) and Palfique LX5 (Tokuyama) composite resins under $1/s^{-1}$ shear rate.

Results: Data (Table 1) were analyzed using statistical software Stata SE 15.1 (StataCorp, College Station, TX, USA). One-way ANOVA and Bonferroni post hoc test were used to compare the viscosity at each temperature ($p<0.05$). For the three composites analyzed, the increase of temperature allowed a significant viscosity reduction ($p<0.05$). From the initial temperature (25 °C), Beautifil II presented a significant higher viscosity when compared to Palfique LX5 and Z100. Palfique LX5 started with the lowest viscosity and with the temperature increasing, it remained with a significant viscosity reduction compared to the other two composites ($p<0.05$). For both Beautifil II and Z100, there was no difference in the viscosity from temperature 50 and 60 °C; while for Palfique LX5 no statistical difference from 35, 50 and 60 °C was observed.

Conclusions: Therefore, it can be concluded that for all the three composites, the temperature of 50 °C reaches the optimal viscosity.

<https://doi.org/10.1016/j.dental.2019.08.062>

62

Resin cements light-cured through different hybrid cad/cam materials



J. Pucci De Moraes*, L.O. Brasil, M.Z.D. Picolo,
M. Giannini, V. Cavalli

Piracicaba Dental School, University of Campinas,
Brazil

Purpose/aim: This study evaluated the influence of the thickness of hybrid materials of the CAD–CAM system on the microhardness and flexural strength of a light-cure resin cement.

Materials and methods: Samples of the three hybrid materials – polymer-infiltrated ceramic network (Vita Enamic), nanoceramic resin (Lava Ultimate), nanohybrid resin (Brava) and one zirconia-reinforced lithium silicate ceramic (Celttra Duo) with different thicknesses (0, 0.5, 1 and 1.5 mm)

Table 1 – Mean Viscosity (SD) at different temperatures.

Mean Viscosity and SD* at different temperatures

	25 °C	35 °C	50 °C	60 °C
Beautifil II	8442.5 (± 1361) ^{a, A}	4592.5 (± 454) ^{a, B}	931.0 (± 187) ^{a, C}	452.5 (± 112) ^{a, C}
Palfique LX5	3012.5 (± 493) ^{b, A}	576.0 (± 58) ^{b, B}	272.75 (± 11) ^{b, B}	206.5 (± 13) ^{b, B}
Z100	4595 (± 442) ^{b, A}	2035.0 (± 103) ^{c, B}	1115.5 (± 118) ^{a, C}	690.0 (± 61) ^{c, C}

a,b,c Different lower-case letters identify statistical difference between groups in the same columns; A,B,C Different Upper-case letters identify statistical difference between groups in the same row. (*SD: Standard Deviation)

were prepared. Resina cement discs (All Cem Venner) were light-cured (1000 mW/cm² for 40 s, Valo, Ultradent) through each indirect material and thickness (n=10). The microhardness and flexural strength of the resin cement were determined and submitted to Anova (two-way) and Tukey HSD test ($\alpha = 5\%$).

Results: 1.5 mm-thick Vita enamic, Lava Ultimate, Celtra-Duo and 1.0 mm-thick Brava samples reduced microhardness of the resin cement compared to direct light-curing (0 mm) ($p < 0.05$). Vita Enamic and Celtra-Duo did not influence flexural strength of resin cement, regardless of thickness ($p > 0.05$). The flexural strength of the cement light-cured through Lava Ultimate was higher than that of the other materials, but decreased with the 1 mm-thick samples ($p < 0.05$).

Conclusions: In conclusion, the microhardness of the resin cement decreased when light-cured through 1.0 mm (Brava) and 1.5 mm-thick (Vita, Lava and Celtra) indirect materials. The flexural strength of the resin cement was not influenced by the thickness of Celtra and Vita Enamic, but it reduced when light-cured through 1.0 mm (Lava Ultimate) and 1.5 mm-thick (Brava) materials.

<https://doi.org/10.1016/j.dental.2019.08.063>

63

Microstructure and mechanical properties of stabilized zirconia ceramics



S. Rada^{1,2,*}, E. Culea², M. Rada¹

¹ National Institute for Research Development of Isotopic and Molecular Technologies, Cluj-Napoca, Romania

² Department of Physics & Chemistry, Technical University of Cluj-Napoca, Romania

Purpose/aim: The main problem of the zirconia based ceramics is the stabilization of tetragonal and/or cubic ZrO₂ crystalline phases at room temperature after sintering. The engineering properties and materials performances of zirconia ceramics are controlled by the crystallinity. The aim of the present study was to investigate the microstructure and mechanical properties of SiO₂, Fe₂O₃, Na₂O and MgO doped 8 mol % yttria stabilized zirconia.

Materials and methods: This work evaluated the effect of the addition of different oxides in the group of ZrO₂ (70, 75, 80 mol %) - Y₂O₃ (8 mol % Y₂O₃) ceramics by the following investigations: X-ray diffraction (XRD), Scanning Electron Microscopy (SEM), InfraRed (IR), UltraViolet-Visible (UV-Vis), Photoluminescence (PL), Electron Paramagnetic Resonance (EPR) and X-ray Absorption (XAS) spectroscopy. The Vickers indentation test was used for determination of fracture toughness.

Results: The 8 mol% Y₂O₃-stabilized ZrO₂ ceramics containing 70, 75 and 80 mol% ZrO₂ and different oxides contents were synthesized through a high temperature solid state reaction process at 1400 °C. The XRD diffractograms show diffraction peaks corresponding to the tetragonal ZrO₂ crystalline phases for all studied ceramics. The analysis of the FTIR spectra indicates that the fractions of tetragonal zirconia phase and the Si-O-Si and Zr-O-Si linkages were increased

with increasing the ZrO₂ content for all studied samples. The EPR spectra are characterized by two resonance lines situated at about g~4.3 and g~2 corresponding to the isolated and clustered Fe⁺³ ions. The EPR analysis indicates higher concentrations of clustered Fe⁺³ ions in the ceramics containing 80 mol % ZrO₂. XANES analysis show that in the studied ceramics the iron ions are octahedral coordinated by six oxygen atoms with slight distortions, which is in consents with the very low pre-edge peak (80 mol % ZrO₂). Significant changes in the Fe environment should be reflected more strongly in the intensity of the pre-edge.

Conclusions: The obtained data show variations in the microstructure and the calculated hardness values of the investigated dental ceramics with respect to the applied indentation load.

<https://doi.org/10.1016/j.dental.2019.08.064>

64

Improvement of resin-based composites physico-mechanical characteristics after thermal post-cure



C.M. Hardy^{1,2}, D. Dive², J.G. Leprince^{1,2}, L.D. Randolph^{1,*}

¹ Louvain Drug Research Institute, Uclouvain, Belgium

² School of Dental Medicine and Stomatology, Uclouvain, Belgium

Purpose/aim: To analyse the extent of physico-mechanical modifications of a range of commercially available resin-based composites (RBCs) for direct restoration after thermal post-cure, a CAD/CAM composite block being used as control.

Materials and methods: Six commercial RBCs for direct restorations were tested (shade A3): Clearfil Majesty Posterior and Clearfil AP-X (Kuraray-Noritake, Japan), Grandio (VOCO, Germany), Filtek Z100 and Filtek Supreme-XTE (3M-ESPE, USA), Essentia (GC-EUROPE, Belgium). The CAD/CAM composite Grandio Disc (VOCO, Germany) was used as control. Rectangular (2x2x25 mm) or disc (5 mm diameter) samples were light-cured with Bluephase G2 (1100mW/cm², Ivoclar-Vivadent), and post-cured thermally in a furnace (90 °C, 15 min). The following properties were measured before and after thermal treatment: monomer conversion by Raman Spectrometry (n=10) (DXR Raman Microscope, Thermo Scientific), Flexural Strength and Elastic Modulus by 3-points bending (n=20) (Lloyd LRX Plus, Lloyd Instruments), Vickers microhardness (n=10) (200 g load, microindenter Durimet, Leitz), and soluble mass and solvent absorption using a high-precision scale (n=3, one week storage in ethanol) (XP2U, Mettler Toledo). The data were analysed using one-way ANOVA, and Weibull distribution were analyzed (shape and scale parameters).

Results: A general increase in conversion, elastic modulus, flexural strength and Vickers microhardness was observed for all materials after thermal treatment, as well as a general decrease in soluble mass and sorption. Most differences observed were statistically significant ($p < 0.05$). The percentage increase ranged from 4.6% to 13.17% for conversion, from

6.42% to 12.84% elastic modulus, from 6.98% to 21.16% flexural strength and from 5.66% to 36.02% Vickers microhardness, and the % decrease from 6.16% to 39.10% for soluble mass and from 48.99% to 73.37% solvent sorption, respectively. The elastic modulus of Grandio Disc was not significantly different from Grandio ($p < 0.05$). However its conversion, Vickers microhardness, and flexural strength significantly increased ($p < 0.05$). The general ranking of materials properties remained similar following thermal treatment. Weibull analysis showed a higher reliability (shape parameter) for the composites after heat treatment. Grandio Disc showed a higher reliability than the post-cured Grandio.

Conclusions: The data showed clear physico-mechanical improvements after thermal post-curing of light-cured RBCs. Such procedure could be used beneficially in indirect bonded restorations as compared to the same RBC bonded directly, notably improving mechanical performance, stability and reliability. However, CAD/CAM RBC blocks may remain a better solution and should be the material of choice in the RBC category.

<https://doi.org/10.1016/j.dental.2019.08.065>

65

Physico-mechanical properties of 3d-printed resin used as temporary crown/bridge restoration



F.A.P. Rizzante^{1,*}, T.L. Bueno²,
G.M.F. Guimarães², G.F. Moura³, R. Roperto¹,
T.S. Porto¹, F. Faddoul¹, A.Y. Furuse²,
G. Mendonça³

¹ Case Western Reserve University, School of Dental Medicine, USA

² Bauru School of Dentistry, University of São Paulo, Brazil

³ University of Michigan School of Dentistry, USA

Purpose/aim: The objective of the present study was to compare physico-mechanical properties of different materials used for temporary restorations.

Materials and Methods: Resin composite (Filtek supreme), Protemp 4 (bisacrylic resin), Jet (acrylic resin), and Nexdent C&B (3D printed resin) samples ($n = 5$) with 10 mm diameter x 2 mm thickness were fabricated and analyzed using Knoop microhardness (25 g force during 5s), surface roughness test (baseline, after 5 thousand brushing cycles with 20 mm movement and 300 g load, and after artificial aging in water at 60 °C during 24 h), and color stability test (initial/after polishing, after brushing cycles, and after artificial aging). All data were checked for normality using Shapiro-Wilk test. Microhardness data was subjected to one-way ANOVA, while surface roughness and color stability were analyzed using one-way repeated measurements ANOVA. All tests were performed with $p < 0.05$.

Results: Considering microhardness test, composite resin showed the highest values, followed by the printed and bisacryl resins. Acrylic resin showed the lowest values (although similar to bisacryl resin). For roughness test, all groups presented similar initial roughness. After brushing, it was observed a tendency of decrease in surface roughness

although the difference was not significant for any group. After artificial aging, an increase in surface roughness was observed, being statistically significant for acrylic resin (compared with results after brushing). The surface roughness further decreased for printed resin after artificial aging (when compared with the initial condition). For color stability, all groups showed similar color alteration between baseline and after brushing cycles, except printed resins (higher color variation). After artificial aging, all temporary materials presented similar and higher color alterations than the resin composite.

Conclusions: Printed resins present at least the same, when not better, properties than other provisional materials (i.e. acrylic resin and bisacrylic resin), while providing the advantages and versatility of a completely digital workflow.

<https://doi.org/10.1016/j.dental.2019.08.066>

66

Effect of Chemical Catalysis on Hydrogen Peroxide Bleaching Efficacy



C.R.G. Torres*, L.F. Cornelio, A.B. Borges

Institute of Science and Technology, Sao Paulo State University, Sao Jose Dos Campos, Brazil

Purpose/aim: The aim of this study was to evaluate the effect of transition metal containing catalysts on the bleaching efficacy of hydrogen peroxide.

Materials and methods: Two bleaching evaluations were performed. For the first one, inside a reactor with controlled temperature were mixed an association of different tooth staining substances (wine, coffee and tobacco), 35% hydrogen peroxide (q.s.p), sodium hydroxide for pH adjustment and different catalysts. A total of 17 iron and 8 manganese containing catalysts, in various concentrations and pHs, were tested. The color change of the solution was evaluated using a transmittance colorimetric spectrophotometer (CM-5, Konica Minolta). The most effective catalyst on this first evaluation was Iron Nitrate (IN), Iron Sulfate (IS), Manganese Porphyrin (MP) and Ferrous Gluconate (FG). In the second evaluation, those most effective substances were tested in relation to its tooth whitening effect. Specimens were obtained from the buccal surface of bovine incisors. The thickness of enamel and dentin were standardized and a flat enamel surfaces were created. The baseline color was evaluated using a reflectance spectrophotometer, obtaining the L^* , a^* and b^* color coordinates. The specimens were divided into five groups ($n = 20$) according to the chemical catalyst added: IN, IS, MP, FG and PC (none –positive control). A negative control (NC) was prepared, which specimens were treated with pure water. The bleaching treatments were performed for 60 min. After that the specimens were stored in artificial saliva for 7 d and the color was evaluated again. The color change was calculated (Delta E). The data were analyzed with one-way ANOVA and Tukey's test.

Results: ANOVA showed significant differences among the groups ($p = 0.0001$). The results of Tukey's test were: NC–1.44(0.50)a; PC–3.50(0.97)b; IN–4.54(1.12)b; IS–4.78(0.78)b; FG–5.6(1,15)b; MP–7.96(1.56)c.

Conclusions: All experimental groups treated with hydrogen peroxide showed a significant bleaching effect. However, the addition of the catalyst MP resulted two times greater bleaching effect than when no catalysis was performed. (FAPESP - 2015/17107-8).

<https://doi.org/10.1016/j.dental.2019.08.067>

67

Physico-Chemical Properties and Cytocompatibility of 36 Commercially Available “Graphene” Materials

V. Rosa^{1,2,3,*}, R. Melhotra¹

¹ Faculty of Dentistry, National University of Singapore, Singapore

² Department of Materials Science and Engineering, National University of Singapore, Singapore

³ Centre for Advanced 2D Materials and Graphene Research Centre, National University of Singapore, Singapore

Purpose/aim: To correlate the physico-chemical properties and cytocompatibility of 36 commercially available “graphene” materials.

Materials and methods: 36 materials advertised as “graphene” were purchased from companies from nine countries. The materials were for characterized by Raman (I2D/IG), AFM (number of layers), XPS (total carbon and C-C sp² content), optical microscopy (lateral size) and by the Brunauer, Emmett and Teller (BET) method. For cytocompatibility, L929 cells were treated with 10 or 25 µg/mL of graphene in basal culture media for 24h. Thereafter, WST-1 and LDH assays were performed. All tests were performed in 3 independent triplicates. Statistical analysis was performed with Spearson’s bivariate correlation test.

Results: 11 out of the 36 materials marketed as graphene were actually graphene oxide as they presented the characteristics D and G modes at 1359 and 1596 cm⁻¹. All the graphene materials presented an average number of layers higher than 10 which is the threshold to be qualified as few-layers graphene. The lowest number of layers at 90th percentile was 13 layers and was observed only for two materials. On an average, the carbon content was high (~90%) but the quantity of C-C sp² bonds was low (~31%). We observed negative correlations between lateral size and BET ($\rho = -0.315$ and -0.320) with cell viability, while other tested characteristics did not significantly affect the cell viability for graphene group. Higher levels of toxicity with graphene oxide were positively correlated to carbon content.

Conclusions: Only 70% of the materials marketed as “graphene” were graphene, as characterized by Raman. None of the materials present a consistent number of layers lower than 10 to be constantly classified as graphene. Only the lateral size (d₅₀) and BET presented marginal negative correlations with increased toxicity. Due to the low quality of the materials available, it is imperative for biomedical researchers to perform proper characterization and purification of the

materials purchased prior to using in the research protocols.

<https://doi.org/10.1016/j.dental.2019.08.068>

68

Bulk-Fill Composites Based on an Elastomeric Methacrylate Monomer



M.G. Rocha^{1,2}, J.F. Roulet^{2,*},
D.C.R.S. Oliveira^{1,2}, M.A.C. Sinhoreti¹,
A.B. Correr¹

¹ Piracicaba Dental School, State University of Campinas, Brazil

² College of Dentistry - University of Florida, USA

Purpose/aim: Evaluate the influence of replacing a regular UDMA with an elastomeric methacrylate monomer on the depth of cure, polymerization shrinkage stress (PSS), mechanical properties, and wear resistance of bulk fill composites (BFCs).

Materials and methods: An elastomeric methacrylate monomer (Exothane 24) was characterized regarding its chemical structure. Six BFCs were made containing Exothane 24 or UDMA in three different concentrations (E1, E2, and E3 or U1, U2, and U3). The bulk fill composites were analyzed regarding their depth of cure using Vickers hardness. The flexural strength and flexural modulus were also assessed by a three-point bend test. The polymerization shrinkage stress (PSS) was analyzed using the universal testing machine method. The composites were submitted to a two-body wear test using a chewing simulator machine (Mechatronics CS-4) and the volumetric wear loss was evaluated using an optical scanner (3M True Definition Scanner). Data were analyzed according to the different experimental designs ($\alpha = 0.05$ and $b = 0.2$).

Results: For the depth of cure, the composite E2 was the only composite that did not have any significant statistical difference in the VHN from top up to 4 mm depth, however the E2 composites had lower degree of conversion than U1, U2, U3 and E3. All composites had the similar flexural strength, except for E3. However, the composites E2 and E3 had lower flexural modulus and PSS (Fig. 1). The volumetric wear loss

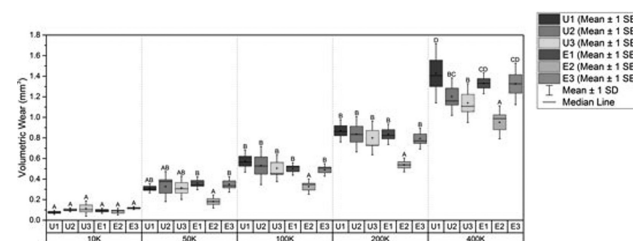


Fig. 1

and wear rate was significantly lower for the E2 composites than the all other composites test.

Conclusions: The substitution of a regular UDMA monomer for an elastomeric methacrylate monomer (Exothane 24) can

significantly reduce the PSS and increase the wear resistance of bulk fill composites.

<https://doi.org/10.1016/j.dental.2019.08.069>

69

Monomer Combination's for Bulkfill Applications'



L.D. Pereira¹, M.P.C. Neto¹,
L.M. Cavalcante^{1,2}, L.F. Schneider^{1,*}

¹ Veiga De Almeida University, Brazil

² Federal Fluminense University, Brazil

Purpose/aim: This study aimed to determine the influence of co-monomer combinations' on the degree of conversion (GC) as a function of depth of model composites for bulkfill applications'.

Materials and methods: four co-monomer combinations' were considered: BisGMA:TEGDMA (70/30 wt%; control group); BisEMA:BisGMA:TEGDMA (65:30:5 wt%; BisEMA-rich group); UDMA:BisGMA:TEGDMA (65:30:5 wt%; UDMA-rich group); BisEMA:UDMA:BisGMA:TEGDMA (32,5:32,5:30:5 wt%; BisE + UDMA group). For each material, a photoinitiator system (CQ + EDMAB) and reinforcing silanized fillers were added (0.7 µm BaAlSi; 45 wt%) to produce flowable, visible-light activated, composites. Degree of conversion (%) was determined at three different depths - 0.05 mm (top), 4 mm and 6 mm - by ATR-FTIR spectroscopy 5 min after light-activation. The cure efficiency was obtained by the bottom-to-top coefficient. Data was analyzed by two-way ANOVA and Tuckey's test (95%).

Results: The UDMA-rich group promoted higher conversion values than the blends at all levels of depth. The UDMA-rich group (96%) and the BisEMA + UDMA group promoted higher bottom-to-top ratio than the BisEMA-rich (89%) and control groups at 4 mm depth. However, at 6 mm depth, only the BisEMA + UDMA group was able to keep a constant degree of conversion whilst the UDMA-rich group was negatively affected.

Conclusions: The use of BisEMA and UDMA in association with BisGMA/TEGDMA promoted the most constant degree of C=C conversion as a function of depth and seems to be a suitable combination for bulk fill applications'.

<https://doi.org/10.1016/j.dental.2019.08.070>

70

RCT Papers in Prosthesis - Compliance with Consort Guidelines - A SR



N. Meckelburg, A. Reis, A. Loguercio,
M. Schroeder*

Universidade Federal do Rio de Janeiro, Rio de Janeiro, Brazil

Purpose/aim: objectives: The literature was reviewed to evaluate 1) the compliance of randomized clinical trials (RCTs) published in peer-reviewed journal with the Consolidated Standards of Reporting Trials (CONSORT) and 2) the risk of

bias of these studies through the Cochrane Collaboration risk of bias tool (CCRT).

Materials and methods: Methods: RCTs were searched at Cochrane Library, PubMed, LILACS, Scopus, and Web of Science to find studies about dental prosthesis. The compliance of these articles with CONSORT was evaluated using a published modified CONSORT instrument using the following scale: 0 = no description, 1 = poor description and 2 = adequate description. Descriptive analyses about the number of studies by journal, follow-up period, and country were recorded. The risk of bias of the RCTs was performed with CCRT. This Systematic Review is still ongoing so data presented here are the preliminary results.

Results: This study is still ongoing, so results were obtained from preliminary data, which seem to be representative of the total. Seventy-eight RCTs remained for assessment. All the analysed studies received at least two scores of 0 and maximum punctuation was 25 points out of 32. Estimated "effect size", "Registration and Protocol", "sample size" and "Allocation Concealment" were more critical items, with 90% receiving a score of 0 for "Effect Size" and 33% receiving a score of 0 for "Registration and Protocol". The overall CONSORT score for the analysed studies was 20.7 points, which represents 64.6% of the maximum CONSORT score (= 32 points). Only 8.3% of the studies were judged as at low risk; 75.0% were classified as having unclear risk and 25.0% as having high risk of bias.

Conclusions: The preliminary data analysed in the study suggest that the adherence of RCTs evaluating dental prosthesis to the CONSORT is low with unclear/high risk of bias.

<https://doi.org/10.1016/j.dental.2019.08.071>

71

Interfacial Gap and Fracture Resistance of Indirect CAD-CAM Restorations



N. Scotti^{1,*}, E.A. Vergano¹, A. Baldi¹,
G. Zoppetto¹, R. Michelotto Tempesta¹,
M. Alovizi¹, D. Pasqualini¹, A. Comba²,
E. Berutti¹

¹ University of Turin, Dental School Lingotto, Italy

² University of Bologna, Dibinem, Italy

Purpose/aim: The aim of this in vitro study was to evaluate the effect of three different CAD-CAM processed materials on the interfacial gap, wear and fracture resistance of endodontically treated molars.

Materials and methods: 48 maxillary molars were selected and endodontically treated. On each specimen a standardized MOD cavity was prepared. Specimens were then divided in two groups (n=24 each) according to the build-up technique employed: (G1) build-up with a bulk fill composite material (Admira Fusion X-Tra, Voco); (G2) fiber post supported build up. Then, a standardized overlay preparation was performed. Specimens were scanned with Cerec Omnicam (Dentsply Sirona) and the indirect restoration was milled with Cerec MXCL. Each group was divided into 3 subgroups (n=8 each) according to the CAD-CAM material employed: (SG1)Grandio-Blocks; (SG2)Cerasmart; (SG3)Celtra Duo. Each overlay, once completed, was luted following a standard-

ized procedure. All specimens were scanned with micro-CT (Skyscan, Bruker) at high-resolution scans (voltage = 100 kV, current = 80A, source-to-object distance = 80 mm, source-to-detector distance = 220 mm, pixel binning = 292, exposure time/projection = 3s). Then, specimens of each group were subjected to mechanical fatigue test in a CS-4.4 chewing simulator (50N, 500.000 cycles). After fatigue, micro-CT scanning was performed to evaluate the interface. Replicas were obtained for external gap evaluation with SEM. Samples were also optically scanned using a laboratory scanner. Micro-CT images, before and after cycling load, were analyzed with Geomagic Software and Mimic to evaluate interfacial gap progression before and after mechanical load. ImageJ analysis was performed to compare visible gap between the three analysis methods. Statistical analysis was performed using a two-way ANOVA test for fracture resistance and a three-way ANOVA for gap progression.

Results: Two-way ANOVA showed that interfacial gap was not significantly influenced by the build-up technique ($p = 0.061$). SG2 and SG3 showed a lower gap ($p = 0.001$) and a higher fracture resistance rate ($p = 0.0001$). Three-way ANOVA showed no significant differences ($p = 0.07$) between optical, SEM and 3D gap evaluation.

Conclusions: Interfacial gap and fracture resistance could be influenced by the CAD-CAM material employed to restore endodontically treated molars. Encouraging results emerged from the present study, with the micro-CT analysis having similar results of a SEM and optical analysis.

<https://doi.org/10.1016/j.dental.2019.08.072>

72

Bond strengths Of universal adhesives achieved by different dentin-etching approaches



M. Sebold*, C.B. André, M. Giannini

Piracicaba Dental School, University of Campinas, Piracicaba, Brazil

Purpose/aim: This study evaluated the effect of four dentin surface treatments (37% phosphoric acid – PA; self-etching – SE; 10–3 solution – 10–3; and 1.4% nitric acid – NA), and post-etching moisture levels on the 24-h microtensile bond strength of two “universal” adhesives containing distinct solvents (alcohol or acetone).

Materials and Methods: One hundred human third molars were used, following a protocol approved by the Ethics Committee in Research of the Piracicaba Dental School – UNICAMP (#CAAE 87550318.0.0000,5418). Teeth were randomly divided into ten groups ($n = 10$): G1) PA–wet bonding+Prime & Bond Active (PBA – Dentsply Sirona); G2) PA–dry bonding+PBA; G3) PA–wet bonding+Gluma Bond Universal (GBU – Kulzer); G4) PA–dry bonding+GBU; G5) PBA SE mode; G6) GBU SE mode; G7) 10–3 + PBA; G8) 10–3 + GBU; G9) NA + PBA; and G10) NA + GBU. Occlusal enamel was removed with a diamond saw, and dentin was polished with a SiC paper (600-grit). Conditioning agents were applied on dentin for 15 s, according to the aforementioned groups, and the etched surfaces were washed and air-dried in all groups, except for G1 and G3, in which dentin

Table 1 – Mean (\pm SD) dentin microtensile bond strength (in MPa) according to dentin treatment and type of adhesive.

Dentin Treatment	Adhesive System Prime & Bond Active	Gluma Bond Universal
37% Phosphoric Acid – Wet	45.9 (\pm 7.6) Aa	40.9 (\pm 5.1) Bab
37% Phosphoric Acid – Dry	37.3 (\pm 6.3) Ab	40.8 (\pm 4.2) Aab
Self-etching Mode	37.9 (\pm 6.2) Abc	39.4 (\pm 4.5) Ab
10–3 Solution	40.5 (\pm 6.1) Abc	44.3 (\pm 5.5) Aa
1.4% Nitric Acid	42.3 (\pm 4.9) Aac	42.6 (\pm 3.4) Aab

Same uppercase letters indicate no differences in rows (comparing adhesive systems for the same dentin treatment, $p > 0.05$). Same lowercase letters indicate no differences in columns (comparing dentin treatments for the same adhesive system, $p > 0.05$).

was kept slightly moist. After bonding, three layers (2 mm) of a composite (Spectra Smart, Dentsply Sirona) were placed onto dentin, and light-cured separately for 20 s. Teeth were sectioned to obtain stick-shaped specimens with a cross section of 1 mm². Specimens were tested in a universal testing machine (EZ Test, Shimadzu) after 24 hours of storage in 100% humidity at 37 °C. Bond strength data was submitted to the Shapiro–Wilk test, followed by 2–way ANOVA (treatment and adhesive system) and Tukey’s test ($\alpha = 0.05$). Results are presented in Table 1.

Results: PBA showed higher bond strength than GBU for the wet-bonding technique using PA, while there was no statistical difference between adhesives for the remaining groups. PBA + 10–3 led to similar results than the SE or the PA–dry bonding approaches. NA + PBA did not differ from PA–wet bonding or the 10–3 groups. The SE mode of GBU resulted in lower bond strength than 10–3, which did not differ from any of the other groups. NA + GBU had similar results compared to all the other groups using the same adhesive.

Conclusions: Experimental conditioners (10–3 and NA) showed promising dentin bond strength results when used with “universal” adhesive systems.

<https://doi.org/10.1016/j.dental.2019.08.073>

73

Effect of surface treatments on bond of cad/cam composite block



L. Chen, T. Sedlacek*, B.I. Suh

Bisco Inc, Schaumburg, USA

Purpose/aim: The aim of this study was to evaluate the effect of different surface treatment methods on shear bond strength of computer-aided design/computer-aided manufacturing (CAD/CAM) composite blocks.

Materials and methods: Four CAD/CAM composite blocks were polished with 320-grit SiC paper, rinsed and dried. All groups were further divided into 3 subgroups according to surface treatment: A) control (no further treatment); B)

Table 1 – Mean shear bond strengths (SD). Different letters indicate significance.

CAD/CAM Blocks	Cerasmart GC	Grandio VOCO	Enamic VITA	Lava 3M
No treatment (polished)	8.6(3.4) a	16.4(6.0) a	12.0(2.8) a	9.7(2.8) a
HF etching + Silane	28.8(4.3) b	24.4(2.9) b	30.8(4.5) b	23.1(4.4) b
Sandblasting + ZPrime Plus	27.6(8.0) b	37.3(7.6) c	29.7(2.8) b	34.2(9.0) c

roughened with 4% Hydrofluoric acid (Porcelain Etchant 25 s, Bisco), followed by application of one coat of silane (Porcelain Primer, Bisco); C) roughened with sandblasting (alumina sand 10s), followed by application of one coat of Z-Prime Plus (Bisco). Shear bond strength was tested using the notched-edge shear bond strength test method (ISO 29022:2013). Resin cement (Duolink Universal, Bisco) was placed on the CAD/CAM surface and light-polymerized (40s at 500mw/cm²). The specimens were then stored in water at 37 °C for 24 h and tested by universal testing machine (Instron, crosshead-speed 1 mm/min). The data were analyzed statistically by one-way ANOVA and Student-t Test.

Results: Mean shear bond strengths ($n=8$) in MPa (standard deviation) are shown in Table 1. Means with different letters in the same column are statistically different ($p < 0.05$).

Conclusions: Both surface treatment methods improved the bond strengths of all of the four CAD/CAM composite blocks.

<https://doi.org/10.1016/j.dental.2019.08.074>

74

Control of dynamic material property development in photopolymers using photochromism



P.K. Shah^{1,*}, J.W. Stansbury^{1,2}

¹ Department of Chemical & Biological Engineering, University of Colorado Boulder, USA

² Department of Craniofacial Biology, University of Colorado Anschutz Medical Campus, USA

Purpose/aim: Photopolymers used as adhesives, coatings, dental materials and for 3D part production are all negatively affected to some degree by both the internal and externally directed stress that develops as a consequence of the polymerization reaction. Photochromism is the phenomenon of light-driven reversible transformation between two isomers possessing different geometrical structures and absorption spectra. Spiropyran (SP) is an example of a photoswitch wherein the two isomers have vastly different properties, providing a way to alter material properties like modulus and stress, when used as an additive during photopolymerization.

Materials and methods: Spiropyran, was added to triethylene glycol dimethacrylate (TEGDMA). Two samples were made with different photoinitiating systems 1) 2,2-dimethoxy-2-phenylacetophenone (DMPA) 2) Camphorquinone/ethyl-4-dimethylaminobenzoate (CQ/EDAB). Shrinkage stress was measured in a tensometer and shear modulus

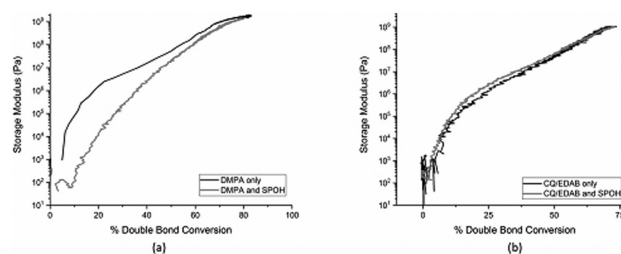


Figure 1

was measured in a photorheometer while simultaneously monitoring double bond conversion with FTIR spectroscopy.

Results: Upon irradiation with UV light, the double bond conversion in TEGDMA with SP/DMPA added to it was higher than the vitrification-limited conversion in TEGDMA/DMPA alone while the shrinkage stress was reduced by over 80%. Higher concentrations of SP resulted in a reduction of the polymerization rate, most likely due to the competitive absorption of UV light between SP and DMPA, while still showing an increased double bond conversion compared to the control without SP. Stress reduction can be due to lowering of the modulus of the material. To test this hypothesis, a photorheometer was used to monitor modulus and double bond conversion during active photopolymerization. Simultaneous monitoring of modulus as well as conversion allowed for following modulus development as a function of conversion, so that the different polymerization kinetic rates of the two systems would not convolute data interpretation. The modulus development in the SP-based system was indeed delayed as compared to the control system, eventually catching up towards the end of the reaction. When a camphorquinone-based visible light initiating system was used instead of DMPA, upon irradiation with visible light, this phenomenon was not observed (Figure 1). UV light favors the isomerization of SP to MC while visible light favors the reverse transformation. Hence the modulus development can be controlled using an appropriate wavelength or a combination of wavelengths of light.

Conclusions: Thus, the photoisomerization of spiropyran was utilized to control modulus development during photopolymerization. Double bond conversion was improved beyond the typical vitrification limit, something that is generally not possible without recourse to heating during polymerization.

<https://doi.org/10.1016/j.dental.2019.08.075>

75

Effect of tooth-brushing with microcurrent on dentinal tubule occlusion



G. Kim, Y. Shin*

Yonsei University, South Korea

Purpose/aim: The aims of this study were 1) to evaluate the effectiveness of tooth-brushing with microcurrent on dentinal tubule occlusion with scanning electron microscope, 2) to compare the dentinal fluid flow rate after tooth-brushing using microcurrent with a sub-nanoliter scaled fluid flow

measuring device and 3) to compare the surface roughness after tooth-brushing with microcurrent.

Materials and methods: Thirty dentin discs were cut perpendicular to the long axis of the tooth each with a thickness of 3.0 mm above the cemento-enamel junction and 3.0 mm below the CEJ. And then the specimens were treated using Colgate Total as below. Group 1: Phosphoric acid-etched specimens without any treatment, Group 2: Phosphoric acid-etched specimens were brushed without microcurrent, Group 3, 4, 5, 6: Phosphoric acid-etched specimens were brushed with microcurrent (20, 100, 200, 500 μ A). A toothbrush was applied to the dentin surface for 1 min/day in the tap water for 7 days. And we analyzed specimen with SEM for preliminary experiment. After SEM analysis, groups 1, 2 and 4 were chosen for dentinal fluid flow measurement using a NFMD. Each specimen's flow was measured for 5 min and dentinal fluid flow rate was calculated as dividing the total dentinal fluid flow by five minutes. One way ANOVA and Tukey's post hoc test were used to determine inter group significance ($p < 0.05$). Also surface roughness was measured using Surface profiler (Bruker). One dentin disc for each group was imaged and analyzed.

Results: Groups 2, 3, 5 and 6 showed remnants of dentifrice abrasives in the dentinal tubules. Group 4 created a dentin surface characterized by irregular crystal-like layer deposits leaving many dentinal tubule orifices occluded. In dentinal fluid flow rate measurement, group 4 showed significantly lower dentinal fluid flow rate than groups 1 and 2 ($p < 0.05$). In all experimental groups, there was an increase in surface roughness compared to group 1. There was no particular relationship between the ampere and Ra values.

Conclusions: All experimental groups showed partially occluded dentinal tubules and the formation of crystal-like structures in specific ampere (100 μ A) indicated that tooth-brushing with microcurrent could occlude dentinal tubules efficiently. The decrease in dentinal fluid flow rate in tooth-brushing with microcurrent group means that dentinal tubules were occluded and the flow of dentinal fluid has decreased. There was no direct correlation between surface roughness and dentinal tubule patency.

<https://doi.org/10.1016/j.dental.2019.08.076>

76

Ultrasonic activation of different solutions on root canal dentin



J.E. Soto-Sainz^{1,*},
J.A. Espinoza-Rodriguez^{1,2,3},
C. Samano-Valencia², A.R. Ayala-Ham¹,
G.Y. Castro-Salazar¹, N.V. Zavala-Alonso³,
R. Ramos-Payan¹, E.M. Aguilar-Medina¹,
E.L. Silva-Benitez¹, J.G. Romero-Quintana¹

¹ Universidad Autónoma De Sinaloa, México

² Benemérita Universidad Autónoma De Puebla, México

³ Universidad Autónoma De San Luis Potosí, México

Purpose/aim: Post systems have been widely used to restore structurally damaged teeth. The most frequent prob-

lem is the elimination of smear layer. The aim of this study was to compare the effectiveness of 37% orthophosphoric acid, 17% EDTA and 10% citric acid with and without ultrasonic activation for smear layer removal.

Materials and methods: 40 upper incisors were extracted due periodontal disease, after obtaining informed consent. Teeth were disinfected, radiographed and stored in 0.2% sodium azide (Sigma Chemical, St. Louis, MO, USA) until their use. The study was approved by the Research Committee. The crowns of the teeth were removed 2 mm below the cemento-enamel junction, working length was adjusted 1 mm shorter than the real. All root canals were treated with rotary twisted files (Sybron Endo, Orange, California, USA) to a main apical size of 50.04 (ML3). Between instruments, root canals were irrigated with 5.25% NaOCl and distilled water, finally were dried with paper points and filled with gutta-percha and sealer. The cervical access was temporarily sealed and the roots were stored in humidity for 7 days at 37 °C. Gutta-percha was removed from the root canal with the drill provided for the post system (D.T. Light-Post of Bisco (Coltène-Whaledent) preserving 4 mm at the apical level and the roots were randomly divided into 8 groups (2 control groups with distilled water) corresponding to the treatment for 1 min with the different irrigating solutions, with or without ultrasonic activation (NSK, Tochigi, Japan), followed by a wash with 5 ml of 2.5% NaOCl and distilled water. Canals were divided longitudinally in labiolingual direction and dehydrated. Finally, samples were sputtered with gold and examined under a scanning electron microscope. Ten images were obtained by each root level. Three calibrated observers scored the degree of smear layer.

Results: Smear layer evaluation scores were analysed using the Kruskal-Wallis H test and Mann-Whitney U-test using the SPSS v20.0 program; revealed that the use of irrigants allows the removal of the smear layer significantly ($P < 0.001$). The ultrasound application showed no significant difference between orthophosphoric and citric acid groups, it was different in the EDTA group 1.47 ± 0.16 ($P < 0.05$).

Conclusions: The elimination of smear layer is one of the challenges when placing a post. The use of different substances such as 17% EDTA activated with ultrasound proved to be a good option for smear layer removal.

<https://doi.org/10.1016/j.dental.2019.08.077>

77

Resin property control throughout conversion based on nanogel functionalization



M. Barros^{1,*}, J. Vigil¹, J. Stansbury^{1,2}

¹ University of Colorado School of Dental Medicine, USA

² Chemical Engineering, University of Colorado Boulder, USA

Purpose/aim: Reactive nanogels have been used to modify the dynamic polymerization process and final polymer properties in resin and composite materials. This study focusses on how the degree of methacrylate functionalization introduced by the nanogel additive alters the pre-cure resin as well as network formation and bulk properties in photopolymerizations.

Materials and methods: A solution of a PEG monomethacrylate (HEMA-5) and bis-phenol-A glycerolate dimethacrylate (BisGMA) at a 70/30 mole ratio was polymerized at 80 °C in 8:1 2-butanone using 1.5wt% azobisisobutyronitrile (AIBN) as the thermal initiator and 15 mol% mercaptoethanol (ME) as chain transfer agent (CTA). The initial nanogel product, which contains a high concentration of hydroxyl groups, was then further reacted with 2-isocyanatoethyl methacrylate at 0, 20 and 50 mol% to re-introduce varying degrees of methacrylate functionality. The remaining hydroxyl groups on each nanogel were reacted with butyl isocyanate. After isolation of the various nanogels by precipitation, they were characterized by GPC, DMA and NMR. Nanogel was loaded at 50wt% in triethylene glycol dimethacrylate (TEGDMA) with 0.1wt% of 2,2-dimethoxy-2-phenylacetophenone (DMPA) added as photoinitiator. Resin viscosity was measured and photopolymerization (365 nm/100 mWcm²) kinetics were followed with real-time near-IR kinetics.

Results: Results associated with the pre-cure resin viscosity, the bulk nanogel glass transition temperature (T_g), the final degree of conversion obtained upon UV irradiation and the maximum rate of polymerization (R_{pmax}) are shown in the Table.

Conclusions: The addition of these low T_g nanogels to TEGDMA at an effectively confluent loading level significantly enhanced the final conversion of TEGDMA and also greatly increased the rate of polymerization. This is likely due to a promotion of autoacceleration from the onset of polymerization while also producing a delay in vitrification for the TEGDMA-swollen nanogels. Further aspects of mechanical properties, shrinkage and stress will be reported but it is clear that nanogels with high reactive group concentrations and used at high loading levels enhance rather than limit the polymerization process in photocurable resin formulations.

<https://doi.org/10.1016/j.dental.2019.08.078>

78

Physicochemical study of Biodentine™-dentine tissue interphase

J.L. Suárez-Franco*, B.I. Cerda-Cristerna, A. Suárez-Porras, R.E. Flores-Ventura, M. Trujillo-Hernández, R. Trueba-García

Facultad De Odontología, Universidad Veracruzana, Orizaba, México

Purpose/aim: Since the introduction of bio-ceramics in the field of endodontics many studies have been conducted evaluating the different physicochemical and biological properties of these materials are holders. In 2011, a bio-ceramic material called Biodentine™ has been promoted as a substitute for bioactive dentine and some authors even claim that this material has better physical and biological properties than other materials based on tricalcium silicate. After the introduction of Biodentine™ in the dental market, its use became popular due to the greater number of advantages that this promised compared to conventional bio-ceramics, they carried out an investigation on the hydration and bioactivity of two mate-

rials based on tricalcium silicate, Biodentine™. The purpose of the present study was to evaluate the chemical composition of the central and peripheral surface of the filling with Biodentine™.

Materials and methods: Recently extracted uniradicular tooth organs were collected, which were washed, disinfected and maintained in hydration with 0.9% sodium chloride. They were selected according to the inclusion criteria and the coronal portion was removed. The root segment was included in self-curing acrylic inside cylindrical glass containers of 0.7 cm in diameter. The cylinders obtained with the included radicular portion were sectioned into three segments with a low speed hand-piece (NSK GS200) and a diamond disk with two lights DIS18 (Temok, Dental Instrumentation) keeping only the middle third, corresponding to the middle third radicular. All the materials were prepared according to the manufacturer's instructions, the portion of the root canal was closed in each of the samples. The morphological characterization of the apatite precipitate was carried out by means of an Electronic JEOL Field Emission Scanning Microscope (Model JSM-00F). The characterization of the chemical composition was carried out by means of an Electronic Scanning Microscope connected to a Dispersive X-ray Energy detector (Inspect™ Scanning Electron Microscope, Japan). The microstructural characterization was performed by means of Raman spectroscopy with a Thermo Scientific™ DXRTM Raman microscope instrument (Thermo Electron Scientific Instruments LLC, Madison, WI USA).

Results: The intensity generated by the apatite peak is greater than that produced in the central zone.

Conclusions: In this study it was proved that all the calcium silicate-based materials analyzed proved to be bioactive, because a precipitate formed on their surface which, according to the analyzes carried out, proved to have amorphous calcium phosphate, which acts as a precursor during the formation of carbonated apatite.

<https://doi.org/10.1016/j.dental.2019.08.079>

79

Reinforcement of dental adhesives with bio-inspired monomers

C. Szczepanski^{1,*}, C. Ligo²

¹ Michigan State University, Michigan, USA

² NorthWestern University, Evanston, USA

Purpose/aim: Dental adhesives are employed to create a sturdy and long-lasting bond between dentin and composite restorations through the formation of a three-dimensional polymer network that interlocks with native bone tissue. To date, the performance of such adhesives is sub-optimal, as the majority of composite failures are observed at restoration margins. This work investigates how the inclusion of bio-inspired monomers can improve the integrity and performance of adhesive materials by integrating adaptable hydrogen bonding moieties within the network architecture. More specifically, the catechol moiety, which is well-known for contributing to the remarkable adhesion observed in mussel byssus and the capacity to form strong bidentate hydrogen bonds, is incorpo-



rated into adhesive formulations and its efficacy at reinforcing and improving the longevity of adhesive materials is explored.

Materials and methods: Catechol methacrylamide (CMAC) was synthesized following procedures previously described in the research literature. Control model adhesive formulations containing urethane dimethacrylate (UDMA), bisphenol A-glycidyl methacrylate (BisGMA), and 2-hydroxyethyl methacrylate (HEMA) were developed with varying HEMA fractions (25–50 wt%). Catechol-modified adhesives were developed by replacing 25–50 mol% of HEMA monomer with CMAC. Both control and catechol-modified adhesive formulations were photopolymerized in bulk, as well as in the presence of water/ethanol mixtures as co-solvent (20–40 wt% relative to the adhesive formulation). Mechanical and thermal integrity of the resultant network materials were assessed using dynamic mechanical analysis (DMA).

Results: When polymerized in bulk (e.g. no solvent), CMAC-modified adhesive formulations had reduced mechanical properties compared to control formulations. This was evident by a measurable reduction in glass transition temperature (T_g), storage modulus (E'), and cross-link density (ρ_x). However, when photopolymerized in clinically relevant conditions (e.g. in the presence of water/ethanol co-solvent), despite more heterogeneous network formation, the presence of catechol-modified monomers improved the integrity of the adhesive formulations. Compared to control formulations, CMAC-modified materials had increased E' , ρ_x , and T_g . The magnitude of these improvements compared to controls was dependent on the level of CMAC modification (e.g., a greater improvement was observed with increasing CMAC fraction), as well as the amount of co-solvent present during photopolymerization.

Conclusions: The addition of bio-inspired monomers containing catechol moieties to model adhesive formulations improves the mechanical integrity of these materials when polymerized in solvent-rich conditions relevant to clinical application. This modification provides a feasible solution to enhance the integrity and long-term performance of dental adhesive materials.

<https://doi.org/10.1016/j.dental.2019.08.080>

80

Inhibitory effects of various ions released from surface active fillers

I. Salim¹, R. Seseogullari-Dirihan¹,
S. Imazato², A. Tezvergil-Mutluay^{1,3,*}

¹ University of Turku, Finland

² University of Osaka, Japan

³ Turku University Hospital, Finland

Purpose/aim: Enzymatic degradation of the collagen matrix by host-derived enzymes such as matrix metalloproteinase (MMP)s or cyteine cathepsins (CC) plays a significant role in the destruction of resin-dentin bonds. Recently surface pre-reacted glass-ionomer fillers (S-PRG filler) incorporated into various restorative materials were introduced. These materials actively release ions. The aim of this study was to

evaluate if these ions released from the fillers could inhibit the enzymatic activity in dentin.

Materials and methods: Demineralized dentin beams (1x2x6 mm) were divided into 8 groups ($n=10/\text{group}$) after baseline dry mass and total MMP activity measurements. The beams were treated with standard solutions containing 100 ppm solutions of boron, fluoride, sodium, silicone, strontium, or 10 ppm aluminium as well as a S-PRG solution for 5 min, and blot dried. Untreated demineralized beams served as controls. The direct inhibitory effect on MMPs was evaluated using a generic MMP activity assay after 1 hr incubation with MMP substrate (Sensolyte, USA). After MMP activity measurements, the beams were incubated in zinc and calcium containing media at 37 °C shaking bath for 1 week. After incubation period the loss of dry mass was determined, aliquots of incubation media were analyzed for CTX for cathepsin K-mediated degradation. Data were analyzed using repeated-measures ANOVA, $\alpha=0.05$.

Results: The total MMP activity was reduced significantly in all groups compared to control ($p<0.05$). The reduction in activity varied between 65% for fluoride to 74% with aluminum ion solutions. After one week of incubation all groups except sodium showed 30–40% reduction in Cathepsin-K mediated degradation which was significant ($p<0.05$). The dry mass changes followed a similar trend after 1 week of incubation.

Conclusions: The result of this work indicated that the ions released from the fillers have the potential to partly inhibit the endogenous enzymatic activity in demineralised dentin matrices.

<https://doi.org/10.1016/j.dental.2019.08.081>

81

Fracture resistance of short-fiber resin composite bilayers

J. Tiu*, R. Belli, U. Lohbauer

University of Erlangen-Nuremberg, Erlangen,
Germany

Purpose/aim: To characterize the toughening development of a flowable short-fiber resin composite (SFRC) veneered with a conventional resin composite using elastic-plastic fracture mechanics.

Materials and methods: Short fiber-reinforced resin composite (SFRC; fibers 200–300 μm , 7 μm , StickTech, GC) were prepared as monolithic or bilayers (Essentia HiFlo, GC), with fibers aligned or randomly oriented, into bar specimens (2.5 x 5 x 25 mm). Specimens were photo-cured (5x20s, 750mW/cm²) notched (monolithic at 0.45w-0.55 w; bilayer at 0.25 w), polished (wet, 4000 grit), and tested (3-point bending, 2.5 kN load cell, 0.01 mm/min). Loading was manually stopped when the curve reached a maximum or a change in compliance was observed. Force and crack extension were recorded, and the specimen was subsequently reloaded up to eight times. Fracture toughness (K1C) values and strain energy release rate JC were calculated according to ASTM E1820 to construct resistance curves fitted with a power law function.

Results: SFRC material showed increasing R-curve behavior, whether fibers are aligned or randomly oriented. Bridging



fibers arrest crack growth at the interface between the veneering composite and SFRC support, with material toughening attributed to frictional forces, crack deflection, and fiber bridging in the wake behind the crack tip, evidenced by SEM fractographic analysis. A process zone of continuous bridging and fiber degradation developed between the crack tip and the notch root, causing the material to reach a steady state of crack growth. Specimens with aligned fibers had more fibers spanning the crack faces resulting in higher fracture toughness and GIC values over specimens with randomly oriented fibers. R-curve constructed from strain energy JC was JC aligned = 0.96(Δa –1888)1.0 for aligned fibers, and JC random = 0.32(Δa –844)1.0 for randomly oriented fibers.

Conclusions: SFRC material exhibits fracture resistance, as seen in the desirable increasing R-curve behavior. Fibers spanning the crack face arrest cracks as it moves through the resin matrix. In a clinical situation, the degree of effectiveness is reliant on the fiber orientations; however, the SFRC bulk fill material veneered with a conventional resin composite is providing tougher support in composite restorations.

<https://doi.org/10.1016/j.dental.2019.08.082>

82

Dentin changes associated with patient age and cavity site



A.T. Weerakoon^{1,*}, I.A. Meyers¹, S. Roy²,
C. Cooper³, T.R. Cox⁴, N.D. Condon⁵,
C. Sexton¹, D.H. Thomson¹, P.J. Ford¹,
A.L. Symons¹

¹ School of Dentistry, University of Queensland, Queensland, Australia

² University of Queensland Centre for Microscopy and Microanalysis, Queensland, Australia

³ Queensland University of Technology, Queensland, Australia

⁴ Faculty of Medicine, Unsw Sydney, Australia

⁵ Institute for Molecular Biosciences, University of Queensland, Queensland, Australia

Purpose/aim: The aim of this study was to examine variations in collagen distribution and cross-linking, and mineral distribution and composition in dentin related to depth in young and mature teeth.

Materials and methods: Posterior ($n=8$ / age group) were collected from Young (≤ 27 years) and Mature (≥ 52 years) patients. Teeth were sectioned mesio-distally, then prepared to shallow (0.5–0.75 mm below the dentin-enamel junction) and deep (0.5–0.75 mm above pulp chamber roof) regions within the coronal dentin. The dentin specimens were used to examine collagen ($n=10$ /age group) or mineral ($n=6$ /age group). For examination of collagen, dentin sections were stained with Picrosirius Red F3BA before observation using polarized and fluorescent light. For examination of dentin mineral, sections were observed using the backscatter detector on a Zeiss Sigma VP field emission Scanning Electron Microscope and analysed using Energy Dispersive X-ray Spectroscopy (SEM-EDS). Photomicrographs were first segmented using machine learning before using a custom, automated

analytical script to measure segmented regions of interest before performing suitable statistical analyses on each group.

Results: Collagen cross-linking increased with patient age and dentin depth. However, collagen distribution remained constant irrespective of patient age, dentin depth and site. In contrast, dentin mineral content and distribution changed with patient age, depth and site. Specifically, the peritubular cuff mineral intensity increased with age irrespective of cavity location. This increase in intensity may not reflect an increase in mineral content. Analysis from SEM-EDS indicates that Calcium and Phosphorus peaks were greatest in inter-tubular dentin regardless of age and site, with the exception of young shallow dentin, where the peritubular mineral peaks were relatively higher as determined by SEM-EDS measurements.

Conclusions: Human dentin collagen and mineral characteristics vary with patient age and site. These findings indicate that physical variations within dentin are fundamental for the development of successful therapies used to repair or restore teeth following pathology. Thus, dental material developers and researchers should consider age-related changes in anatomical variation in dentine when developing, testing and applying regenerative and restorative products.

<https://doi.org/10.1016/j.dental.2019.08.083>

83

Structural and mechanical effects of ionizing radiation on human enamel



M. Wendler^{1,*}, G. Jerez², I. Luque-Martinez²,
M. Lopez³, A. Bedran-Russo⁴, M. Muñoz²

¹ Faculty of Dentistry, University of Concepcion, Chile

² Faculty of Dentistry, Universidad De Valparaíso, Chile

³ Faculty of Engineering, University of Concepcion, Chile

⁴ College of Dentistry, University of Illinois at Chicago, Chicago, USA

Purpose/aim: An increased incidence of enamel delamination has been observed in cancer patients undergoing radiotherapy treatment. This has been related to substrate deterioration, although no clear relation between ionizing radiation and the microstructure and mechanical properties of enamel has been yet established. Thus, the purpose of this study was to examine the in vitro effect of ionizing radiation on the crystallinity index (CI) and mineral content, as well as on the fracture toughness (KIC), of human enamel.

Materials and methods: Transversal slices ($n=10$) were obtained from the cusps of caries-free extracted human molars, in order to obtain specimens displaying a longitudinal enamel rod orientation. After fine polishing with SiC paper (P4000), 5 specimens were subjected to Raman spectroscopy (RS) in order to collect three spectra from each sample (4000–500 cm^{-1} range, 4 cm^{-1} resolution and 32 co-additions). The organic and hydroxyapatite contents, as well as the CI, were obtained using analytical methods and Fourier trans-

form analysis of the Raman spectra. The K_{1c} of the enamel was measured on the remaining specimens using the indentation K_{1c} (IF) method at three different distances from the dentin-enamel junction (5 indentations at each position, with a 10 N load and 15 s dwell time). Specimens were then submitted to ionizing (gamma) radiation at 70 Gy in a Co irradiation unit. RS and the IF test were re-conducted on the irradiated samples. Results were analyzed using non-parametric statistics (Wilcoxon-Mann-Whitney test, $\alpha < 0.05$).

Results: A significant decrease in the amide III/phosphate and the carbonate/phosphate ratios of the enamel ($p < 0.05$), accompanied by a significant drop of the CI, were observed after irradiation. The reduction in the K_{1c} displayed by the irradiated enamel reflected the impact of the microstructural changes on the mechanical properties of the material.

Conclusions: Ionizing radiation causes molecular changes in the organic and non-organic content of enamel, resulting in loss of the bond symmetry of the apatite structure and, consequently, a reduction of the mechanical properties.

<https://doi.org/10.1016/j.dental.2019.08.084>

84

Endocrown luting procedures: analysis of dual luting cements conversion rate



S. Chirico^{1,2,*}, A. Ionescu¹, L. Breschi²,
E. Brambilla¹, M.M. Gagliani¹

¹ Department of Biomedical, Surgical and Dental Sciences, University of Milan, Italy

² DIBINEM, University of Bologna, Italy

Purpose/aim: The purpose of this study was to investigate the conversion of dual cements polymerized by LED curing light and used to lute endocrowns, made by lithium silicate with high and low translucency milled by a CAD/CAM device.

Material and methods: A freshly extracted sound first maxillary premolar and a first maxillary molar were used and prepared - according to Bindl and Mörmann criteria - to receive an endocrown. The preparations were digitally scanned by an intraoral scanner (Cerec Bluecam, Software Version 4.2, Sirona Dental System) and 24 endocrowns were produced by a milling machine (Cerec MCXL Wounder, Sirona) using zirconia-reinforced lithium silicate (LS) (Calibra Duo, Dentsply) blocks. Half of the specimens (N=12) were prepared for the molars and the remaining half were designed and produced for premolars. Each group - molar and premolar - was further divided into two subgroups: one in which the restorations were made by a high translucency LS block (N=6) and the other was obtained by a low translucency LS block (N=6). After applying an insulator (Separating Fluid, Ivoclar) to the tooth and the tested dual cement to the endocrown, we placed the endocrown on the tooth and cured for 60 s using a LED light curing unit (Valo, Ultradent) with irradiance of 1000 mW/cm² from the occlusal site. In addition, 10 blocks of dual cement, size 5 x 7 mm and thickness of 1 mm as a control group (GC) we prepared. They were polymerized for 60 s through a transparent Mylar acetate strip. The conversion rate of the dual cement was evaluated by measuring the Vickers Hardness of the mate-

rial at the bottom of the preparation and compared it with the GC.

Results: The highest mean Vickers hardness values were recorded in GC: 41.9 (3.7), followed by the molar group (M) in lithium disilicate (LS) with high translucency (HT) (M_LS_HT): 39.7 (6.8). The lowest values were recorded in the premolar group (P) in LS with low translucency (LT) (P_LS_LT): 16.8 (1.1).

Conclusions: The conversion rate of the dual cement under LS endocrowns is strongly dependent on both the translucency of the material and the type of the tooth.

<https://doi.org/10.1016/j.dental.2019.08.085>

85

Stress relaxation via covalent dynamic bonds in nanogel containing resins



G. Gao*, X. Han, N. Swan, X. Zhang,
C. Bowman, J. Stansbury

Chemical and Biological Engineering, University of Colorado Boulder, USA

Objective: Polymerization stress is common in photopolymerization reactions in which monomers are rapidly converted to constrained polymer networks that cannot dissipate stress by viscous flow beyond gelation. Nanogels with covalent dynamic bonds that are able to both reduce in-situ polymerization stress and provide for the relaxation of strain-induced post-polymerization stress are examined here.

Methods: Nanogels were synthesized by reaction between a tetrathiol and a diacrylate using an excess of thiol to controllably achieve nano- rather than macro-gel. A nanogel (RAFT NG) with integral allyl sulfide linkages capable of reversible addition-fragmentation transfer activity was prepared along with a Control NG that lacks allyl sulfide functionality. Nanogel characterization involved dynamic light scattering, rheology, Ellman's test and dynamic mechanical analysis. A thiol-ene matrix resin was modified with 0 to 20 wt% of nanogel and the resulting photopolymers were analyzed for reaction kinetics, polymerization shrinkage stress, mechanical properties and post-polymerization stress relaxation potential.

Results: Control NG and RAFT NG have similar sizes (~250 nm), glass transition temperatures (~-15 °C), residual thiol concentration (~1.2 mmol/g) and shear thinning behavior. Photopolymerization of RAFT NG/thiol-ene resin results in slightly lower reaction rate and final conversion compared with the Control NG/thiol-ene. However, 10wt% RAFT NG-containing resins reduced shrinkage stress to about 40 % that with the Control NG. Mechanical properties including tensile strength, Young's modulus and T_g are maintained ($p < 0.05$) up to 10 wt% RAFT NG addition. Further, the fully cured RAFT NG photopolymers can achieve ~60 % relaxation of strain-induced stress in the glassy state upon UV exposure that reactivates network adaptation in the presence of radicals.

Conclusions: Incorporation of nanogels with internal allyl sulfide structure into thiol-ene resins, substantially reduced stress during and following polymerization. This work provides a novel functionalized nanogel with the ability to improve the properties and potential durability of crosslinked polymer networks with applications to dental composites.

(Funding: IUCRC for Applications and Fundamentals of Photopolymerization)

<https://doi.org/10.1016/j.dental.2019.08.086>

Paffenbarger Award Finalists

P1

3D printable resins combining extreme strength with toughness



R. Bailey^{1,*}, M. Barros¹, P.K. Shah²,
J.W. Stansbury^{1,2}

¹ Department of Craniofacial Biology, University of Colorado Anschutz Medical Campus, USA

² Department of Chemical & Biological Engineering, University of Colorado Boulder, USA

Purpose/aim: Continued advances in digital dentistry are reliant on the development of additive manufactured polymeric materials with mechanical properties that enable credible expansion into interim or even longer-term functional intraoral application. 3D printing of restorative/prosthetic devices requires relatively low viscosity, readily photocurable resins that provide aesthetic, high conversion polymers with high isotropic strength along with excellent durability. This study focuses on a class of physically reinforced covalent network polymers that are designed to uniquely deliver both high strength and toughness.

Materials and methods: Several urethane (meth)acrylate monomers were individually formulated with methacrylic acid and a variety of hydrophobic comonomers to produce resins with ambient viscosities at or below 100 mPa.s that are suitable for printing with a DLP device. The resins containing a UV/visible light photoinitiator and a complementary photo-absorber were used to print standard disc and bar test specimens using 50 μ m layers at 5 s exposure per layer on an Octave printer (405 nm). Printed specimens were washed in isopropanol and subjected to a post-cure process using both 365 and 405 nm LED with an optional integrated thermal treatment. Conversion was monitored by near-IR for the various post-cure regimes. Mechanical test specimens were tested dry or following water storage to gravimetrically verified equilibrium saturation.

Results: As an example of the high performance potential associated with these physically reinforced covalent networks, one of the resin compositions was printed and post-cured to give optically clear, unfilled polymer with dry and wet flexural strength of 193.6 & 16.4 MPa and 183.1 & 23.9 MPa, respectively ($n=10$). The dry/wet flexural modulus was 4.07 & 0.63 GPa and 3.76 & 0.46 GPa, respectively. The maximum single-specimen flexural properties obtained were 215 MPa in ultimate strength and 5.2 GPa in modulus with a deflection to failure of 235%. After tuning the resin formulation and the printer parameters, equivalent strength and modulus were obtained for printed samples and analogous bulk molded samples.

Conclusions: The urethane-carboxylic acid physical interaction in these resins lowers initial viscosity and promotes exceptional mechanical strength that is uniquely coupled

with excellent toughness. The presence of water does not compromise the physically reinforced network. The ability to 3D print high performance, clear polymers allows viable consideration of suitably pigmented resins as interim intraoral dental devices.

<https://doi.org/10.1016/j.dental.2019.08.087>

P2

Development of porous calcium-hydroxide-linked scaffolds for dentin cell-homing therapy



E.A.F. Bordini^{1,3,*}, F.B. Cassiano¹,
E.S. Bronze-Uhle², L.E. Pacheco², G. Zabeo²,
J. Hebling¹, M.C. Bottino³,
C.A. De Souza Costa¹, D.G. Soares²

¹ Araraquara School of Dentistry, São Paulo State University, Araraquara, Brazil

² Bauru School of Dentistry, University of São Paulo, Bauru, Brazil

³ School of Dentistry, University of Michigan, Ann Arbor, USA

Purpose/aim: This study describes a method to create highly porous calcium-hydroxide-linked chitosan (CH-Ca[OH]₂) scaffold to be used as a cell-free tissue engineering system for dentin regeneration.

Materials and methods: The synthesis was based on calcium hydroxide (Ca[OH]₂) incorporation into chitosan solution followed by freezing-drying, to modulate porosity degree and donate calcium for complexation. Chitosan concentration and freezing protocol were adjusted to optimize the porous architecture. Surface topography was evaluated by scanning electron microscopy (SEM), and pore degree/diameter were calculated (ImageJ). Calcium incorporation was detected by Fourier-transform infrared spectroscopy (FTIR)/energy-dispersive spectroscopy (EDS). Degradability degree was then tuned by glutaraldehyde vapor cross-linking, and cumulative calcium release was calculated (o-cresolphthalein). Thereafter, dental pulp stem cells (DPSCs) were seeded onto chitosan (CH) and CH-Ca(OH)₂ scaffolds, and cellular viability (Live/dead), proliferation (Alamar blue), and adhesion/spread (F-actin) were analyzed. Mineralized matrix deposition (Alizarin red) was analyzed on scaffolds adapted to human dentin discs. Finally, the chemotactic (live/dead) and bioactive potential (DSPP, DMP-1, ALP, Col1; RT-PCR) was investigated by means of 3D-cell culture model into artificial pulp chambers coupled to simulated pulp pressure (pAPC).

Results: SEM/EDS analysis demonstrated that incorporating Ca(OH)₂ into 2% chitosan solution followed by gradual freezing (-20 °C/-80 °C/-198 °C) creates a calcium-containing chitosan scaffold with an organized and interconnected porous network; whereas, CH scaffold had a disorganized one. Pore diameter and overall porosity increased significantly from 86.9 μ m and 32.17% on CH, to 202.1 μ m and 86.89% on CH-Ca(OH)₂, respectively. The FTIR analysis suggested that Ca(OH)₂ induced a bubbling effect due to carbonation followed by carbonic gas release, and confirmed that calcium complexation occurred. Degradability degree was stabilized by

glutaraldehyde cross-linking, and sustained calcium release was detected for the CH-CH-Ca(OH)₂ scaffold throughout 21 days. The live/dead and F-actin images demonstrated that CH-Ca(OH)₂ architecture allowed for viable cells to spread throughout its structure with increased cell proliferation ($p < 0.05$), whereas cells in CH were agglomerated in clusters. Increases on mineralized matrix deposition and gene expression of odontoblastic markers were detected for CH-Ca(OH)₂ in comparison to CH scaffold ($p < 0.05$). Also, DSP+ cells from 3D culture were found adhering to CH-Ca(OH)₂ scaffold on pAPC assay.

Conclusions: The incorporation of CH-Ca(OH)₂ on chitosan scaffolds under gradual freezing by phase separation is capable to create a highly organized porous network, optimizing DPSCs infiltration and proliferation, along with sustained calcium release capable to induce chemotaxis and to improve the odontogenic potential of DPSCs, being thus an interesting alternative for cell-homing therapy.

<https://doi.org/10.1016/j.dental.2019.08.088>

P3

Photoreactive nanogels for local treatment of the oral cavity



H. Escobedo*, J.W. Stansbury, D.P. Nair

University of Colorado Anschutz Medical Campus,
Aurora, USA

Purpose/aim: The aim of this study is to synthesize photoreactive nanogels with tunable drug release kinetics that can be tailored for the localized delivery of therapeutics within the oral cavity.

Materials and methods: A one-pot, solution polymerization reaction in which of 2-hydroxyethyl acrylate, tetraethylene glycol dimethacrylate, and acrylic acid monomers (60:20:20 molar ratios, designated as the HTA nanogels) with 2, 2'-azobis (2-methylpropionitrile) (1 wt%) and 2-mercaptoethanol (20 mol%) was stirred at 80 °C in the solvent methyl ethyl ketone (MEK) until the double bond 70% conversion was implemented to synthesize the nanogels. The solvent to monomer ratio was systematically altered from two-(2X), four-(4X), six-(6X), and eight-fold (8X) excess of MEK. Characterization of the 2X to 8X nanogels were done with FTIR spectroscopy, gel permeation chromatography, dynamic light scattering, viscometer, and dynamic mechanical analysis. The 4X-HTA nanogel were functionalized with 10% or 100% moles of 2-isocyanatoethyl methacrylate (IEM). Rhodamine B (RhB) was utilized as a small molecule drug mimic and incorporated within the 4X-HTA. The release kinetics of the different photo-aggregated, RhB-loaded methacrylated 4X-HTA nanogels via light exposure (365 nm, 10 mW/cm², and 30 s) was quantified for over 30 days.

Results: By altering the solvent excess during synthesis, tailored nanogels with molecular weight from 1.9 kDa to 47.9 kDa and hydrodynamic radius between 0.9–3.2 nm with the ability to swell more than 30 times their initial volume were synthesized. The 4X-HTA methacrylated nanogels with 0%-, 10%-, and 100% - reactive functionality yielded significantly different surface charges with zeta potential values of -6.4 mV, -13.3 mV, and -16.7 mV ($p < 0.05$) respectively. The

4X-HTA nanogel with maximum photoreactive functionality was shown to most efficiently control the burst release of the model small molecule drug (RhB) upon light exposure release at 7% at 24 h in comparison with the nanogels with less-to-no reactive functionality (40 % and >75% at 24 h respectively).

Conclusions: Photoreactive nanogels with tunable drug release kinetics can be synthesized using the protocol outlined in this study. The potential to control the encapsulation and drug release kinetics via the concentration of photoreactive groups on the surface and the photo-induced aggregation of the nanogels offers the unique ability to control the *in situ* drug release of oral therapeutics.

<https://doi.org/10.1016/j.dental.2019.08.089>

P4

Mini-interfacial fracture toughness when bonding indirect restorations with light-curable composite



C.M.F. Hardy*, V. Landreau, M. Valassis,
B. Mercelis, B. Van Meerbeek, J.G. Leprince

UCLouvain, Louvain-la-Neuve, Belgium

Purpose/aim: Using solely light-curable highly-filled resin-based composite to lute thick indirect restorations presents practical advantages. The goal of this work was to validate the rationale of this strategy by measuring the mini-interfacial fracture toughness (mini-iFT) by testing the influence of (a) the luting composite type (light- vs. dual-cure), (b) the indirect restoration thickness (2 vs. 6 mm), and (c) the filler content (50vs.75 wt%) of the resin-based composite used for immediate dentin sealing (IDS) after cavity preparation.

Materials and methods: 64 extracted wisdom teeth were cut to expose dentin, which was then immediately sealed with Clearfil SE Bond 2 (Kuraray Noritake, Japan) and a thin layer of an experimental resin-based composite ("IDS"; 50/50 wt% TEGDMA/BisGMA, camphorquinone/amine (0.2/0.8 wt%) as photoinitiator, and 40/10wt % vs. 65/10 wt% of barium-glass microfiller and fumed silica nanofiller, respectively). Both the IDS and the 2-vs.6-mm thick CAD/CAM composite blocks (Katana Avencia A3, Kuraray Noritake) were sandblasted, conditioned by Clearfil Ceramic Primer Plus (Kuraray Noritake) and luted together with either a pre-heated (68 °C) highly-filled light-cure composite (ClearfilAP-X, Kuraray Noritake) or a control dual-cure composite cement (Panavia V5, Kuraray Noritake). Light-curing was performed with BluephaseG2 (1100 mW/cm², Ivoclar Vivadent, Liechtenstein); irradiation times were adjusted in order for luting composites to reach similar degree of conversion (Raman spectrometry), i.e. 40s and 240s through 2-mm and 6-mm thick blocks, respectively. The prepared samples were then cut in sticks ($n = 40$) with a 1.5x2 mm cross-section; a notch with controlled dimensions was cut at the interface between IDS and luting composite. The sticks were submitted to 4-point bending to determine the mini-iFT (0.05 mm/min; 5848 MicroTester, Instron, USA). The fractured interfaces were verified by SEM and the results were analyzed by 3-wayANOVA and Weibull analysis (JMP Pro14).

Results: There was no significant ($p = 0.38$) difference in mini-iFT for the 2-vs.6-mm thick blocks. However, a significant

($p < 0.0001$, power = 0.999) difference in mini-iFT was found between the luting composites in favor of Clearfil AP-X, as well as regarding the filler content of IDS ($p = 0.0011$; power = 0.9) in favor of the 50wt% filler content. Weibull distribution revealed a higher shape parameter, i.e. increased reliability of the procedure when using ClearfilAP-X.

Conclusions: This work provides the proof of concept that 2- and 6-mm thick indirect restorations can safely be luted with a pre-heated solely light-curable highly-filled composite, which even is beneficial in terms of mini-iFT as compared to using a dual-cure luting composite. IDS with a lower filler content resulted in a higher mini-iFT.

<https://doi.org/10.1016/j.dental.2019.08.090>

P5

Rechargeable dual function dental sealant against cariogenicity of streptococcus mutans



M.S. Ibrahim^{1,2,*}, A.S. Ibrahim³,
A.A. Balhaddad^{1,2}, M.D. Weir¹, T.W. Oates¹,
H.H.K. Xu^{1,4}, M.A.S. Melo¹

¹ University of Maryland School of Dentistry,
Baltimore, USA

² College of Dentistry, Imam Abdulrahman Bin
Faisal University, Dammam, Saudi Arabia

³ Health Monitoring Centers, Ministry of Health,
Jeddah, Saudi Arabia

⁴ University of Maryland School of Medicine,
Baltimore, USA

Purpose/aim: Nanoparticles of amorphous calcium phosphate (NACP) and dimethylaminohexadecyl methacrylate (DMAHDM) are being heralded as an excellent candidate for bioactivity purposes. However, the limitation of calcium and phosphate ion-depletion effect with loss of bioactivity over time and the less understanding of antibacterial effect against cariogenic bacteria hamper the development of these materials. Here, we report our work on (1) development of an efficient dual DMAHDM-NACP bioactive resin-based formulation capable to substantial initial ion release and a long-term repeated recharge capability, and (2) investigations of the *S. mutans* cariogenic response against the DMAHDM-NACP resin-based formulations intended as dental sealants.

Materials and methods: A parental formulation consisted mainly of pyromellitic glycerol dimetacrylate (PMGDM)/ethoxylated bisphenol A dimetacrylate (EBPADMA) was tuned, aiming the maximum mass ratio of DMAHDM and NACP. Flexural strength (FS), flexural modulus (FM), flowability (Fw) and Ca/PO₄ ion release profile before/after ion recharging cycles as a function of the NACP concentration were evaluated. In addition, the effect of these new sealants on *S. mutans* cariogenicity was assessed by colony-forming unit (CFU) counts, cell biomass (CV), metabolic activities (MTT), lactic acid production (LA), polysaccharide production (EPS), oxygen stress tolerance and acid stress tolerance. Data were analyzed using one-way analysis of variance (ANOVA) and Bonferroni's multiple comparison tests at an alpha of 0.05.

Results: A stable antibacterial, high ion releasing, and rechargeable formulation was reached when NACP con-

centration reached 20 wt.% combined with 5% DMAHDM. 20%NACP-containing sealants showed a release of 3.64 ± 0.11 mmol/L ($p < 0.05$) of Ca ions and 3.41 ± 0.10 mmol/L of PO₄ ions during the 70-day period. After each recharging cycle, the formulations satisfactorily released Ca and PO₄ ions with no decay after subsequent recharges. FS, FM, and Fw were similar to controls. Our results uncovered for the first time that sealant formulations containing DMAHDM have significant antibacterial activities. Furthermore, these formulations showed a critical role on *S. mutans* virulence factors. Sealants containing DMAHDM in their compositions strongly reduced *S. mutans* biofilm by 90-95% ($p < 0.05$). The ability of *S. mutans* to survive and resist high acid and oxygen stresses, MTT, CV, EPS, and LA were also significantly reduced.

Conclusions: The tuned formulations showed promising remineralizing abilities through ions release and recharge. Overall, our data support that sealants with 5%DMAHDM may disrupt the biofilm of *S. mutans* by targeting its virulence factors. This outcome opens the door for an important pathway on the suppression of cariogenic biofilm around dental materials.

<https://doi.org/10.1016/j.dental.2019.08.091>

P6

Dark-curing photoinitiators that extend the cure depth in composite materials



K. Kim^{1,*}, J. Sinha¹, A.M. Salazar¹,
C.B. Musgrave¹, J.W. Stansbury^{1,2}

¹ University of Colorado, Boulder, Colorado, USA

² School of Dental Medicine, Aurora, Colorado, USA

Purpose/aim: Achieving maximum conversion throughout an optically thick photopolymer (i.e. filled composites) requires extended irradiation of the exposed surface to ensure near-comparable levels of conversion at the light-attenuated, opposite surface. Due to the efficient termination in radical polymerizations, conversion immediately stops with only limited post-cure potential if access to the curing light and continued radical production is interrupted. A strategy to uniformly maximize final conversion within photopolymers by extending radical initiation beyond the temporal exposure of the curing light is advanced here through a photo-activated initiation with immediate radical production upon photolysis and latent redox radical generation that arise from the controllably prolonged reactions between photo-generated amines and peroxide, which effectively extends the cure depth.

Materials and methods: The resin was 90 wt% triethylene glycol dimethacrylate (TEGDMA) and 10 wt% α -methylene- γ -butyrolactone, the cyclic analogue of methyl methacrylate. Dark-curing photoinitiators (DCPI) was synthesized, while the control photoinitiator (CTPI) was benzophenone with N,N-dimethyl-p-toluidine (DMPT) coinitiator. The DCPI generates initiating radicals and releases DMPT upon UV irradiation ($\lambda_{max} = 340$ nm), which ensures rapid surface cure and latent redox initiation between photo-released DMPT and benzoyl peroxide (BPO) over extended time periods. The concentrations of photoinitiators and BPO are respectively 0.50 and 0.56 wt% relative to the resin. A 365 nm LED was used at an

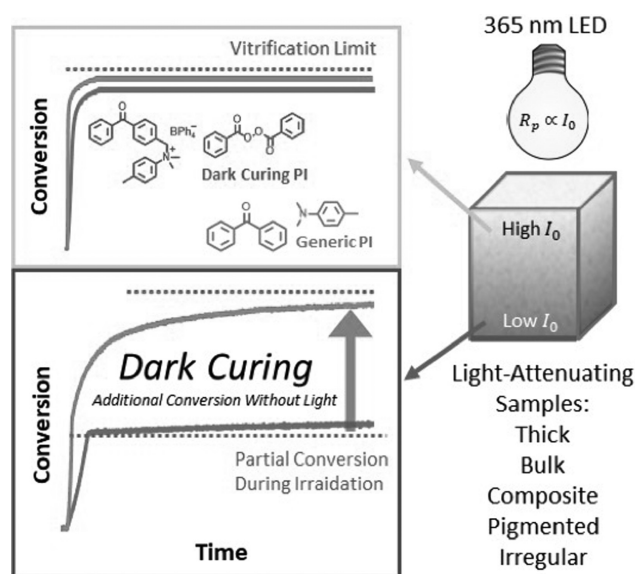


Figure 1

incident irradiant intensity of 30 mW/cm^2 . The continuous polymerization after a short irradiation (dark-curing) was confirmed by real-time FTIR, sampling the vinyl absorption band at 1637 cm^{-1} .

Results: Under limited irradiation of a thin specimen to mimic the condition of an under-cured layer within a deep composite, the DCPI achieved an initial conversion of $\sim 20\%$ during the active photocuring. However, the continuous generation of radicals from efficient room temperature redox reactions achieved an additional $\sim 23\%$ conversion over 1 h without reliance on irradiation or heating. Such dark-cure results are juxtaposed against the analogous experiments with CTPI, whose conversion rapidly plateaued at the 20% conversion. Additional examples showing control of the rate/extent of the dark-cure redox reaction will be highlighted along with the ability to tune the DCPI into the visible light wavelength range (Fig. 1).

Conclusions: The potential to reach full conversion under non-ideal photocuring conditions or throughout highly light-attenuating, thick films, such as bulk fill dental composites, can be reliably accomplished with the DCPI approach. This offers the prospect to shift to a new paradigm where the final degree of conversion does not have to be determined directly by the duration of irradiation.

<https://doi.org/10.1016/j.dental.2019.08.092>

P7

Development of higher substituted thiols for improved thiol-ene dental materials



K. Long*, A. Ortego, M. Olin, C. Bowman

University of Colorado Boulder, USA

Purpose/aim: Thiol-ene materials have been proposed as alternatives to methacrylate based dental materials. To improve thiol-ene materials, secondary thiol monomers were

Final Conversions for Thiol-Ene Small Molecule Tests with NMR analysis

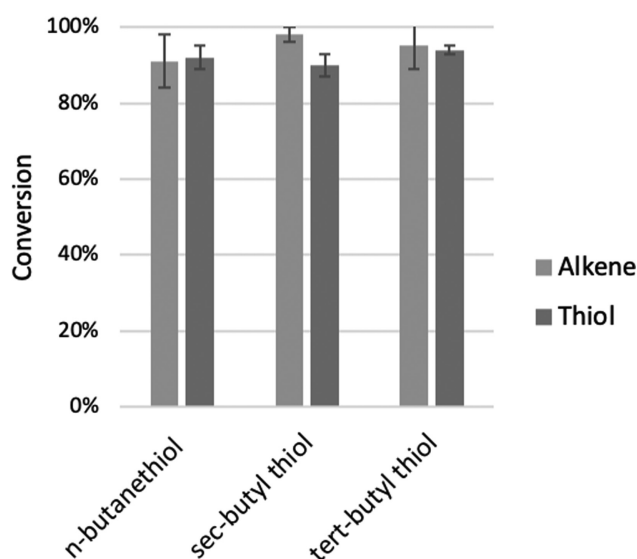


Figure 1

first proposed to have reduced odor and extended stability in monomer solutions. This study investigates how the substitution of the thiol affects the thiol-ene polymerization.

Materials and methods: Preliminary small molecule studies were completed using isomers of butane thiol. Analogous primary, secondary, and tertiary monomers were synthesized. Reaction kinetics (rate and conversion) were studied using FT-IR and NMR analyses. Mechanical properties were examined using DMA, MTS, and shelf life studies were conducted.

Results: Small molecule studies reveal that primary, secondary, and tertiary thiols have near identical rates under “standard conditions” (30 mW/cm^2 light intensity, 1 wt% initiator loading). Under reduced conditions, it was discovered that increasing the substitution decreased the rate of reaction (Fig. 1). Polymeric studies show that the rate decreases with increasing substitution, but has a larger decrease in rate for tertiary thiols. The mechanical rates did not differ greatly when the substitution of the thiol was increased.

Conclusions: Kinetic results demonstrate that secondary and tertiary thiols can be incorporated into the thiol-ene reaction without severe adverse effects. Even though the rate did decrease with increasing substitution, the amount the rate decreased is highly dependent on both the thiol and alkene structures. Mechanical tests show that the substitution does not greatly alter mechanical properties.

<https://doi.org/10.1016/j.dental.2019.08.093>

P8

Residual stresses in bilayer crowns: a vfem studyC.S. Rodrigues^{1,2,*}, S. Dhital³, L.G. May², J. Kim³, Y. Zhang¹¹ New York University, USA² Federal University of Santa Maria, Brazil³ University of Connecticut, USA

Purpose/aim: Previous literature stated that chipping of the porcelain in bilayer restorations might be associated with tensile residual thermal stresses in the porcelain overlay. This study aimed to elucidate the effects of cooling rates and veneer/core thickness ratios on residual stresses developed in porcelain-veneered zirconia (PVZ) and metal-ceramic (MC) restorations using a novel viscoelastic finite element method (VFEM).

Materials and methods: First, a PVZ bar specimen was modeled to carry out the VFEM analysis, and residual stresses were predicted. Then, residual stresses in these PVZ bar specimens, were measured by the Vickers indentation method to validate the VFEM model with experimental data. As an excellent agreement was observed, the model was used to predict residual stress profiles in bilayer crowns. Two bilayer systems were studied: porcelain-veneered zirconia (Vita VM9/3Y-TZP) and metal-ceramic (InLine PoM/CoCr4). Models with two different veneer/core thickness ratios were prepared (2:1 and 1:1) and two cooling protocols were simulated (Fast: ~300 C/min, Slow: ~30C/min) using a heat transfer, followed by the residual stress analysis. The physical properties of zirconia, metal, and porcelains used in the FEM simulations were all measured as a function of temperature. Zirconia and metal exhibited linear elastic properties whereas porcelains showed a viscoelastic behavior.

Results: MC models showed lower stresses in the porcelain layer than PVZ. Model 1:1 showed decreased tensile stresses in the veneer of both bilayer systems, especially when slow cooling was applied (PVZ slow: ~34 MPa, PVZ fast: ~55 MPa, MC slow: ~17 MPa, MC fast: ~40 MPa). Model 2:1 revealed similar maximum tensile stresses in the porcelain over metal and zirconia when fast cooling was applied (PVZ: ~56 MPa, MC: ~53 MPa). However, stresses decreased due to slow cooling (PVZ: ~46 MPa, MC: ~23 MPa). Slow cooling induced a wide range of compressive stress regions in PVZ crowns.

Conclusions: Metal framework led to lower residual stresses at the porcelain layer in all simulations. Nevertheless, when zirconia is chosen as framework, a slow cooling protocol is essential to decrease the tensile residual stresses. Using a thinner porcelain overlay combined with a slow cooling protocol is advised to minimize residual stresses in bilayer restorations.

<https://doi.org/10.1016/j.dental.2019.08.094>

Marshall Awards Finalists

M1

Methacrylamide-methacrylate hybrid monomers for dental applications

A. Fugolin*, M.G. Logan, S. Lewis, J.L. Ferracane, C.S. Pfeifer

Oregon Health & Science University, Portland, USA

Purpose/aim: Methacrylamides have shown increased resistance to enzymatic/hydrolytic degradation compared to methacrylates, due in part to the absence of labile ester bonds. However, methacrylamides are highly hydrophilic, jeopardizing mechanical performance due to water sorption. In this study, hybrid methacrylamide-methacrylate monomers were designed with the hypothesis that the increased crosslinking provided by the difunctional species would reinforce the hydrophilic network, while still providing adequate interaction with the moist dentin. Polymerization kinetics and water sorption/solubility were used as screening tools for bond strength evaluation.

Materials and methods: HEMA, TEGDMA (controls) or secondary methacrylamides (HEMAM – commercially available, 2EM and 2dMM – newly synthesized) either bearing a hydroxyl group or a methacrylate functionality (Hybrids-Hy) were added at 40 wt% to BisGMA. 2-dimethoxyphenyl acetophenone and diphenyl iodonium hexafluorophosphate (0.2/0.4 wt%) were added as photoinitiators. Polymerization kinetics was followed in real-time during polymerization for 300s at 630 mW/cm² by near-IR spectroscopy. Water Sorption/solubility (WS/SL) were measured according to ISO 4049. Storage Modulus in shear (G') was obtained by rotational rheometry. Ethanol was added at 40 vol% to selected compositions and tested for dentin microtensile bond strength (μ TBS) in caries-free human third molars, 48 h after restoration. Single bond (SB) was tested as commercial control. Data were analyzed with one-way ANOVA/Tukey's Test ($p = 0.05$).

Results: Results for kinetics, WS/SL, and G' are presented in Figure 1. In general, hybrid monomer had lower maximum rate of polymerization (RPMAX), final degree of conversion (DC) and DC at RPMAX compared to the

Table 1. Average (SD) of maximum rate of polymerization (RP_{MAX}), degree of conversion at RP_{MAX} (DC at RP_{MAX}), final degree of conversion (Final DC), water sorption (WS), solubility (SL), and storage modulus (G') for all tested monomers copolymerized with BisGMA in 40 wt%. Values followed by the same letter within the same column indicate statistical similarity ($p > 0.05$).

Diluent Monomer	Polymerization Kinetics			WS ($\mu\text{g}/\text{mm}^3$)	SL ($\mu\text{g}/\text{mm}^3$)	G' (MPa)
	RP _{MAX} (%·s ⁻¹)	DC at RP _{MAX} (%)	Final DC (%)			
TEGDMA	0.11 (0.02) A	19.6 (5.3) A	78.0 (2.7) BC	35.54 (1.84) EF	-4.24 (6.03) B	119.81 (0.63) B
HEMA	0.07 (0.01) AB	21.0 (3.5) A	89.0 (1.9) A	93.90 (4.77) C	-12.73 (1.59) C	122.93 (14.68) AB
HEMAM	0.05 (0.006) B	13.0 (1.5) AB	83.2 (3.2) AB	183.03 (5.74) A	-11.67 (0.92) C	130.56 (24.04) AB
HEMAM Hy	0.03 (0.005) C	8.7 (1.9) B	63.5 (0.8) D	38.73 (1.84) EF	-1.59 (0.00) B	160.73 (8.03) A
2EM	0.09 (0.01) AB	16.8 (2.3) AB	73.6 (1.4) C	101.31 (1.48) B	6.37 (2.25) A	119.79 (18.38) B
2EM Hy	0.08 (0.02) AB	14.7 (3.8) AB	63.3 (2.0) D	44.03 (0.92) E	0.00 (0.00) AB	135.07 (8.33) AB
2dMM	0.09 (0.02) AB	15.7 (3.4) AB	76.7 (2.2) C	79.05 (0.92) D	6.37 (0.00) A	130.87 (13.85) AB
2dMM Hy	0.07 (0.01) AB	12.5 (2.5) AB	59.4 (1.2) D	33.42 (3.18) F	-0.53 (2.43) AB	115.70 (7.01) B
p value	<0.001	0.007	<0.001	<0.001	<0.001	0.024

Figure 1

OH-bearing counterparts. HEMA and TEGDMA presented the highest values. Hybrid monomers had lower values of WS/SL compared to OH-bearing monomers. HEMAM-Hy had the highest WS/SL and TEGDMA, 2EM, and 2dMM-Hy the lowest. SB showed the highest values of μ TBS after 48 h (53.4 ± 9.8 a MPa), statistically higher than the other formulations, which in turn were all statistically similar to each other (HEMA = 42.3 ± 9.0 ab, HEMAM = 31.1 ± 8.4 b, HEMAM-HY = 28.5 ± 10.7 b, 2dMM = 29.7 ± 4.3 b, and 2dMM-Hy = 27.9 ± 6.0 b MPa, respectively). In the near future, we will be able to determine bonding stability for specimens stored for 6 months. Overall, hybrid monomers showed lower reactivity than their analogous OH-bearing analogs, but markedly higher stability in water. Storage modulus was highly dependent on the monomer structure. Early μ TBS was similar for all experimental materials compared to the HEMA control.

Conclusions: The new monomers are promising alternatives for dental adhesive formulations. However, bond stability is a crucial aspect, and this investigation is currently underway.

<https://doi.org/10.1016/j.dental.2019.08.095>

M2

Antimicrobial properties of PMMA resin containing graphene

A.C. Ionescu^{1,*}, S. Sauro², P.M. Pires³,
A. López-Castellano¹,
A.M. Alambiaga-Caravaca¹, E. Brambilla¹

¹ University of Milan, Department of Biomedical,
Surgical and Dental Sciences, Milan, Italy

² Universidad Cardenal Herrera-CEU, Valencia,
Spain

³ Federal University of Rio De Janeiro, Rio De
Janeiro, Brazil

Purpose/aim: Modern prosthetic dentistry is increasingly focusing on digital procedures, including CAD/CAM technologies. In this context, PMMA is being widely employed as material for prosthetic and restorative devices. Secondary caries is still the main reason for the failure of dental resin-based restorations. Therefore, an antimicrobial activity expressed by these materials is regarded as beneficial for their longevity. This study aimed to test the physical, chemical, and microbiological behavior of a PMMA resin for CAD/CAM applications containing graphene.

Materials and methods: Specimens ($n=48$) were made from <50 ppm graphene-containing PMMA disks and from conventional PMMA disks for CAD/CAM applications. Specimens were finished with abrasive paper up to 4000 grit, and a half was subjected to soaking in absolute ethanol for 24 h. This protocol was introduced to evaluate the microbiological behavior of the tested samples after softening of the surface, thus accelerating aging of the surfaces of restorative resins.

Material characteristics were assessed in terms of surface roughness, microhardness, ultimate tensile strength, solubility, and water sorption. Elution of methyl-methacrylate after specimen treatment was determined using HPLC. After 24 h pre-incubation with sterile human saliva, the

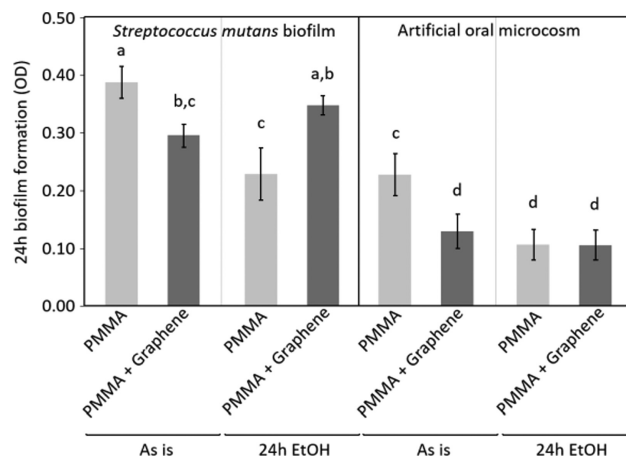


Fig. 1

microbiological behavior of the materials was assessed using two models: *Streptococcus mutans* biofilm formation in a continuous-flow bioreactor simulating shear forces (30 ml/h) for 24 h, and artificial oral microcosm based on mixed plaque inoculum developed using the same setup for 24 h. The viable biomass adhering to the specimens' surfaces was measured using a tetrazolium dye-based test. Statistical analysis included verification of normality of distribution and homoscedasticity, then multi-way ANOVA and Student's t-test ($\alpha = .05$).

Results: Finishing protocol produced no significant differences in surface roughness between tested materials. Ethanol treatment significantly reduced surface microhardness in both materials, but to a lesser extent on graphene-containing PMMA. No difference in ultimate tensile strength was found between materials. Graphene-containing PMMA showed significantly lower water sorption and solubility compared to conventional PMMA. After ethanol treatment, a significantly lower amount of leachates was identified for graphene-containing PMMA. Graphene addition significantly reduced biofilm formation compared to control in both microbiological models (Fig. 1). Interestingly, specimen treatment produced the opposite (*S. mutans* model) or no effect (artificial oral microcosm) on biofilm formation.

Conclusions: Graphene-added PMMA is a promising material from both mechanical and microbiological point of view. Ethanol treatment influenced surface characteristics of the materials, leaving on graphene-added PMMA a surface more prone to bacterial colonization.

<https://doi.org/10.1016/j.dental.2019.08.096>

M3

Mechanical and antimicrobial properties of novel bioactive dental restorative composites

C.B. Tanaka^{1,*}, F. Gonçalves², D.P. Lopes²,
L.H. Catalani³, R.R. Braga³, J.J. Kruzic¹

¹ University of New South Wales, Australia

² Ibirapuera University, Brazil

³ University of São Paulo, Brazil

Purpose/aim: The aim of this study was to investigate the effect of adding either chitosan particles or chitosan particles loaded with di-calcium-phosphate anhydrous (DCPA) to a resin composite on mechanical and antimicrobial properties against *Streptococcus Mutans*.

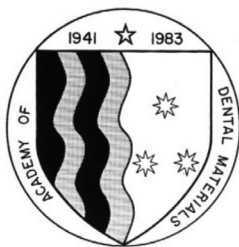
Materials and methods: Composites with 60 wt% barium glass filler content and a mix of 1:1 molar ratio of TEGDMA and BISGMA were prepared while adding 0.5 or 1.0 wt% sub-micron particles of chitosan or chitosan loaded with DCPA. Flexural strength and fracture toughness were performed after two different soaking treatments: 24 h or 90 days in DI water. Mechanical properties of new bioactive composites were compared along with the control composite (containing only barium glass) by two-way ANOVA and Tukey's multiple comparison test ($p \leq 0.05$). Antimicrobial properties were evaluated by crystal violet biofilm assay. The specimens were incubated in a *Streptococcus Mutans* solution at 37 °C and 5 % CO₂ for 24 h. The biofilms were quantified by crystal violet

staining (optical density 595 nm). The results were compared by Kruskal-Wallis and Student-Newman-Keuls multiple comparison test ($p \leq 0.05$).

Results: The results showed that the mean flexural strength for 24 h hydration of 0.5 % chitosan, 85.0 ± 8.7 MPa, was statistically similar to control group 78.7 ± 7.2 MPa and showed ~20% higher strength compared with the other groups. After 90 days hydration, there was no significant difference between the strength of any of the materials ($p > 0.05$); however, the mean flexural strength of all experimental material significantly increased by approximately 23 % after 90 days of water hydration except for the 0.5% chitosan group that presented a reduction of ~8 %. The fracture toughness was similar (0.85 ± 0.04 MPa. \sqrt{m}) for all experimental materials and for both hydration periods of 24 h and 90 days. Crystal violet biofilm assay showed a significant lower biofilm quantity for the experimental materials compared with control ($p < 0.001$), however, there were no differences between any of the chitosan and chitosan/DCPA groups.

Conclusions: The mechanical properties of a novel bioactive restorative composite are not affected by the presence of chitosan or chitosan/DCPA submicron spheres and present antimicrobial properties against *Streptococcus Mutans*. A potential for ions releases also can be attributed to this design material but more studies are needed to evaluate their efficiency to remineralization tooth structures.

<https://doi.org/10.1016/j.dental.2019.08.097>



ACADEMY OF DENTAL MATERIALS

www.academydentalmaterials.org

General information:

The Academy of Dental Materials is a body composed of individuals interested in the science of dental materials. The Academy of Dental Materials exists solely for the purpose of advancing the science and technology of dental biomaterials. This is accomplished by sponsoring annual scientific meetings, conferences, an international journal, transactions of scientific proceedings, awards for students, awards for outstanding scientists, and the confirmation of Fellowship for special members.

Membership information and instructions:

Membership dues are kept at a minimal level to encourage membership (US\$ 149 Regular and Fellow, US\$ 40 Student, US\$ 55 Post-Doctoral, and US\$ 2000 Corporate). These rates include an online subscription to the *Dental Materials* journal. Regular and ADM Fellow members can choose to additionally receive a hard copy of the journal for an additional US \$26 (or US\$ 175 total). Academy members receive a discounted registration fee for the annual ADM meeting. ADM meetings are conducted using a style that promotes interaction among participants. The opportunity for student and faculty presentations is afforded through poster presentations during meeting days. For membership application forms, meeting information, and general instructions, please contact: Dr. Ricardo M. Carvalho, DDS, PhD, FADM, Email: rickmc@dentistry.ubc.ca

Corporate membership information:

As a Corporate Member, the company will be recognized in the *Dental Materials* journal (circulation approximately 1,800). The corporation name and logo will appear on a special page (in each issue of the journal) acknowledging the Corporate Members. In addition, a complimentary online and hard-copy subscription to *Dental Materials* will be sent to the corporate contact during the year of membership. Meeting sponsorship is independent of corporate membership. The Corporate Member fee is US\$ 2000 per year. For corporate membership information, please contact: Lynn Reeves, Executive Manager, E-mail: admin@academydentalmaterials.org, Phone: (858) 272-1018 FAX: (858) 272-7687

Fellowship and Student Award information:

Academy members in good standing may apply for Fellowship in the Academy. Applications must include a current c.v. and two letters of recommendation from current Fellows of the Academy. The criteria to apply for Fellowship are (1) achievement of advanced degrees: at least a master's degree and preferably a Ph.D., Odont Dr., or equivalent degree; (2) publication of at least ten peer-reviewed, scientific articles in refereed journals of which the candidate should be first author on one-half of the articles; (3) at least five years of leadership through research, training, service, and/or education beyond formal education; and (4) normally at least five years membership in the Academy.

University Student Award

Each year, the members of the Academy of Dental Materials affiliated with various Dental Schools around the world, present awards to their most outstanding students or student researchers in the field of dental materials.

For information regarding Fellowship in the Academy and annual dental student awards, please contact: Dr. Milena Cadenaro
E-mail: mcadenaro@units.it.

Student Travel Award

The ADM offers Student Travel Awards to facilitate attendance and participation in the ADM annual meeting by outstanding students currently enrolled in an education program in areas relevant to the mission of the ADM.

Paffenbarger Award

Students pursuing graduate studies in dental materials or biomaterials sciences and dental students who have conducted research in dental materials or biomaterials sciences are encouraged to compete in the **Paffenbarger Award** competition at the annual meeting of the Academy. The winner of the award competition receives a prize of US\$ 1,750, the second- place winner receives US\$ 1,250, and the third-place winner receives US\$ 1,000. All 3 students also receive free registration for the next ADM Meeting. In addition to the Paffenbarger Award, the Academy presents an annual award at each dental school to the student who has demonstrated outstanding academic achievement in dental materials science. For information regarding the Paffenbarger Award competition, please contact: Dr. Arzu Tezvergil-Mutluay E-mail: arztez@utu.fi

Marshall Postdoctoral Award

The ADM offers the **Marshall Postdoctoral Award** to recognize and encourage excellence in dental biomaterials research performed by individuals in the transitional post-doctoral stage of their careers. The winner of this award competition receives US\$ * and free registration to the following year's ADM annual meeting.

Founder's Award information:

The ADM has initiated an award to honor Dr. Evan Greener in recognition of his contributions to the Academy. The **Founder's Award** will be given to an ADM Member who is nominated by one or more fellow ADM members as exhibiting excellence in dental materials research and in service to the Academy. Nominations should document the contributions of the individual and should be sent to the President of the Academy: Dr. Jeffrey Stansbury E-mail: Jeffrey.stansbury@ucdenver.edu. The nominations will be reviewed by the Board of Directors for acceptance. This is an honorary award, not a cash award, but up to US\$ 1000 will be provided to the awardee for expenses in attending the annual Academy meeting to receive the award in person.

MEMBERSHIP APPLICATION

Complete all blank lines

Please print or type

PROFESSIONAL INFORMATION

LAST NAME: _____ FIRST NAME: _____

INSTITUTION/COMPANY/UNIVERSITY: _____

DEPARTMENT: _____

STREET ADDRESS: _____
(please note that journal will be sent to this address)

CITY: _____ STATE: _____

COUNTRY: _____ ZIP: _____

PHONE#: _____ FAX #: _____

E-MAIL: _____

IMPORTANT NOTE: STUDENTS AND POSTDOCTORAL APPLICANTS MUST SEND A CONFIRMATION LETTER OF STUDENT/POSTDOCTORAL STATUS FROM EITHER A SPONSORING MEMBER OR THEIR LEARNING INSTITUTE.

FILING INFORMATION

MEMBERSHIP: Please check one of the following categories and see reverse side for information:

- ☐ MEMBER - option 1 US\$175/year (includes **printed and online** journal) (US\$100 for first year only).
- ☐ MEMBER - option 2 US\$149/year (includes only the online journal) (US\$74 for first year only).
- ☐ STUDENT MEMBER* US\$40/year (includes only the online version journal).
 - ☐ *STUDENT MEMBER – I do **not** have a PhD title
 - ☐ *STUDENT MEMBER – I **am** enrolled in a Masters, PhD or dental degree program
- ☐ POSTDOCTORAL MEMBER* US\$55/year (includes only the online version journal).
 - *Confirmation Letter of Student/Postdoctoral Status required to accompany application
 - ☐ *POSTDOCTORAL MEMBER*I have **not** been a PhD member in the ADM for longer than 4 years

PAYMENT: Please check one of the following:

☐ Check ☐ Money Order ☐ Visa ☐ MasterCard ☐ Discover TOTAL: US\$ _____

Account or Card No.: _____ 3-digit security code: _____

Expiration date: _____ Cardholder's Name: _____

Signature: _____

SIGNATURE OF THE APPLICANT: _____ DATE: _____

SEND FORM AND PAYMENT TO:

Academy of Dental Materials
Attn: Lynn Reeves
4425 Cass Street, Suite A
San Diego CA 92109 USA
Email: Lynn@RES-Inc.com
Phone: +01-858-272-1018
FAX: +01-858-272-7687

